Quantification of feedstock characteristics before and during hydrothermal liquefaction under subcritical conditions of water

Sylvia Yawa Elikplim Edifor

BSc. (Chem) Hons.

Thesis submitted for the degree of Doctor of Philosophy

School of Chemical Engineering and Advanced Materials

Faculty of Engineering, Computer & Mathematical Sciences

The University of Adelaide, Australia

June 2021

TABLE OF CONTENTS

DECLARATION vi

ACKNOWLEDGEMENTS vii

PREFACE viii

Chapter 1: Introduction 1

1.1. Background 2

1.2. Scope and Structure of the Thesis 4

Chapter 2: Literature Review 6

2.1. Introduction 7

2.2. Municipal sewage sludge 7

2.2.1. Types of sewage sludge 8

2.2.2. MSS management and disposal 10

2.2.3. Alternative use of sludge and biosolids 11

2.3. Hydrothermal Processes 12

2.3.1. Hydrothermal liquefaction 13

2.3.2. Batch and continuous HTL processes 14

2.3.3. Feedstock characteristics 19

2.4. Rheometry 19

2.4.1. Ex-situ viscosity measurement 20

2.4.2. In-situ viscosity measurement 23

2.5. Mixer type rheometry 25

2.5.1. Choice of impellers for mixer type rheometry 26

2.5.2. Methods of mixer-type rheometry 27

2.6. Viscosity variation of feedstock during HTL 31

2.6.1. Selection of model compounds 32

2.6.2. Selection of no-lignin biomass 33

2.6.3. Factors affecting viscosity variation 34

2.7. Implication and significance of the current study 35

2.8. Objectives of the thesis 36

2.9. References 36

Chapter 3: The influence of feedstock characteristics on processability of biosolid slurries for conversion to renewable crude oil via hydrothermal liquefaction 48

Chapter 4: Rheological studies of municipal sewage sludge slurries for hydrothermal liquefaction biorefinery applications 62

Chapter 5: Viscosity variation of model compounds during hydrothermal liquefaction under subcritical conditions of water 78

Chapter 6: Real-time viscosity variations of sewage sludge during hydrothermal liquefaction under subcritical water conditions 100

Chapter 7: Conclusions 142

7.1. Conclusions from individual studies 143

7.1.1. The influence of feedstock characteristics on the processability of biosolid slurries for conversion to renewable crude oil via hydrothermal liquefaction 143

7.1.2. Rheological studies of municipal sewage sludge slurries for hydrothermal liquefaction biorefinery applications 144

7.1.3. Viscosity variation of model compounds during hydrothermal liquefaction under subcritical conditions of water 145

7.1.4. *Real-time viscosity variations of sewage sludge during hydrothermal liquefaction under subcritical water conditions* 146

7.2. Recommendations for future work 146

ABSTRACT

Hydrothermal liquefaction (HTL) is a thermal process that converts organics in biomass and waste into renewable crude-like oil. Sewage sludge is a typical waste material that can produce crude-like oil via HTL under subcritical conditions due to its organic-rich content. The composition and properties of sewage sludge significantly influence the feedstock's processability, the conversion of organics, and the crude-like oil yields. HTL feedstock properties, specifically viscosity and density, are important flow properties that affect HTL product formation at different reaction conditions. Knowledge of the feedstock viscosity helps estimate slurry transportation through pipelines, pumping power and heat transfer requirements for design purposes.

To determine the flow properties before HTL for pipeline specification, the settling characteristics of biosolid slurry was determined using batch settling experiments. Results of the settling test were used to assess the stability of the slurry during transportation. The effect of solid concentration and particle size of biosolids on slurry stability and pumpability was evaluated. Stability of biosolid slurries improved with an increase in solid concentration. The rheological properties of sewage sludge obtained from different parts of the wastewater treatment plant were also estimated. Generally, sludge slurries were determined to be non-Newtonian fluids. Rheological parameters of sludge feedstock, including yield stress, flow behaviour and consistency indices, were obtained from rheological models. A comparative study was made on the rheology and pumping power required for different sludge types to determine the transportability of these slurries based on a plant capacity of 1000 tonnes/year.

To determine the flow properties of sewage sludge during HTL process, the real-time viscosity of sewage sludge slurries was quantified using a modified batch reactor. The torque-rotational speed data of the impeller was converted to shear stress-shear rate data to estimate viscosity. The Couette and Metzner-Otto methods were shown to be valid for real-time viscosity

measurement under subcritical conditions. Apparent viscosity changes of lipid, proteins and carbohydrate model compounds at different reaction conditions were estimated. Model compounds exhibited unique viscosity profiles based on the mass yields and chemical speciation of HTL products. Apparent viscosity changes in reacting sludge slurries were determined at variable solid concentration, temperature and pressure. Significant differences were observed between the apparent viscosity profiles of sludge slurries and the apparent viscosity profiles of mixtures of model compounds with similar organic compositions. The effects of lignin, inorganics and the dominance of specific macromolecules on the apparent viscosity of sludge were analysed through a comparative study with the apparent viscosity of microalgae and determined to have significant effects on the apparent viscosity profile of sludge slurries.

The major contributions from this PhD investigation can be applied to determine the real-time viscosity of fluids and slurries under subcritical conditions. The study on the rheology of sludge is vital for pipeline specification and reactor design purposes. The changes in apparent biomass viscosity can be predicted for design purposes and process monitoring during reactor operations in an HTL plant.

DECLARATION

I certify that this work contains no material which has been accepted for the award of any other degree or diploma in my name, in any university or other tertiary institution and, to the best of my knowledge and belief, contains no material previously published or written by another person, except where due reference has been made in the text. In addition, I certify that no part of this work will, in the future, be used in a submission in my name, for any other degree or diploma in any university or other tertiary institution without the prior approval of the University of Adelaide and where applicable, any partner institution responsible for the joint-award of this degree.

I acknowledge that copyright of published works contained within this thesis resides with the copyright holder(s) of those works.

I also give permission for the digital version of my thesis to be made available on the web, via the University's digital research repository, the Library Search and also through web search engines, unless permission has been granted by the University to restrict access for a period of time.

I acknowledge the support I have received for my research through the provision of an Australian Government Research Training Program Scholarship.

…… …… 24/06/2021

Sylvia Yawa Elikplim Edifor Date

ACKNOWLEDGEMENTS

Firstly, I would like to thank God for this experience, and my supervisors Professor David Lewis, Dr Philip van Eyk and Dr. Patrick Biller, for their support, supervision and guidance over the last few years. I would like to express my heartfelt gratitude to them for their patience, motivation, encouragement, counsel and faith in me throughout my PhD journey. I would also like to thank Associate Professor Quoc Dzuy Nguyen for impacting knowledge, guidance, time and providing constructive feedback as an expert in the field of rheology.

I would like to acknowledge Southern Oil Refining and the Australian Council Linkage Project (LP150101241) for the financial support during my PhD study. I would also like to thank Mr. Bill Pemberton of Melbourne Water, Mr. Mark Swain and Mr. Gary Smith of SA Water and Queensland Urban Utilities for providing me with sewage sludge and biosolid feedstock for my experimental work.

I acknowledge the assistance of Dr Tony Hall and Dr Quihong Hu for their immense support and expertise during the analytical studies of my feedstock and product. I would also like to express my sincere thanks to Jason Peak, Aubrey Slater, Jozef Kumberger and Simon Golding of the ECMS Workshop for their technical support.

I would like to thank my colleagues in the HTL research team (Jasim Al-Juboori, Reem Obeid, Arafat Md Hossain, Thomas Brailey Scott, Andres Chacon Parra, Chye Yi Leow and Robran Kim Cock) at the University of Adelaide for their support and feedback.

Finally, I would like to thank my parents and siblings for their patience and support throughout my PhD journey. I would also like to thank Prof. Addai-Mensah, Janet Skinner, Dr Maxwell Lartey, Eve, Kwami, Jojo, Nuella Lartey and my friends (Josephine Hinneh, Pei Lay Yap, Gule Li, Felix Adu-Agyare, Caleb Acquah and Peace Adesina) for their encouragement and emotional support during my PhD.

PREFACE

This thesis is submitted as a portfolio of publications according to the 'Specifications for Thesis 2021' of the University of Adelaide. The journals in which the articles were published are given in the following table:

Journal Title	**2019 Impact Factor**
Industrial & Engineering Chemistry Research	3.573
Chemical Engineering Research and Design	3.350

The main body of this work is published in the following journal papers:

a. Edifor, S. Y., Van Eyk, P., Biller, P., & Lewis, D. M. (2020). The influence of feedstock characteristics on the processability of biosolid slurries for conversion to renewable crude oil via hydrothermal liquefaction. *Chemical Engineering Research and Design, 162*, 284-294. doi: 10.1016/j.cherd.2020.08.016

b. Edifor, S. Y., Nguyen, Q. D., van Eyk, P., Biller, P., & Lewis, D. M. (2021). Rheological studies of municipal sewage sludge slurries for hydrothermal liquefaction biorefinery applications. *Chemical Engineering Research and Design, 166*, 148-157. doi: 10.1016/j.cherd.2020.12.004

c. Edifor, S. Y., Nguyen, Q. D., Van Eyk, P., Biller, P., Hall, T., & Lewis, D. M. (2021). Viscosity variation of model compounds during hydrothermal liquefaction under subcritical conditions of water. *Industrial & Engineering Chemistry Research, 60*, 980-989. doi: 10.1021/acs.iecr.0c04845

d. Edifor, S. Y., Nguyen, Q. D., Van Eyk, P., Biller, P., Hall, T., & Lewis, D. M. (2020). Real-time viscosity variations of sewage sludge during hydrothermal liquefaction under

subcritical water conditions. The University of Adelaide. Unpublished work written in manuscript style.

Chapter 1:

Introduction

1.1. Background

An increase in population density and urbanisation increases the competition for limited resources, including water and energy, which leads to over-dependency on utilities. Expansion of water and energy industries will be necessary to meet the increasing demand for utilities of which Wastewater treatment plants (WWTPs) are no exception (Vergara-Araya et al., 2020). Management, treatment and disposal of wet solid residue in WWTPs are costly with high environmental concerns. Implementation of waste-to-energy (WTE) technologies present an economical solution that reduces the cost of waste management and produces useful energy simultaneously. WTE technologies can be the physical, chemical or thermal treatment of waste resources. The hydrothermal liquefaction (HTL) process is a typical example of WTE technology.

HTL is a thermal degradation process that can convert organic matter in biomass and wet waste streams into crude-like oil, solid products, aqueous products and gas under subcritical water conditions. This thermal process mimics the geological formation of fossil fuels in the Earth but requires a shorter residence time to convert biomass organics into crude-like oil. The renewable crude-like oil can be upgraded into liquid transportation fuels with similar properties to fossil-derived fuels. HTL involves a series of complex reactions that subjects the organic feedstock under subcritical water conditions at a temperature of about 350°C and pressures of about 200 bar (Castello et al., 2018). The water acts as a reactant (Shakya et al., 2015), solvent, catalyst (Toor et al., 2011) and a suitable medium for specific reactions to occur in the crude-like oil formation process via HTL.

Production of heavy oil from sewage sludge via thermal technologies begun in the 1970s and continued in the 1990s, where Itoh et al. (1994) explored alternative utilisation of sewage sludge to reduce solid waste by profitably producing oil. Since then, other researchers have investigated the thermal treatment of sludge on different scales across the world. Globally, an

increase in population increases sewage sludge production. Large volumes of sewage sludge produced due to increased population indicate the availability and abundance of this feedstock to produce renewable energy as a form of waste management. HTL of sewage sludge is a promising technology for future treatment and management of solid residues from WWTPs, while recovering energy simultaneously. Hence, HTL of sewage sludge is potentially viable for managing large volumes of solid waste and producing useful fuel.

Municipal sewage sludge from different stages of a WWTP has been hydrothermally liquefied in few studies (Anthony III, 2015; Biller et al., 2017; Marrone, 2016; Nazari et al., 2017; Snowden-Swan et al., 2016; Vardon et al., 2011) on batch and continuous scales due to its rich organic matter, high carbon recovery and high calorific value. The utilisation of sludge for such an efficient and beneficial use is challenging due to the complex behaviour of sewage sludge slurries obtained from different parts of the WWTP. Rheological sludge properties, especially slurry viscosity, are essential for material and heat transfer processes during HTL of sludge under subcritical conditions. Both heat and material transfer processes are crucial in plant design, reactor design, pipeline and instrumentations of a plant, process control and process monitoring of a continuous system as well as economic analysis of a plant. Therefore, it is expedient to determine the viscosity of the feedstock slurry for design purposes.

This body of work investigates the rheological properties of sewage sludge and biosolid feedstock for material transportation (pumping). Secondly, this PhD investigation elucidates and quantifies the real-time viscosity of reacting sewage sludge slurries, individual model compounds and mixtures of model compounds of the macromolecules in sewage sludge (lipid, protein and carbohydrate) under subcritical condition of water. This information is applicable in HTL plant design and the design of other thermochemical processes as viscosity is useful for heat transfer calculations and reactor design purposes.

1.2. Scope and Structure of the Thesis

Chapter 2 comprises a comprehensive literature review based on a scientific study on the HTL plant design. This chapter discusses the various sections of a typical HTL plant from the raw material source (sewage sludge) to product formation. This chapter highlights the importance of viscosity as a flow and heating property of biomass feedstock during material transportation in pipelines and pumps, and heat transfer processes applicable in a wide range of sludge processing industries. The review discusses relevant literature on the different types of viscosity measuring techniques and suggests a suitable method for real-time viscosity measurement during the HTL process.

The first journal article presented in Chapter 3 is a study on the influence of feedstock characteristics on the processability of biosolid slurries for conversion to renewable crude-like oil via HTL. The stability and pumpability of biosolid slurries with different particle sizes and solid concentrations were determined for pipeline specification and pump design purposes. The pumping power requirement for biosolid slurries was determined as an important parameter that influences both capital and operational costs in an HTL Plant.

The second journal article presented in Chapter 4 investigates the rheological properties of different types of sludge slurries obtained from different stages in a WWTP. The rheological properties that affect flow properties of sewage sludge slurries during HTL application were modelled using three viscosity models. Model validation and verification were conducted to determine the best model that fits the experimental data. The pumping power required for pumping each type of sludge slurry was estimated and compared to the others.

The third journal paper presented in Chapter 5 is a study on the viscosity variation of model compounds during HTL under subcritical water conditions. This study reports the changes in viscosity of model compounds including lipids, proteins and carbohydrates. Viscosity variation

of mixtures of single model compounds and mixtures of model compounds in a batch reactor was estimated to predict the viscosity variation of actual biomass.

The fourth journal paper presented in Chapter 6 focusses on the real-time viscosity variation of sewage sludge slurries during HTL under subcritical water condition. A batch reactor was calibrated to function as a rheometer for real-time viscosity measurement under subcritical conditions. Viscosity measurement was conducted using two equations which were verified and validated under subcritical water condition. Changes in the apparent viscosity of reacting sludge slurries were determined and compared to the apparent viscosity variations of mixtures of model compounds and the apparent viscosity of algae.

Chapter 7 comprises of the conclusions of this study, including recommendations for future work based on the research findings.

References for Chapters 2 and 6 are listed at the end of each chapter. References for Chapters 3, 4 and 5 are listed in the attached journal papers.

Chapter 2:

Literature Review

2.1. Introduction

This chapter reviews the scientific literature on the feedstock characteristics of sewage sludge during hydrothermal liquefaction under subcritical water conditions. This review discusses the properties of different types of sewage sludge, the HTL process and the various stages in a typical HTL plant. Additionally, this review highlights the importance of the HTL reacting slurry's viscosity as it is an important flow property for design purposes, process monitoring, operations, and estimation of heat transfer properties. The different types of viscosity measuring methods stating the design limitations of the existing methods are discussed, and the in-situ viscosity measurement methods for accurate viscosity measurement of HTL reacting slurries with minimal errors are proposed in this review.

2.2. Municipal sewage sludge

Municipal sewage sludge (MSS) refers to the solid waste produced by the municipality and obtained from residential, industrial, institutional wastewater and landfill leachate (Pöykiö et al., 2019). Sewage sludge is the semi-solid residue produced after the treatment of sewage. MSS contain complex organic materials, inorganic minerals, microbes (Sharma et al., 2020), microplastics (Rolsky et al., 2020) and other hazardous substances. The organic fraction of MSS comprises of lipid, carbohydrate, protein and lignin in varying percentages depending on the source of the waste while the inorganic component of MSS includes mineral elements and heavy metals. MSS is rich in nutrients such as Nitrogen and Phosphorous, which are beneficial for soil conditioning (Pöykiö et al., 2019). Heavy metals in sewage sludge include lead, cadmium, zinc, copper and nickel (Wang et al., 2005). Sewage sludge contains active pathogens (bacteria and viruses), dead microbes (Extracellular polymeric substances, EPS) and micro-pollutants. EPS are biopolymers that are mainly composed of polysaccharides and proteins (Redmile-Gordon et al., 2020) responsible for retaining moisture, trapping nutrients, thickening slurries and aggregating sludge particles. Other non-categorised hazardous

compounds in MSS include dioxins, propionyl-CoA carboxylase (PCCB), phenolic compounds, pesticides and detergents.

2.2.1. Types of sewage sludge

The first stage in the wastewater treatment process is screening. As shown in Figure 1, untreated wastewater flows into a drum screen where large objects are separated from the liquid waste. The screened fluid then flows through a grit chamber to remove particulates, sand and stones in the sewage. De-gritted wastewater is transported into a primary clarifier where concentrated sediments are separated from liquid sewage through gravity sedimentation (Ranieri et al., 2011). Concentrated sediments containing more than half of the suspended solids in the wastewater, contaminants, organic materials, nutrients and inorganics materials at this stage are known as primary sludge (National Research Council et al., 1996). Primary sludge is the first type of sewage sludge produced during the treatment of wastewater.

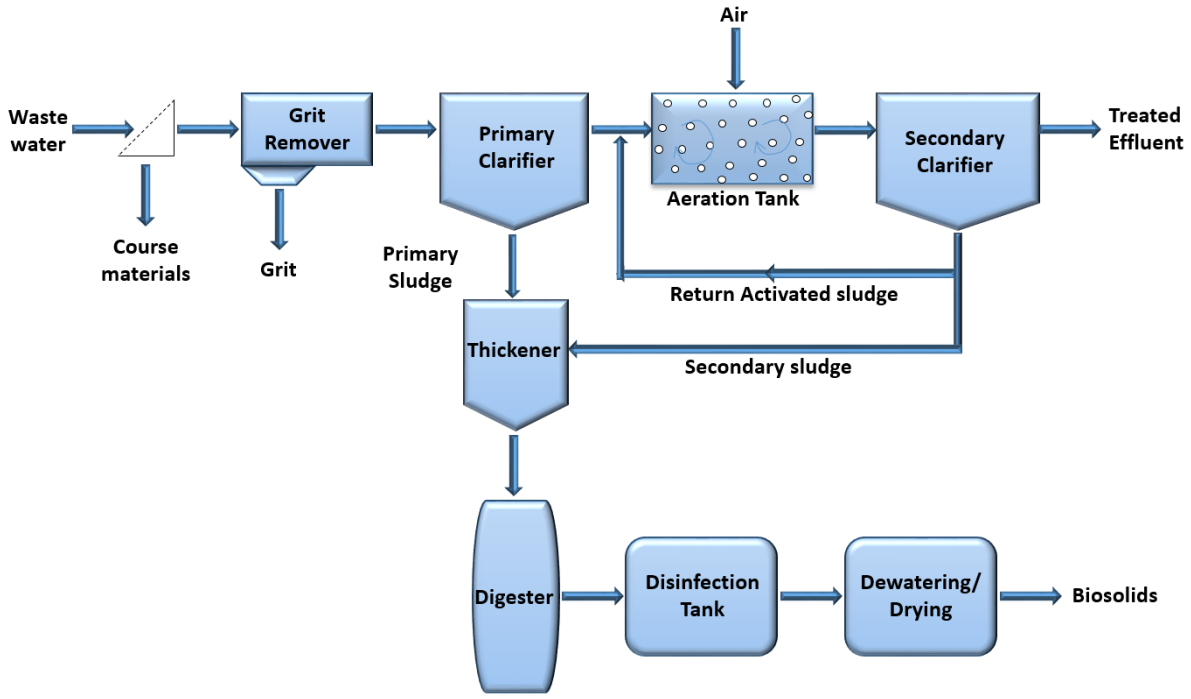

Figure 1. Process flow diagram of a conventional wastewater treatment plant

The effluent from the primary clarifier is aerated in an aeration tank where bacteria consume the sewage sludge's organic components to activate it. A secondary clarifier separates the concentrated activated sludge from the secondary effluent. The concentrated activated sludge obtained after bacterial decomposition is also known as secondary sludge (Environmental Protection Agency, 1998). Secondary sludge is the second type of sewage sludge produced in a WWTP.

A fraction of the activated sludge, also known as return activated sludge, is recycled into the aeration tank to activate the effluent from the primary clarifier. The remaining fraction of activated sludge flows into a thickener. Primary and secondary sludge from the primary and secondary clarifiers are thickened and digested in an anaerobic digester where micro-organisms consume organic materials in the sludge. The digested sludge is further treated by disinfection, dewatering and drying to reduce the moisture content and the pathogen content by 90% (Australian Water Association, 2012). After anaerobic digestion, treated solids which are nutrient-rich organic materials with reduced moisture content from 96-94% to about 30 -70% and reduced pathogen content to a standard and acceptable level for reuse are termed biosolids (Brown et al., 2017). Biosolids contain organic compounds, inorganic and trace elements, a minimal amount of pathogens and nutrients that can serve as an alternative for inorganic fertilisers and soil conditioners (Leonie & Graeme, 2009). Biosolids are the solid residues obtained at the end of the wastewater treatment process.

Sludge treatment processes affect the physicochemical properties of the different types of sewage sludge produced in a WWTP (Water Environment Federation, 2012). As shown in Table 1, solid contents of primary, secondary and digested sludge are <12%. Sludge contains high total organic carbon (TOC) and high organic contents (> 70wt%) which can be recovered. The sewage sludge properties differ from one WWTP to another due to the variable sources of

the feedstock, different operations and wastewater treatment processes peculiar to each WWTP (Baudez et al., 2007).

Table 1. Characteristics of sewage sludge produced during wastewater treatment (Metcalf & Eddy, 2003)

Type of sludge	Total solids, %	TOC[a], wt% dry	Ash[a], wt% dry
Primary sludge	6-12	44.6	7.5
Secondary sludge	1.5-4	40.9	16.2
Digested sludge	3-10	35.3	28.1

[a] Marrone et al. (2018)

Biological treatment of wastewater in WWTP produces solid waste which contains residual pathogens that were not destroyed during the treatment process. These by-products obtained after wastewater treatment, including primary sludge, secondary sludge, digested sludge and biosolids can be sampled at different stages of the treatment process. Due to the pathogenic content of these by-products, sludge and biosolids need to be further treated, managed and disposed of properly with less environmental impacts.

2.2.2. MSS management and disposal

The gradual increase in worldwide population and urbanization increases waste generation. Generation of an enormous amount of waste poses a global challenge with a growing demand for an environmentally safe and economical waste management solution. According to the Australian and New Zealand Biosolids Partnership (2020), Australia produced over 370,000 tonnes of dry biosolids in 2019. The end-use of biosolids, including agriculture, land rehabilitation, landfill and stockpiling costs $100 million annually (Australian Water Association, 2012; Darvodelsky, 2011). This clearly shows that the traditional treatment and management of sludge and biosolid is expensive.

According to the waste management hierarchy, the best way to manage MSS is by reusing it compared to disposal (Khoshnevisan et al., 2020). Economically, energy recovery from waste presents reliable waste management and reduced waste disposal cost by producing useful energy. Production of renewable crude like-oil from sludge via hydrothermal liquefaction will increase sludge value (Skaggs et al., 2017). The rich organic fraction of sludge can be converted into a high-value product by applying technologies such as WTE technologies. WTE pathway is potentially sustainable and beneficial. It provides an alternative solution to waste management and disposal by reducing about 50% solid mass while simultaneously producing a novel source of fuel from an innovative process that supplements non-renewable fossil fuel. Hence, the application of WTE technologies can be a viable and economical solution for managing sludge and biosolids.

2.2.3. Alternative use of sludge and biosolids

Production of heavy oil from sewage sludge via WTE technologies begun in the 1970s where Hess and Cole (1973) proposed an alternative sludge treatment process using high-pressure thermal treatment. Further investigations on the conversion of sludge into oil via WTE technologies have progressed over the years and proven the feasibility of thermochemical processes (Itoh et al., 1994; Shah et al., 2020; Xu & Lancaster, 2009; Yokoyama et al., 1997).

The conversion of both sludge and biosolids into liquid transportation fuel is a better alternative to traditional sludge management as it manages waste and produces renewable fuel simultaneously. Unlike biosolids, the conversion of organic-rich matter in fresh sludge is highly desirable, as the conversion of sludge will reduce the cost of treating sludge to produce biosolids and increase crude-like oil yields due to the high organic content in sludge. Sludge is a stable and homogenous feedstock with a low solid concentration that can be easily transported through pipelines. However, fresh sludge is dilute and requires dewatering to increase the throughput, crude-like oil yields and process efficiency during crude-like oil production via

thermal conversion processes. Contrarily, biosolid feedstocks contain lower organic compositions and high solid content which can be complex and difficult to process due to its high solid composition. Production of biosolids does not only increase sludge treatment cost, but it also occupies land space when stockpiled and landfilled for years. Effective sludge management should consist of a method to convert both freshly produced sludge and already existing waste (stockpiled biosolids). To harness the energy value in fresh sludge and reduce MSS in already existing stockpiled biosolids, it might be useful to mix both biosolids and sewage sludge feedstock for crude-like oil production.

A mixture of biosolids and sludge will be beneficial as both feedstocks complement each other by providing enough solids for HTL by thickening sludge, reducing the operation cost required for dewatering, increase the organic and carbon contents and improving the nature of the feedstock properties for improved heat and material transfer process. Prior to mixing both feedstocks, it would be essential to elucidate the behaviour of the individual feedstock under thermochemical process conditions as an early step towards process optimisation.

2.3. Hydrothermal Processes

WTE technologies are potentially sustainable techniques for converting waste into energy through chemical processes, biochemical processes such as fermentation and thermochemical conversion processes which includes hydrothermal processes (HTP), pyrolysis, combustion and gasification (Khan & Kabi, 2020; Mukherjee et al., 2020; Nazari, 2016). HTP is advantageous over other thermochemical processes as it skips the energy-intensive drying stage. Waste materials including industrial, municipal solid and agricultural waste residues (Sharma et al., 2020) are nutrient-rich raw materials and fuel sources that can generate heat and electricity through HTP.

HTP which includes hydrothermal carbonisation (HTC), hydrothermal liquefaction (HTL) and hydrothermal gasification (HTG) are promising processes with a potential of converting a wide range of biomass feedstock into energy, solid, liquid and gaseous fuel (Rajasekhar Reddy & Vinu, 2018). HTC is targeted at producing solid fuel, also known as hydrochar at temperatures below 250ºC. Hydrochar has similar properties to low-rank coal. HTL occurs between 250ºC - 370ºC and produces a desired liquid fuel. The liquid fuel can be upgraded into petroleum fuels, as it possesses similar properties as fossil-derived fuel. Fractional distillation of the produced crude-like oil produced from HTL of sewage sludge slurries has the potential to be upgraded and refined to meet the Fuel Quality Standards. The boiling point profile of the crude-like oil aligns with gasoline (13.4wt%), jet fuel (16.1wt%), light diesel (11.9wt.%), heavy diesel (17.2 wt%) and residual fuels having a high heating value (HHV) of 32-42 MJ/kg and high carbon content of 80-88wt.% (Castello et al, 2019). Upgrading of these fractions could meet relevant fuel standards. HTG produces synthetic gas at reaction temperatures above 370ºC (Elliott et al., 2015). This study focuses on the production of renewable crude-like oil via HTL.

2.3.1. Hydrothermal liquefaction

HTL is a thermochemical depolymerisation process that converts organic-rich materials in wet biomass under subcritical and supercritical water conditions. It involves a series of complex reactions that produce crude-like oil under subcritical conditions between 250ºC to 370ºC at pressures between 100 -350 bar (Castello et al., 2018). Water in the feedstock acts as a medium, catalyst and solvent that solubilises non-polar compounds at subcritical conditions during the production of renewable crude-like oil. Under HTL conditions, macromolecules in the wet organic materials interact through hydrolysis, depolymerisation, dehydration and decarboxylation processes to produce crude-like oil, aqueous, solid and gas phases in the presence of water. HTL can be conducted as a batch process or a continuous process.

2.3.2. Batch and continuous HTL processes

HTL of sewage sludge has been widely studied on both batch and continuous operations. A typical HTL batch process has been described by Obeid et al. (2019) where HTL is conducted in a batch reactor. The prepared feedstock is loaded into the reactor and pre-pressurised with a gas (N_2). As shown in Figure 2, the loaded reactor is placed into a heated fluidised bed, and the reactor is heated to the operating temperature. After the desired reaction time has elapsed, the reactor is removed from the fluidised bed, and the products are cooled to lower temperatures. The produced gas is released. HTL liquid and solid products are separated and analysed (Obeid et al., 2019). One advantage of using a batch system is the ability to process higher solid concentrations. However, batch systems have a limitation of throughput as they require a limited amount of feedstock to be processed at any given time.

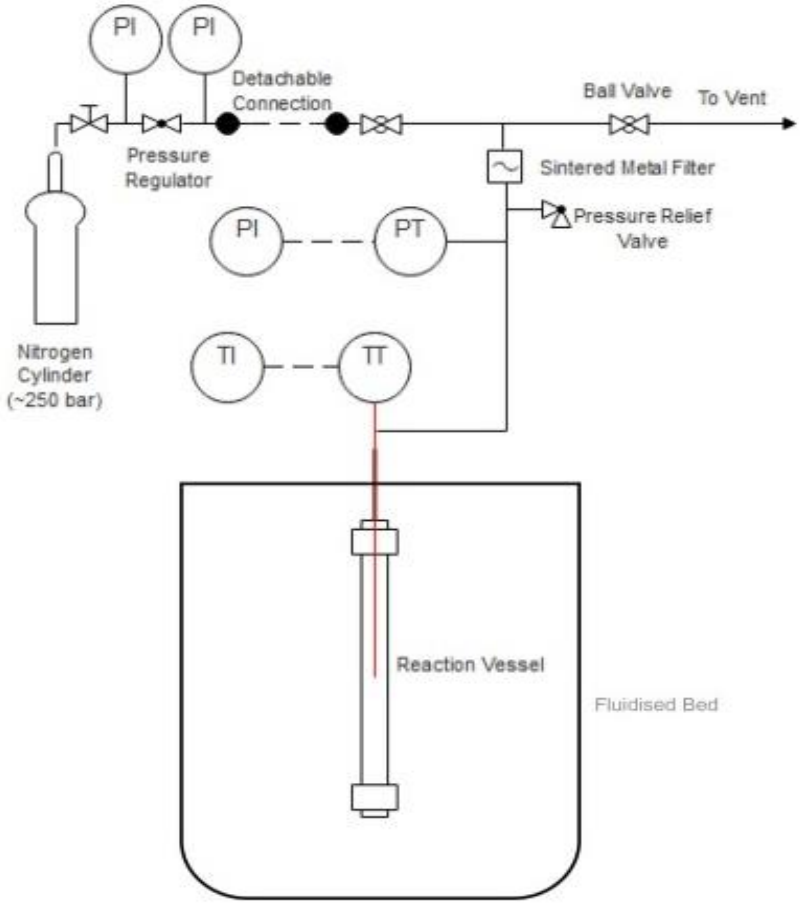

Figure 2: HTL Batch reactor set-up (Obeid et al., 2019)

For HTL continuous processes, continuous stirred tank reactors (CSTR), tubular reactors or a combination of CSTR and a tubular reactor are mostly employed (Balaman, 2019; Elliott et al., 2015; Marrone, 2016). CSTR and tubular reactors are used to process a homogeneous feed to maximise conversion of organics in the feedstock continuously. Even though these reactors are advantageous for high throughput and continuous production of crude-like oil, transportation issues such as settling of particles in nonhomogeneous slurry feedstock and high solid loading can lead to plugging of the tubes (especially in tubular reactors) and changes in the heat transfer properties of the fluid.

In a typical HTL plant design using tubular reactors, as shown in Figure 3, prepared sludge feedstock slurry is pumped under atmospheric and high pressures in two stages. Pressurised slurries are transported through heat exchangers to pre-heat the reacting slurry to the desired temperature. The pressurised and pre-heated slurry flow through tubular reactors where the feed is heated to the operating temperature in an alumina-filled bed that is fluidised by compressed air (Jazrawi et al., 2013). In other continuous systems, the pressurised and pre-heated fluid flows into a CSTR, which is electrically heated to the operating temperature (Elliott et al., 2015). One advantage of using a CTSR is that the reacting feedstock is continuously stirred to maintain homogeneity and constant heat transfer during the HTL process. The products from the reactor are cooled in a heat exchanger and separated. Solid products (char) are separated from the liquid products by filtration. The crude-like oil is upgraded and refined.

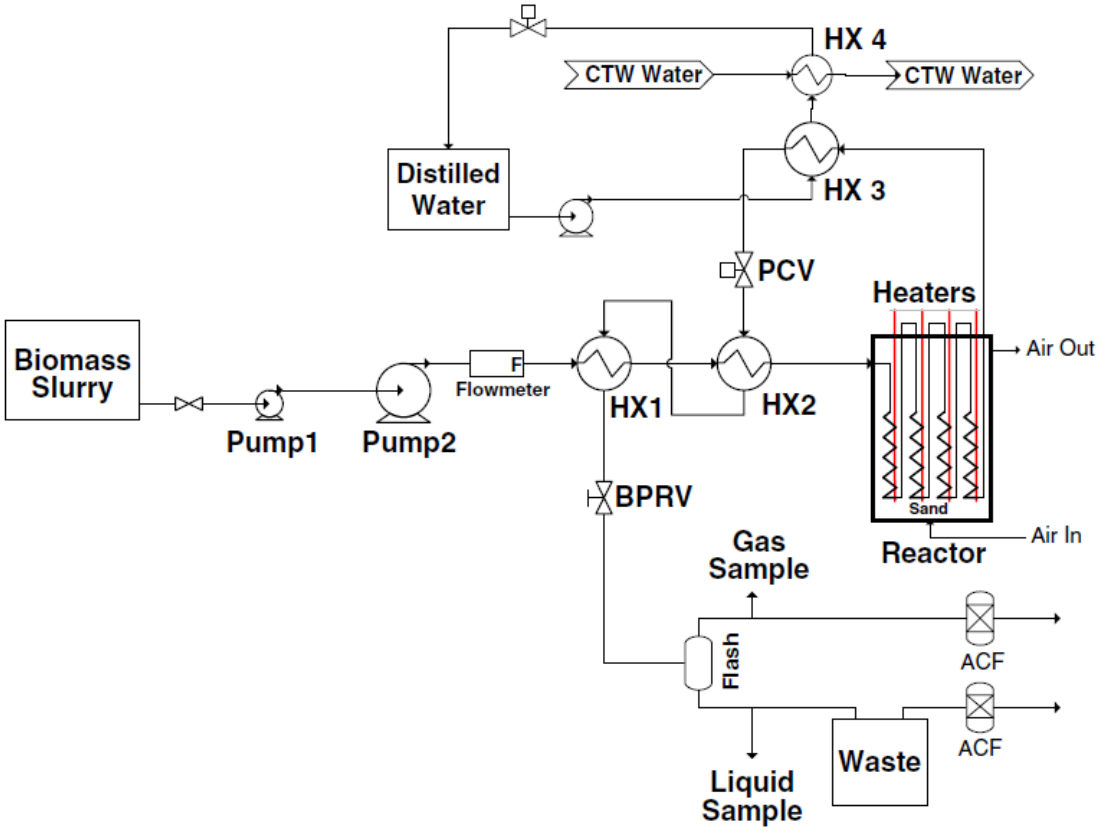

Figure 3: Process diagram of HTL plant designed at the University of Sydney (Jazrawi et al., 2013)

The bench-scale HTL plant designed by the Pacific Northwest National Laboratory (PNNL) where a CSTR is used in combination with a tubular reactor is shown in Figure 4. Two pressurised feed tanks are used for continuous delivery of the HTL feed at a constant flow rate. The feed is pumped through a pre-heater to heat the feed to about 130°C. The pre-heated feed flows into a CSTR where the feed is electrically heated to the operating temperature and stirred using a magnetically driven impeller. The process slurry from the CSTR is transported through a plug flow reactor at the operating temperature. The solid inorganic products are separated from the product stream in a filter at the same operating temperature. The pressurised filtrate products are cooled in a heat exchanger below 70°C. The gas is vented to depressurise the

system, and the crude-like oil phase is separated from the aqueous phase using a separation funnel.

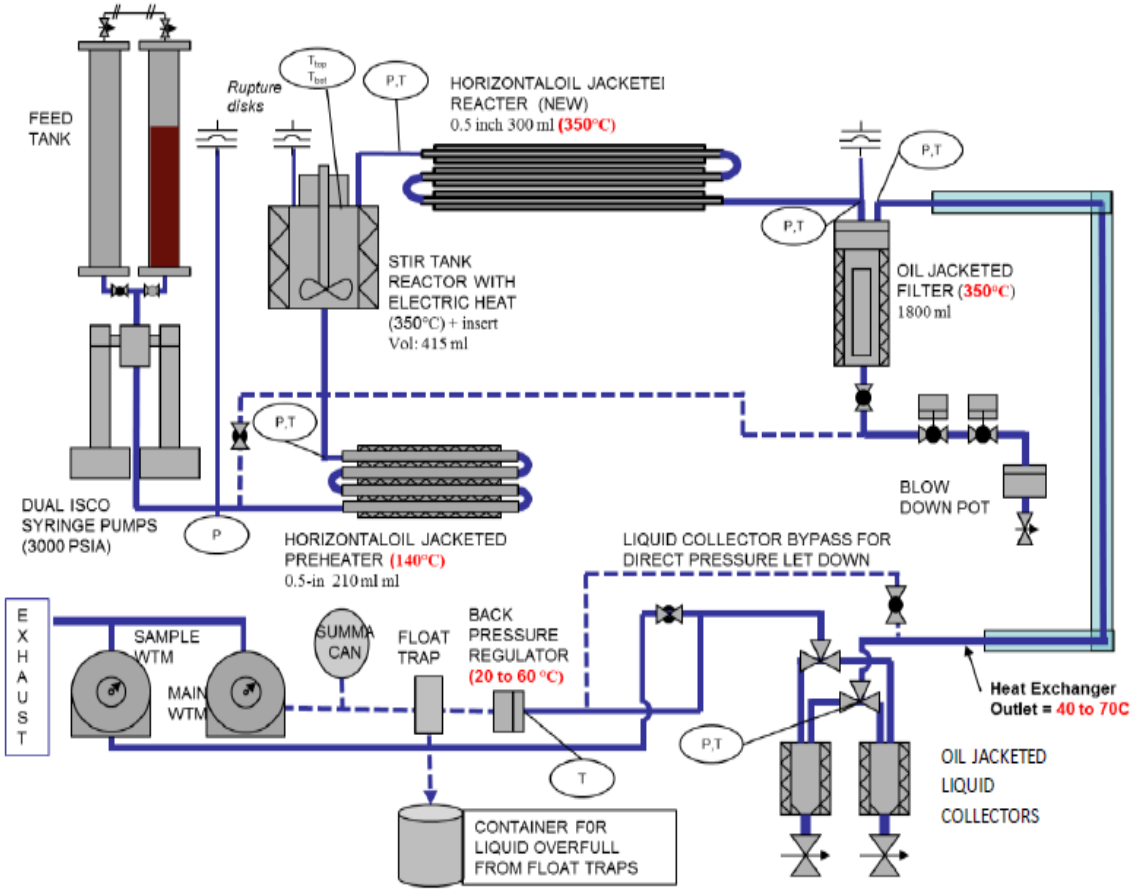

Figure 4. Process flow diagram of the PNNL bench-scale HTL plant (Marrone, 2016)

A primary objective of producing renewable fuels, where renewable diesel is the main target is to enhance low carbon emissions with the aim of meeting the Clean Fuel Standard. Commercial readiness for the use of renewable diesel produced from the HTL of renewable sources such as sewage sludge can be measured by the availability of the feedstock and the global acceptance of renewable energy.

There is an increasing interest from industry and government toward commercialisation of renewable energy in general, and the opportunity for renewable crude-oil provides short to medium term opportunities to transition to alternate heavy transportation fuels. In 2020, the

Australian Government announced its decision to invest $1.5 billion into six major manufacturing sectors with Recycling and Clean energy listed as a priority sector (Australian Government, 2021). This announcement in the National Manufacturing Priority Road map presents a great opportunity for growth in the Clean Energy sector as it encourages the recycling and re-use of organic waste such as sewage sludge into clean energy. Additionally, the provision of such funds will create a platform for emerging technologies in a bid to achieve a low carbon economy through the production of alternative source of renewable energy.

Previous studies on HTL processes have analysed biomass on laboratory scales, demonstration and pilot plants with the aim of scaling up to meet the industrial requirement. A commercial plant to produce renewable crude-like via HTL of sewage sludge feedstock is currently non-existent although there is progress in this area of research, government support and industrial partners' willingness to commercialise the results from research.

The bottlenecks in scaling up HTL plants to industrial level include the inconsistent quality of product properties obtained from a laboratory-scale experiment (Eboibi et al., 2014), the progressive changes of the reactants' properties during the HTL process and the limited design data for scaling up. Scaling up processes requires an in-depth understanding of the basic principles governing material transport and heat transfer for such a process. Small-scale laboratory studies are necessary for estimating the feasibility and validity of studies before scaling up. Such studies help to solve unknown parameters, bring up challenges and optimise the process with minimal losses (Ebrahimi et al., 2009). The plant design of the HTL process will cover a wide range of studies ranging from thermodynamics, fluid transport, heat transfer processes and simultaneous heat and mass transfer. The characteristics of sludge feedstock which mainly affect slurry transport and heat transfer processes are yet to be determined for HTL plant design purposes.

2.3.3. Feedstock characteristics

Feedstock characteristics influence the fluid flow mechanism, residence time and flow velocity in pipelines and tubular reactors. These characteristics include particle size, solid concentration, settling rate, slurry density and slurry viscosity. The feedstock properties, especially viscosity, affect the material transportation (pumping and fluid flow) of slurries. Additionally, slurry viscosity is used to estimate heat transfer properties of reacting slurries.

The particle size distribution, density, solid concentration, rheology, pumpability, stability and settling ability of sludge are reported independently from several investigations (Akhtar & Amin, 2011; Elliott et al., 2015; Park et al., 2011; Sintamarean et al., 2017; Spellman, 1996). Studies on dilute sewage sludge rheology were conducted for WWTP applications. However, the rheological characteristics of concentrated sewage sludge (>10wt%) under elevated pressures for HTL applications are yet to be investigated. Rheological properties of concentrated and pressurised sludge slurries will be useful for specification and design of pipelines, pumps and HTL reactors as well as analyse the pumping energy, heating requirement and process monitoring during operations.

2.4. Rheometry

Rheometry is the measure of the flow and deformation properties of fluids. This includes the experimental measurement of fluid shear viscosity, an important flow property for design, process monitoring and process control purposes. Fluid shear viscosity includes dynamic viscosity and kinematic viscosity. Dynamic viscosity is the resistance of a fluid to deformation at a given shear rate as kinematic viscosity is the fluid's resistance to flow under the influence of gravity. The known value of the dynamic fluid viscosity can be used to estimate the kinematic viscosity once the density of the fluid is known.

Generally, viscometers and rheometers are used to measure fluid dynamic viscosity. In the past, ex-situ viscosity measurements were used for consistency checks and quality control in industries. Industrial application and technological advancement have led to the need for measuring fluids during reactions and other processes. This has eventually led to the search for alternative measuring processes to predict dynamic viscosity of fluids at different process conditions. Development of at-line and on-line viscosity measuring techniques apply the basic principles of viscometer measurement to provide more accurate fluid viscosity values at different process conditions during a process.

2.4.1. Ex-situ viscosity measurement

Ex-situ viscosity measurements, also known as off-line viscosity measurement, are an indirect way of measuring a fluid's viscosity by sampling the fluid from a process and measuring its viscosity in a viscosity measuring equipment. Standard conventional rheometers are used for off-line viscosity measurements and for determining the rheological parameters of fluids at different conditions. Rheometers can be generally classified into shear rheometers and extensional rheometers.

Extensional rheometers measure the deformation of materials under controlled extensional stress or strain by mechanically stretching the material (Collett et al., 2015). Shear rheometers measure the deformation of materials under controlled shear rate and shear stress. Shear rheometers, also known as rotational rheometers, are the most common type of rheometers widely used. Dynamic viscosity of fluids using rotational rheometers is estimated by measuring the amount of torque required to deform the fluid under a given shear rate. Rotational rheometers have different configurations which include the cone-plate, parallel plate and the couette. In the operation of most rotational rheometers, there are two members, a mobile and a stationary member. The mobile part is driven, and the torque on that rotating member is

measured to determine the shear stress. The rotational speed of the mobile member is used to determine the shear rate.

According to Barnes et al. (1989), the gap between the mobile member and the rheometer stationary part affects the shear rate. The influence of the gap is such that for narrow gap-cylinder configurations where the ratios of the radii of the inner cylinder and the outer cylinder are greater than 0.97, the angular speed of the rotational member Ω_1, the radii of the inner cylinder R_i and the outer cylinder R_o are related to the shear rate $\dot{\gamma}$ in the given equation:

$$\dot{\gamma} = \frac{R_o \Omega_1}{R_o - R_i} \tag{1}$$

The shear stress is estimated from the torque on the rotational member in equation 2:

$$\sigma = \frac{T}{2\pi R_o^2 L} \tag{2}$$

Where T is the torque on the shaft of the rotational member and L is the effective immersed length of the sheared liquid. From both equations, the viscosity can be calculated as:

$$\eta = \frac{T(R_o - R_i)}{2\pi R_o^3 \Omega_1 L} \tag{3}$$

The narrow-gap configuration is effective for accurate viscosity derivations but also pose many challenges, especially when dealing with relatively large particles. Employing the use of a wider-gap configuration where the ratio of R_i to R_o is less than 0.97, the shear rate of the fluid will be given by

$$\dot{\gamma} = \frac{2\Omega_1}{n\left(1 - \frac{R_i}{R_o}^{2/n}\right)} \tag{4}$$

Where n is the power-law index obtained from plotting a log-log graph of T versus $\Omega_1$and taking the slope of the graph as the value of n. The shear rate of the fluid using the wide-gap

configuration depends on the property of the fluid. Shear stress of the liquid is determined at the inner cylinder in the given relation:

$$\sigma = \frac{T}{2\pi R_i^2 L} \tag{5}$$

The viscosity of the sheared fluid measured with a wide-gap configuration is given by

$$\eta = \frac{Tn\left(1 - \frac{R_i}{R_o}^{2/n}\right)}{4\pi R_i^3 \Omega_1 L} \tag{6}$$

The rheological characteristics of dilute sewage sludge slurries (<10 wt% dry solids) has been extensively studied at atmospheric pressures for WWTPs applications (Cao et al., 2016; Noguchi et al., 2011; Wolny et al., 2008; Zhang et al., 2017). Nonetheless, there is no information on the rheological behaviour of concentrated and pressurised sludge slurries for HTL applications. This information is essential for pipeline design and pump specification especially during feedstock transport from the feedstock preparation unit (feed tank) to the heat exchanger as shown in the upstream process in Figure 3 and Figure 4. Secondly, this information can be applied to other pressurised systems that require slurry transport of concentrated sewage sludge feedstock. An investigation on the rheology of sewage sludge slurries for HTL applications is yet to be conducted.

Conventional rotational rheometers have a limitation on the operating temperatures and pressures. As shown in Table 2, the maximum pressure and temperature of existing rheometers manufactured by Anton Paar are 1000 bar and 300ºC, respectively. The listed rheometers are unsuitable for measuring in-process viscosities of HTL reacting slurries between 300ºC and 350ºC. Hence, the traditional rheometers cannot accurately measure fluid viscosity during HTL under subcritical and supercritical water conditions due to design limitations.

Table 2. Conventional rotational rheometers

Company	**Anton Paar**		**Vinci Technologies**	**Haake**	**TA Instruments**		**Brookfield Ametek**
Model of rheometer	MCR		Rheo-1000 High pres.	D400/300	DHR-2	AR-G2 & AR2000ex	PVS
Accessory	Pressure Cell		-	Pressure Cell	Pressure cell		-
Mode of pressure input	Self & gas	Self & liquid	-	-	Self & gas	Self & gas	-
Temp, ºC	-10 to 200	25 to 300	200 (max)	300	-10 to 300	-10 to 150	-40 to 260
Press, bar	400	1000	1000	400	138	138	69

2.4.2. In-situ viscosity measurement

In-situ viscosity measurements, are also known as real-time viscosity measurements, are direct measuring techniques that measure fluid viscosity in its original state and capture the true viscosity value in the fluid's current condition. Real-time viscosity measurements consist of at-line viscosity measurements, including magnetic resonance imaging (MRI), ultrasound Doppler velocimetry and attachments of traditional rheometers, for example, rotational, vibrational and capillary rheometers (Goloshevsky et al., 2005; Wunderlich et al., 2006). MRI and ultrasound Doppler velocimetry techniques are accurate viscosity measuring techniques yet very expensive and sophisticated. Off-line rheometers can be attached to process lines for in-process viscosity measurements by sampling a portion of the process fluid in a bypass and measuring the viscosity. However, viscosity measurement on a bypass of a process line can be a challenge especially for non-Newtonian fluids that have a high settling property. This

technique estimates a near-viscosity value that may not be equivalent to the true value as the reaction conditions are altered when a fraction of the process fluid is sampled for measurement in the attached rheometer.

On-line or in-line viscosity measurements are examples of in-situ measurements. One typical on-line viscosity measuring technique is the use of heat transfer capacity. The viscosity of fluids greatly affects heat transfer processes; hence, the knowledge of the heat transfer capacity can be used to estimate the process fluid's viscosity. Wunderlich et al. (2006) investigated the bulk fluid viscosity in a stirred tank reactor (STR) by measuring the heat transfer capacity using a calibration heater. The heat transfer capacity *UA* was estimated as the quotient of the change in the calibration heat power by a change in the temperature difference between the reactor and the jacket when the calibration heater was turned on. The heat transfer coefficient is a function of heat transfer resistance of the walls of the vessel as well as the convection heat transfer coefficient from the reactor side and the jacket side where the convection heat transfer coefficients are dependent on the Nusselt number (Wunderlich et al., 2006). Nusselt number is a function of the Reynolds number (Re), Prandtl number (Pr) and the viscosity number. The dimensionless numbers, Re and Pr, are both dependent on the viscosity of the fluid. Viscosity measurement using calorimetry can be accurate. However, this technique only works for STRs, where a change in the state of the calibration heater (temperature change) occurs.

On-line viscosity measurement can also be estimated using the power input of a stirrer in an agitated vessel. The measured torque (M) on the impeller shaft at a known impeller speed (N) can be directly related to the HTL reacting fluid's dynamic viscosity (η) which is a ratio of the shear stress to shear rate (Yang, 1961) in the given relation**:**

$$\eta = \frac{\tau}{\gamma} = \frac{k_\tau M}{k_\gamma N} \tag{7}$$

The shear stress constant (k_τ) and shear rate constant (k_γ) are determined from the geometric properties of the impeller and reactor vessel (Aït-Kadi et al., 2002). From the viscosity correlation, an increase in torque on the impeller shaft corresponds to an increase in fluid viscosity at a constant speed. Thus, an increase in the energy input during agitation (as a measure of torque) of the STR indicates an increase in the fluid's viscosity at a constant speed (Loomis, 2014; Tan & Li, 2017). In this case, the mechanical energy input measured in terms of voltage can be directly related to the torque on the impeller shaft (Schelden et al., 2017).

On-line viscosity measurement using the torque and rotational speed of an impeller is only valid under laminar flow conditions in STRs and mixers. Hence, this technique can be applicable to HTL CSTRs for on-line viscosity measurement under room conditions and subcritical water conditions.

2.5. Mixer type rheometry

A mixer-type rheometer consists of a cylindrical vessel and an impeller similar to the cup and bob analogy in rotational rheometers. Reactors for on-line viscosity measurements have been designed for high temperature-high pressure systems using coal oil slurries from reviewed literature. Okutani et al. (1980) proposed the first application of a high temperature-high pressure reactor/rheometer to determine the viscosity of coal paste by pre-pressurising with hydrogen at maximum operating conditions of 550ºC and 29 MPa. A few decades later, Ren et al. (2011) designed a similar system with modern features, including a torque sensor for detecting the torque on the motor for viscosities measurement of coal oil slurries pre-pressurised with H_2 at 5 MPa and heated at a rate of 5ºC/min. Viscosity measurements were limited to lower operating conditions, a narrow range of viscosity measurements and non-reactive systems. There is limited scientific literature on the viscosity measurement of feedstock in a complex multi-component reactive system such as HTL of sewage sludge and biosolids. Hence, there is a need to modify an existing system for sludge feedstock viscosity

measurement under subcritical conditions applying a mixer-type rheometer principle. Viscosity measurement under subcritical condition will be useful to elucidate the sludge feedstock variabilities at different reaction conditions.

Mixer type rheometry is a suitable measuring technique for determining the viscosity of reacting fluids during HTL. This technique can measure viscosities of settling slurries (for example, biosolids) where particle size of the solid component can lead to slurry instability during the measuring process. Slurry instability is measured by the settling characteristics and non-homogeneity of the mixture. The choice of the impeller is a critical step as the impeller can maintain slurry stability during viscosity measurements to minimise measuring errors.

2.5.1. Choice of impellers for mixer type rheometry

There are different impeller configurations for mixer-type rheometers that enhance mixing and heat transfer in autoclaves. Sewage sludge slurries tend to remain stable with particles continuously suspending for a longer time. On the other hand, particles in biosolids slurries tend to settle. Using sewage sludge slurries and biosolids for HTL applications will require higher solid loadings, which have great potentials of possessing high viscosities that will be confirmed through offline viscosity measurements. The anchor and helical impellers are suitable for viscosity measurements of viscous fluids (Jo et al., 2017). Solids that originate from the inorganic composition of sludge and solid intermediate products produced during HTL have a great tendency to settle in the reactor vessel without agitation. The anchor impeller can be suitable as it gives a tangential flow of fluid in the vessel, thereby keeping the fluid homogeneous. Anchor impellers are suitable for viscosity measurement in settling slurries. This is due to the small clearance between the anchor impeller blades and the mixing vessel walls, which reduces the unyielding zone over the vessel and keeps the slurry homogeneous throughout the measuring process, thus reducing the settling rate of the particles.

The anchor impeller is a U-Shaped 2-bladed impeller. In sizing the anchor impeller, the clearance between the impeller and the vessel walls should be big enough to accommodate larger particles of the sample to reduce measuring errors and small enough to reduce the formation of dead zones around the walls of the vessel. The most challenging task in using such a geometric impeller is transforming the measured torque and shaft speed into shear stress and shear rate values. The fluid properties may be derived after several experiments and data analysis to determine the geometric and shear constants essential for viscosity estimation using various methods for viscosity determination.

2.5.2. Methods of mixer-type rheometry

Viscosity in mixer-type rheometers is estimated using a measure of torque on the impeller shaft at a given rotational speed. Impeller torque and speed data can be converted into fluid viscosity using the Couette and Metzner-Otto methods. Each method uses the impeller and cylindrical vessel's geometrical parameters to determine the rheological constants of shear rate and shear stress for viscosity estimation.

2.5.2.1.Couette

Couette analogy can be adopted in any reactor configuration with an impeller attachment using power predictions of agitated vessels containing non-Newtonian fluid and obeying the power-law model (Choplin & Marchal, 2010). Couette analogy is applicable in both batch and continuous systems where the mixing device in a vessel is assumed to be a virtual cylindrical bob**.**

The Couette analogy concept is used to interpret data obtained from the measurements on the anchor impeller's speed and torque following the approach of Aït-Kadi et al. (2002). Aït-Kadi et al. (2002) applied correlations of different geometries of mixers in an agitated vessel using Couette's analogy. They determined the internal radius, R_i, of the mixing device by relating it

to the radius of the cylindrical vessel (R_e), length of the mixing chamber (L), impeller rotational speed (N), torque on the impeller shaft (M), consistency index (k), gear ratio (g) and the flow index (n) of the power law model in the following equation:

$$R_i = \frac{R_e}{\left[1 + \frac{4\pi N}{n}\left(2\pi k L {R_e}^2 \frac{1+g^{n+1}}{M}\right)^{\frac{1}{n}}\right]^{\frac{n}{2}}} \tag{8}$$

In the Couette theorem, the impeller's internal radius represents the equivalent diameter of a concentric cylinder as used in the cup and bob geometry of conventional rheometers (Bbosa et al., 2017). The shear rate/shear stress data was then determined at a given position gap. The radius for the optimal position (r) for a small gap where $(R_e\text{-}R_i)/R_e$ <<1 was estimated by equation 9.

$$r = \frac{R_i + R_e}{2} \tag{9}$$

Shear rate (γ) at the optimal position can be computed as the product of the shear rate constant (k_γ) and the impeller speed in the following relation:

$$\dot{\gamma}(r) = k_\gamma \cdot N = \frac{4\pi}{n} \frac{\left(\frac{R_e}{r}\right)^{\frac{2}{n}}}{\left(\frac{R_e}{R_i}\right)^{\frac{2}{n}} - 1} \cdot N \tag{10}$$

Shear stress was estimated as a product of the shear stress constant and the torque on the impeller shaft at specific impeller rotational speeds using equation 11.

$$\tau = k_\tau \cdot M = \frac{1}{2\pi r^2 L} \cdot M \tag{11}$$

The fluid's viscosity is a quotient obtained from dividing the shear stress data by the corresponding shear rate data.

2.5.2.2.Metzner Otto

Metzner and Otto proposed a concept that relates the mean shear rate to the rotational speed of an impeller where shear rate is directly proportional to the impeller speed and the constant of proportionality is the Metzner-Otto constant, ks (Jo et al., 2017; Luan et al., 2014). This constant depends on the shape of the impeller and the tank's geometry but independent of the fluid properties. The Metzner and Otto concept works for determining the apparent viscosities of both Newtonian and non-Newtonian fluids using the power consumption (*P*), and dimensionless numbers such as Power number (N_P) and the impeller Reynolds number (*Re*).

The power consumption of the anchor impeller using a Newtonian viscosity standard is estimated using equation 12 (Luan et al., 2014)

$$P = 2\pi NM \tag{12}$$

The power number for the Newtonian fluid is inversely related to the Reynolds number under laminar conditions in equation 13:

$$k_P = N_p Re \tag{13}$$

N_P and *Re* for a Newtonian fluid are functions of fluid density ρ, fluid viscosity η and the impeller diameter *D* as shown in equations 14 and 15.

$$N_P = \frac{P}{\rho N^3 D^5} \tag{14}$$

$$Re = \frac{\rho N D^2}{\eta} \tag{15}$$

The Herschel-Bulkley model can describe the rheological property of a non-Newtonian fluid viscosity standard:

$$\tau = \tau_y + k\dot{\gamma}^n \tag{16}$$

Where $\dot{\gamma}$, τ, k, n and τ_y represents shear rate, shear stress, consistency index, flow index and yield stress. The Metzner and Otto constant, k_s can be determined from the Reynolds number (Re^I) and the power constant ($N_P{}^I$) of the non-Newtonian fluid in equations 17 to 20:

$$N_P{}^{\mathrm{I}} = \frac{P}{\rho N^3 D^5} \tag{17}$$

$$Re^{\mathrm{I}} = \frac{\rho N^{(2-n)} D^2}{k} \tag{18}$$

$$k_p{}^{\mathrm{I}} = N_P Re^{\mathrm{I}} \tag{19}$$

$$k_s = \left(\frac{k_{pn}}{k_p}\right)^{\frac{1}{n-1}} \tag{20}$$

Alternatively, *ks* can be determined using the effective shear rate relation which is derived from the effective viscosity and effective Reynolds number using the power-law model for a non-Newtonian fluid as shown in equations 21 to 25 (Jang et al., 2019):

$$Re_{eff} = \frac{N_p}{K_p} \tag{21}$$

$$\eta_{eff} = \frac{\rho N D^2}{Re_{eff}} \tag{22}$$

$$\eta_{eff} = \frac{\rho N D^2}{Re_{eff}} = k\gamma_{eff}{}^{n-1} \tag{23}$$

$$\gamma_{eff} = \left(\frac{\eta_{eff}}{k}\right)^{1/n-1} \tag{24}$$

$$\gamma_{eff} = k_s N \tag{25}$$

The torque (M) on the impeller shaft is related to the equivalent diameter in equation 26 (Bbosa et al., 2017)

$$d_e = D * \left[1 + \frac{2\omega}{n}\left(\frac{\pi h K {D_v}^2}{2M}\right)^{\frac{1}{n}}\right]^{-n/2} \quad (26)$$

Where ω, h and D_v represents the rotational speed of the impeller, effective immersed length of impeller height and vessel diameter. The shear stress constant can be estimated using the properties of the Newtonian fluid and the geometry of the impeller using equation 27, which is similar to equation 11:

$$k_\tau = \frac{2}{\pi h {d_e}^2} \quad (27)$$

The viscosity of the fluid is estimated by

$$\eta = \frac{k_\tau M}{k_s N} \quad (28)$$

In-situ viscosity measurements can be conducted by converting the measured torque and rotational speed to shear stress and shear rate data using the Couette principle and the Metzner-Otto analogy. However, these viscosity measuring methods have not been applied to HTL feedstock under subcritical water conditions. The viscosity of reacting slurries is yet to be investigated under subcritical water conditions during the HTL of biomass feedstock.

2.6. Viscosity variation of feedstock during HTL

Sewage sludge contains organic component (lipids, proteins, carbohydrates and lignin) and inorganics (clays and minerals) that reacts in the presence of pressurised water to produce HTL products at elevated temperatures. The various components of the feedstock sludge can contribute to the formation of specific compounds due to peculiar interactions and reactions that occur at a given reaction condition. The changes in the viscosity of the reacting feedstock under different reaction conditions are yet to be quantified. It would be interesting to understand how the viscosity of the HTL sludge feedstock changes with temperature and

pressure to produce the four fraction products (aqueous, solids, gas and crude-like oil products) under HTL conditions. It is important to elucidate and quantify the viscosity variations of reacting feedstock during HTL as viscosity is a major parameter in transport phenomena and heat transfer analysis, especially in the HTL reactors as shown in Figure 3. Knowledge of the energy required in transporting and heating the slurry is vital for design purposes as well as cost analysis of the HTL plant design. This information will not be limited to HTL applications, but it would be useful in other thermochemical systems.

2.6.1. Selection of model compounds

To fully elucidate the viscosity changes in sludge, it will be useful to understand the viscosity changes of the individual components of sludge. This information will be applicable to other biomass feedstock, which comprises variable compositions of lipids, protein, carbohydrates, and lignin to elucidate the bulk slurry changes at different reaction conditions.

There is significant scientific research on the HTL reaction mechanism, kinetics, and the effects of process conditions using models of lipids, proteins, carbohydrates, and lignin in biomass. Sunflower oil, soy protein and granulated sugar are models for lipids, proteins and carbohydrates that have been extensively studied and readily available (Gollakota & Savage, 2018; Luo et al., 2015; Obeid et al., 2019; Sheehan & Savage, 2016). Other researchers have also investigated on the process optimisation and reaction kinetics of mixtures of model compounds to mimic the actual biomass (Gollakota & Savage, 2018; Lu et al., 2018; Lu et al., 2020; Obeid et al., 2020). However, there is no information on the thermophysical changes, particularly viscosity changes, of model compound feedstock slurry during HTL under subcritical water conditions. The viscosity variations of individual models, binary and ternary mixtures of model compounds under different HTL reaction temperatures and pressures are yet to be investigated. This information will be useful for fundamental studies. Furthermore,

viscosity variations of mixtures of model compounds will be essential in predicting the viscosity variations in actual biomass.

2.6.2. Selection of no-lignin biomass

The organic fraction of sewage sludge contains <30% of lignin (Goto et al., 1999; Hattori & Mukai, 1986; Su et al., 2015). The effects of lignin cannot be ignored in the viscosity variations of sludge feedstock. There is a significant number of scientific literatures on HTL of alkaline lignin which is a common model for lignin macromolecule (Alhassan et al., 2020; Cao et al., 2020; Lyckeskog, 2016; Peng et al., 2019; Schuler et al., 2017). However, there is currently no information on the viscosity changes of reacting pure lignin feedstock during the HTL process. At room conditions, lignin is largely insoluble in water. When lignin model compounds are mixed with water, they form a sticky paste that sticks to the containing vessel walls and the stirrer (Schulze et al., 2019). The sticky nature of lignin makes viscosity estimation using the torque and rotational speed measurements of the impeller very difficult, especially at lower temperatures. Due to the small clearance (gap) between the bottom of the anchor impeller and the reactor vessel, viscosity measurements will be challenging with lignin slurry unless a different impeller configuration is used. Nonetheless, the effects of lignin on the viscosity changes in sewage sludge feedstock can be analysed by comparing the viscosity changes in a 'no-lignin containing' biomass to the viscosity changes in sewage sludge and the viscosity variations in mixtures of model compounds that mimic the composition of each actual biomass (sewage sludge and no-lignin containing biomass). Microalgae is a suitable HTL feedstock due to its high protein and lipid composition that increases crude-like oil yields. Microalgae have been extensively studied in scientific literature and can be considered a no-lignin containing biomass (Barreiro et al., 2015; Djandja et al., 2020; Elliott et al., 2013; Gu et al., 2020; Tian et al., 2017). The viscosity changes in microalgae during HTL under subcritical conditions is yet to be investigated.

2.6.3. Factors affecting viscosity variation

Viscosity of reacting fluids depends on pressure, temperature, shearing forces from the impeller during agitation, phase changes, and products' composition. Fluids consist of molecules held together by intermolecular bonds and attractive forces. When fluids are heated up, the fluid molecules attain energy and begin to move. These molecules' movement commences when the attained energy exceeds the bond energy that initially kept the molecules in their initial positions. When molecules move apart from each other, there is less resistance to the fluid's free flow, and this reduces in the internal frictional forces between these molecules. Consequently, viscosity, which is the measure of the resistance to flow in fluids decreases with an increase in temperature, and this is typical for liquids. Nonetheless, biomass viscosity under subcritical conditions may be challenging to predict due to the combined effect of pressure and temperature.

The formation of intermediates and products during HTL can greatly affect the viscosity of the reacting slurry. The presence of solids, the production of crude-like oil, the appearance and disappearance of certain chemical compounds in the product stream can influence the viscosity changes in a reacting slurry as the presence solids, and high molecular weighted compounds increase viscosity. However, the formation of these products may behave differently at elevated temperatures and pressures. Thus, the viscosity of reacting sludge slurry cannot be easily predicted.

HTL involves a series of multiple reactions that occur under different process conditions of temperature, pressure and shear influence. There is currently no scientific literature that explains the effect of pressure, temperature, agitation, phase change and chemical speciation of reacting biomass on the changes in viscosity under subcritical water conditions during HTL. An investigation on the effects of temperature, pressure, agitation and product formation during HTL of sewage sludge feedstock under subcritical water conditions is yet to be assessed.

2.7. Implication and significance of the current study

HTL of sewage sludge has been widely studied on different scales (laboratory and pilot plants). This process is viable for simultaneous waste management and energy recovery. However, there is currently no industry commercialising this viable process using sewage sludge due to insufficient scale-up data. Scaling up such a chemical engineering plant requires vital information on the feedstock for the reactor and pipeline design purposes. Viscosity is an important feedstock property that affects the flow processes in a chemical plant. Fluid viscosity can also be used in estimating heat transfer properties for equipment design. Hence, knowledge of the process fluid's viscosity is essential for pipeline, pump and reactor design in an HTL Biorefinery and other similar chemical engineering plants.

One major challenge with using sewage sludge, particularly biosolid as an HTL feedstock, is the feedstock's complexity. There is insufficient information in the scientific literature on the characteristics of concentrated sludge slurries (>10% dry solid concentration) under pressure. Most investigations on the rheological characterisation of sewage sludge are limited to dilute sludge slurries at atmospheric conditions for WWTP applications. The feedstock's rheological properties at room temperatures help determine the design parameters for feedstock flow in pipeline and pumps (before HTL).

Knowledge of the variations in the viscosity of reacting sludge slurries during HTL under subcritical condition is vital for heat transfer calculations necessary for the reactor design. The viscosity data is also useful for process control and monitoring during plant operations. Sludge is a complex feedstock that comprises of different macromolecules. The macromolecules in sludge can be mimicked by using model compounds. Elucidating the changes in the apparent viscosity of slurries of model compounds and mixtures of model compounds aids in predicting the rheological behaviour of actual biomass under subcritical conditions.

Viscosity data can be fed directly into a CFD model to analyse and describe the engineering system's behaviour, optimise and simulate the fluid flow and heat transfer through the application of fundamental laws of mechanics and heat transfer to the slurry in order to scale up to industrial level. A CFD model, similar to the one developed by Chen et al. (2020), will require detailed and relevant input variables and process operation data for HTL of sewage sludge and biosolids, which involve fluid flow, pumping energy, chemical reactions, kinetics, material and heat transfer processes.

2.8. Objectives of the thesis

This study aims to quantify sludge feedstock characteristics before and during HTL to determine the flow and heating properties for design purposes and process monitoring. This aim will be achieved by completing the following objectives:

a. To characterise biosolid slurries for improved material transport and pumping of HTL feedstock in upstream processes of biorefineries.

b. To determine the rheological properties of different types of sewage sludge slurries obtained from different parts of the WWTPs.

c. To elucidate viscosity variations in feedstock slurries during HTL of model compounds under subcritical water conditions.

d. To quantify viscosity changes in sewage sludge slurries as a function of reaction temperature at elevated pressures.

2.9. References

Aït-Kadi, A., Marchal, P., Choplin, L., Chrissemant, A.-S., & Bousmina, M. (2002). Quantitative Analysis of Mixer-Type Rheometers using the Couette Analogy. *The Canadian Journal of Chemical Engineering*, *80*, 1166-1174.

Akhtar, J., & Amin, N. A. S. (2011). A review on process conditions for optimum bio-oil yield in hydrothermal liquefaction of biomass. *Renewable and Sustainable Energy Reviews, 15*, 1615-1624.

Alhassan, Y., Hornung, U., & Bugaje, I. M. (2020). Lignin Hydrothermal Liquefaction into Bifunctional Chemicals: A Concise Review. In V. Beschkov (Ed.), *Biorefinery Concepts, Energy and Products*.

Anthony III, J. R. (2015). *Hydrothermal Liquefaction of Municipal Sludge and Biosolids.* (Master of Science in Engineering), The University of Texas at Austin, Austin.

Australian and New Zealand Biosolids Partnership, A. (2020). *Australian Biosolids Statistics*. Australia: Australian Water Association Retrieved from https://www.biosolids.com.au/guidelines/australian-biosolids-statistics/.

Australian Government,A. (2021). *Recycling and Clean Energy. National Manufacturing Priority Road Map*. Retrieved from https://www.industry.gov.au/data-and-publications/recycling-and-clean-energy-national-manufacturing-priority-road-map

Australian Water Association, A. (2012). *The Management of Biosolids in Australia*. Retrieved from https://www.awa.asn.au/Documents/Position_Paper_Biosolids.pdf.

Balaman, S. Y. (2019). Biomass-Based Production Systems. *Decision-Making for Biomass-Based Production Chains* (pp. 25-54): Academic Pres.

Barnes, H. A., Hutton, J. F., & Walters, K. (1989). *An Introduction to Rheology* (Vol. 3). UK: Elsevier.

Barreiro, L. D., Gómez, B. R., Hornung, U., Kruse, A., & Prins, W. (2015). Hydrothermal Liquefaction of Microalgae in a Continuous StirredTank Reactor. *Energy & Fuels, 29*, 6422-6432.

Baudez, J. C., Ginisty, P., Peuchot, C., & Spinosa, L. (2007). The preparation of synthetic sludge for lab testing. *Water Science and Technology, 56*(9), 67-74.

Bbosa, B., DelleCase, E., Volk, M., & Ozbayoglu, E. (2017). Development of a mixer-viscometer for studying rheological behavior of settling and non-settling slurries. *J Petrol Explor Prod Technol, 7*, 511-520.

Biller, P., Johannsen, I., dos Passos, J. S., & Ottosen, L. D. M. (2017). Primary sewage sludge filtration using biomass filter aids and subsequent hydrothermal co-liquefaction. *Water Research, 130*, 58-68.

Brown, C., Ellson, A., Ledger, R., Sorensen, G., Cunliffe, D., Simon, D., McManus, M., Schrale, G., McLaughlin, M., Warne, M., Liston, C., M, M., Sickerdick, L., Desmier, R., & Smith, G. (2017). *Draft - South Australian Biosolids Guidelines for the safe handling and reuse of biosolids*. Adelaide.

Cao, X., Jiang, Z., Cui, W., Wang, Y., & Yang, P. (2016). Rheological properties of municipal sewage sludge: dependency on solid concentration and temperature. *Procedia Environmental Sciences, 31*, 113-121.

Cao, Y., Zhang, C., Tsang, D. C. W., Fan, J., Clark, J. H., & Zhang, S. (2020). Hydrothermal Liquefaction of Lignin to Aromatic Chemicals: Impact of Lignin Structure. *Industrial & Engineering Chemistry Research, 59*, 16957-16969.

Castello, D., Pedersen, H. T., & Rosendahl, L. A. (2018). Continuous Hydrothermal Liquefaction of Biomass: A Critical Review. *Energies, 11*(3165).

Castello, D., Haider, M. S., & Rosendahl, L. A. (2019). *Catalytic Upgrading of Hydrothermal Liquefaction Biocrudes: Different challenges for different feedstock. Renewable Energy, 141*,420-430.

Chen, X., Tian, Z. F., Van Eyk, P. J., Lewis, D., & Nathan, G. G. J. (2020). *Numerical simulation of hydrothermal liquefaction of algae in a lab-scale coil reactor*. (ECMF-2020-0057).

Choplin, L., & Marchal, P. (2010). Mixer-type rheometer. In C. Gallegos (Ed.), *Rheology* (Vol. II, pp. 32-51). United Kingdom: Encyclopedia of Life Support Systems.

Collett, C., Ardon, A., Bauer, U., Chapman, G., Chaudan, E., Hallmark, B., Pratt, L., Torres-Perez, M. D., & Wilson, D. I. (2015). A portable extensional rheometer for measuring the viscoelasticity of pitcher plant and other sticky liquids in the field. *Plant Methods, 11*(16). doi: 10.1186/s13007-015-0059-5

Darvodelsky, P. (2011). *Biosolids Snapshot*. New South Wales.

Djandja, O. S., Wang, Z., Chen, L., Qin, L., Wang, F., Y., X., & Duan, P. (2020). Progress in Hydrothermal Liquefaction of Algal Biomass and Hydrothermal Upgrading of the Subsequent Crude Bio-Oil: A Mini Review. *Energy & Fuels, 34*, 11723-11751.

Eboibi, B. E., Lewis, D. M., Ashman, P. J., & Chinnasamy, S. (2014). *Effect of operating conditions on yield and quality of biocrude during hydrothermal liquefaction of halophytic microalga Tetraselmis sp.* Bioresour Technol.

Ebrahimi, A., Bandari, M., & Parvari, M. (2009). Effect of Mixer Rotational Speed on Heat Transfer Coefficient in Preparation of Nickle Perovskite From Laboratory to Bench Scale. *Iranian Journal of Chemical Engineering, 6*(3).

Elliott, D. C., Biller, P., Schmidt, A. J., & Jones, S. B. (2015). Hydrothermal liquefaction of biomass: Developments from batch to continuous process. *Bioresour Technol, 178*, 147-156.

Elliott, D. C., Hart, T. R., Schmidt, A., Neuenschwander, G. G., Rotness, L. J., Olarte, M. V., Zacher, A. H., Albrecht, K., Hallen, R. T., & Holladay, J. E. (2013). Process development for hydrothermal liquefaction of algae feedstocks in a continuous-flow reactor. *Algal Research, 2*, 445-454.

Environmental Protection Agency, E. P. A. (1998). How Wastewater Treatment Works...The basics. U.S.

Gollakota, A., & Savage, P. E. (2018). Hydrothermal Liquefaction of Model Food Waste Biomolecules and Ternary Mixtures under Isothermal and Fast Conditions. *Sustainable Chemistry & Engineering, 6*, 9018-9027.

Goloshevsky, A. G., Walton, J. H., Shutov, M. V., de Ropp, J. S., Collins, S. D., & McCarthy, M. J. (2005). Nuclear magnetic resonance imaging for viscosity measurements of nonNewtonian fluids using a miniaturized RF coil. *Measurement Science and Technology, 16*, 513-518. doi: 10.1088/0957-0233/16/2/025

Goto, M., Nada, T., Kodama, A., & Hirose, T. (1999). Kinetic Analysis for Destruction of Municipal Sewage Sludge and Alcohol Distillery Wastewater by Supercritical Water Oxidation. *Industrial & Engineering Chemistry Research, 38*, 1863-1865. doi: 10.1021/ie980479s

Gu, X., Martinez-Fernandez, J. S., Pang, N., Fu, X., & Chen, S. (2020). Recent development of hydrothermal liquefaction for algal biorefinery. *Renewable and Sustainable Energy Reviews, 121*.

Hattori, H., & Mukai, S. (1986). Decomposition of Sewage Sludges in Soil as Affected by their Organic Matter Composition. *Soil Science and Plant Nutrition, 32*(3), 421-432.

Hess, H. V., & Cole, E. L. (1973). United States Patent No.

Itoh, S., Suzuki, A., Nakamura, T., & Yokoyama, S. (1994). Production of heavy oil from sewage sludge by direct thermochemical liquefaction. *Desalination, 98*, 127-133.

Jang, H. K., Hong, S. O., Lee, S. B., Kim, J. M., & Hwang, W. R. (2019). Viscosity measurement of non-Newtonian fluids in pressure-driven flows of general geometries based on energy dissipation rate. *Journal of Non-Newtonian Fuid Mechanics, 274*.

Jazrawi, C., Biller, P., Ross, A. B., Montoya, A., Maschmeyer, T., & Haynes, B. S. (2013). Pilot plant testing of continuous hydrothermal liquefaction of microalgae. *Algal Research*, 268-277.

Jo, H. J., Jang, H. K., Kim, Y. J., & Hwang, W. R. (2017). Process viscometry in flows of non-Newtonian fluids using an anchor agitator. *Korea-Australia Rheology Journal, 29*(4), 317-323.

Khan, I., & Kabi, Z. (2020). Waste-to-energy generation technologies and the developing economies: A multi-criteria analysis for sustainability assessment. *Renewable Energy, 150*, 320-333.

Khoshnevisan, B., Tabatabaei, M., Tsapekos, P., Rafiee, S., Aghbashlo, M., Lindeneg, S., & Angelidaki, I. (2020). Environmental life cycle assessment of different biorefinery platforms valorizing municipal solid waste to bioenergy, microbial protein, lactic and succinic acid. *Renewable and Sustainable Energy Reviews, 117*.

Leonie, M., & Graeme, K. (2009). *Use of biosolids in agriculture*. New South Wales.

Loomis, P. (2014). *Biosolids and Energy Process Development at the Blue Plains AWTP*. Paper presented at the NJWEA Annual Conference Biosolids Workshop.

Lu, J., Liu, Z., Zhang, Y., & Savage, P. E. (2018). Synergistic and Antagonistic Interactions during Hydrothermal Liquefaction of Soybean Oil, Soy Protein, Cellulose, Xylose, and Lignin. *Sustainable Chemistry & Engineering, 6*, 14501-14509. doi: 10.1021/acssuschemeng.8b03156

Lu, P., Shu, D., Chi, Y., Chen, D., & Zeng, H. (2020). Interactions Between Carbohydrate and Protein During Hydrothermal Liquefaction of Food Waste. *Environmental Engineering Science, 00*(00). doi: 10.1089/ees.2020.0204

Luan, D., Chen, Q., & Zhou, S. (2014). Numerical Simulation and Analysis of Power Consumption and Metzner-Otto Constant for Impeller of 6PBT. *Chinese Journal of Mechanical Engineering, 27*(3), 635-640. doi: 10.3901/CJME.2014.03.635

Luo, L., Dai, L., & Savage, P. E. (2015). Catalytic Hydrothermal Liquefaction of Soy Protein Concentrate. *Energy & Fuels, 29*, 3208−3214. doi: 10.1021/acs.energyfuels.5b00321

Lyckeskog, H. N. (2016). *Hydrothermal Liquefaction of Lignin into Bio-Oil. Influence of the Reaction Conditions and Stability of the Bio-Oil Produced.* (Doctor of Philosophy), Chalmers University of Technology, Gothenburg, Sweden. (27753305)

Marrone, P. (2016). *Genifuel Hydrothermal Processing Bench-Scale Technology, Evaluation Report* (Vol. LIFT6T14): IWA Publishing.

Marrone, P. A., Elliott, D. C., Billing, J. M., Hallen, R. T., Hart, T. R., Kadota, P., Moeller, J. C., Randel, M. A., & Schmidt, A. J. (2018). Bench-Scale Evaluation of Hydrothermal Processing Technology for Conversion of Wastewater Solids to Fuels. *Water Environment Research, 90*(4), 329-342. doi: 10.2175/106143017X15131012152861

Metcalf, & Eddy. (2003). Wastewater engineering-Treatment and Reuse *Waste Management* (4th ed.). New York: McGraw Hill.

Mukherjee, C., Denney, J., Mbonimpa, E. G., Slagley, J., & Bhowmik, R. (2020). A review on municipal solid waste-to-energy trends in the USA. *Renewable and Sustainable Energy Reviews, 119*.

National Research Council, Division on Earth and Life Studies, Environmental and Resources Commission on Geosciences, & Consumption, C. o. t. U. o. T. M. W. E. a. S. i. t. P. o. C. f. H. (1996). Municipal Wastewater and Sludge Treatment *Use of Reclaimed Water and Sludge in Food Crop Production* (pp. 45-60). Washington, D.C: National Academy Press.

Nazari, L. (2016). *Hydrothermal Liquefaction of High-Water Content Biomass and Waste Materials for the Production of Biogas and Bio-Crude Oil.* (Doctor of Philosopy), The University of Western Ontario, Canada.

Nazari, L., Yuan, Z., Ray, M. B., & Xu, C. (2017). Co-conversion of waste activated sludge and sawdust through hydrothermal liquefaction: Optimization of reaction parameters using response surface methodology. *Applied Energy, 203*, 1-10.

Noguchi, T., Noda, Y., Yamasaki, Y., Inoue, S., Matsumura, Y., Kawai, Y., Shimizu, Y., & Minowa, T. (2011). The Rheological Characteristics of Biomass Slurry under High Pressure and High Temperature. *Journal of the Japan Institute of Energy, 90*.

Obeid, R., Lewis, D., Smith, N., & Van Eyk, P. (2019). The elucidation of reaction kinetics for hydrothermal liquefaction of model macromolecules. *Chemical Engineering Journal, 370*, 637-645.

Obeid, R., Lewis, D. M., Smith, N., Hall, T., & van Eyk, P. (2020). Reaction Kinetics and Characterization of Species in Renewable Crude from Hydrothermal Liquefaction of Mixtures of Polymer Compounds To Represent Organic Fractions of Biomass Feedstocks. *Energy & Fuels, 34*(1), 419-429.

Okutani, T., Yokoyama, S., & Maekawa, Y. (1980). Viscosity of coal paste under high hydrogen pressure. *Fuel, 59*.

Park, S. J., Bae, J. S., Lee, D. W., Ra, H. W., Hong, J. C., & Choi, Y. C. (2011). Effects of Hydrothermally Pretreated Sewage Sludge on the Stability and Dispersibilty of Slurry Fuel Using Pulverized Coal. *Energy & Fuels, 25*, 3934-3939.

Peng, C., Zhang, G., Han, J., & Li, X. (2019). Hydrothermal conversion of lignin and black liquor for phenolics with the aids of alkali and hydrogen donor. *Carbon Resources Conversion, 2*, 141-150. doi: doi.org/10.1016/j.crcon.2019.06.004

Pöykiö, R., Watkins, G., & Dahl, O. (2019). Characterisation of Municipal Sewage Sludge as a Soil Improver and a Fertilizer Product. *Ecol. Chem. Eng S., 26*(3), 547-557. doi: 10.1515/eces-2019-0040

Rajasekhar Reddy, B., & Vinu, R. (2018). Feedstock Characterization for Pyrolysis and Gasification. In S. De, A. K. Agarwal, V. S. Moholkar, & B. Thallada (Eds.), *Coal and Biomass Gasification: Recent Advances and Future Challenges* (pp. 3-36). Singapore: Springer Singapore.

Ranieri, E., Leverenz, H., & Tchobanoglous, G. (2011). An Examination of the Factors Involved in Agricultural Reuse: Technologies, Regulatory and Social Aspects. *Journal of Water Resource and Protection, 3*, 300-310. doi: 10.4236/jwarp.2011.35038

Rolsky, C., Kelkar, V., Driver, E., & Halden, R. U. (2020). Municipal sewage sludge as a source of microplastics in the environment. *Current Opinion in Environmental Science & Health, 14*, 16-22.

Schelden, M., Lima, W., Doerr, E. W., Wunderlich, M., Rehmann, L., Buchs, J., & Regestein, L. (2017). Online measurement of viscosity for biological systems in stirred tank bioreactors. *Biotechnol Bioeng*, *114*(5), 990-997. doi: 10.1002/bit.26219

Schuler, J., Hornung, U., Kruse, A., Dahmen, N., & Sauer, J. (2017). Hydrothermal Liquefaction of Lignin. *Journal of Biomaterials and Nanobiotechnology, 8*, 96-108. doi: 10.4236/jbnb.2017.81007

Schulze, P., Leschinsky, M., Seidel-Morgenstern, A., & Lorenz, H. (2019). Continuous Separation of Lignin from Organosolv Pulping Liquors: Combined Lignin Particle Formation and Solvent Recovery. *Industrial & Engineering Chemistry Research, 58*, 3797−3810. doi: 10.1021/acs.iecr.8b04736

Shah, A. A., Toor, S. S., Conti, F., Nielsen, A. H., & Rosendahl, L. A. (2020). Hydrothermal liquefaction of high ash containing sewage sludge at sub and supercritical conditions. *Biomass and Bioenergy, 135*.

Shakya, R., Whelen, J., Adhikari, S., Mahadevan, R., & Neupane, S. (2015). Effect of temperature and Na 2 CO 3 catalyst on hydrothermal liquefaction of algae. *Algal Research, 12*, 80-90. doi: 10.1016/j.algal.2015.08.006

Sharma, S., Basu, Shetti, N. P., & Aminabhavi, T. M. (2020). Waste-to-energy nexus for circular economy and environmental protection: Recent trends in hydrogen energy. *Science of the Total Environment, 713*.

Sheehan, J. D., & Savage, P. E. (2016). Products, Pathways, and Kinetics for the Fast Hydrothermal Liquefaction of Soy Protein Isolate. *Sustainable Chemistry & Engineering, 4*, 6931−6939. doi: 10.1021/acssuschemeng.6b01857

Sintamarean, I. M., Pedersen, T. H., Zhao, X., Kruse, A., & Rosendahl, L. A. (2017). Application of Algae as Cosubstrate To Enhance the Processability of Willow Wood for Continuous Hydrothermal Liquefaction. *Industrial & Engineering Chemistry Research, 56*(15), 4562-4571. doi: 10.1021/acs.iecr.7b00327

Skaggs, R. L., Coleman, A. M., Seiple, T. E., & Milbrandt, A. R. (2017). Waste-to-Energy biofuel production potential for selected feedstocks in the conterminous United States. *Renewable and Sustainable Energy Reviews*.

Snowden-Swan, L. J., Zhu, Y., Jones, S. B., Elliott, D. C., Schmidt, A. J., Hallen, R. T., Billing, J. M., Hart, T. R., Fox, S. P., & Maupin, G. D. (2016). Hydrothermal Liquefaction and Upgrading of Municipal Wastewater Treatment Plant Sludge: A Preliminary Techno-Economic Analysis.

Spellman, F. R. (1996). Wastewater Biosolids to Compost. Retrieved 07/09/2017 https://books.google.com.au/books?id=MQ1AOJgFVWcC&pg=PA16&lpg=PA16&dq=with+total+solids+of+2500ppm&source=bl&ots=iwRk0Ur7g6&sig=EeOtfJUdkNXg3EU914VgBCFG1sU&hl=en&sa=X&ved=0ahUKEwium8PopJLWAhUDW7wKHbH1BF4Q6AEIMzAC#v=onepage&q=with%20total%20solids%20of%202500ppm&f=false

Su, Y., Zhu, W., Gong, M., Zhou, H., Fan, Y., & Amuzu-Sefordzi, B. (2015). Interaction between sewage sludge components lignin (phenol) and proteins (alanine) in supercritical water gasification. *International Journal of Hydrogen Energy, 40*, 9125-9136. doi: 10.1016/j.ijhydene.2015.05.072

Tan, P., & Li, Z. (2017). *Reducing Sludge Viscosity and Improving Dewaterability through a Thermochemical Hydrolysis Process*. Paper presented at the WEF Residuals and Biosolids Conference

Tian, C., Liu, Z., & Zhang, Y. (2017). Hydrothermal Liquefaction (HTL): A Promising Pathway for Biorefinery of Algae. *Algal Biofuels*, 361-391. doi: 10.1007/978-3-319-51010-1_18

Toor, S. S., Rosendahl, L., & Rudolf, A. (2011). Hydrothermal liquefaction of biomass: A review of subcritical water technologies. *Energy, 36*(5), 2328-2342. doi: 10.1016/j.energy.2011.03.013

Vardon, D. R., Sharma, B. K., Scott, J., Yu, G., Wang, Z., Schideman, L., Zhang, Y., & Strathmann, T. J. (2011). Chemical properties of biocrude oil from the hydrothermal liquefaction of Spirulina algae, swine manure, and digested anaerobic sludge. *Bioresour Technol, 102*, 8295-8303.

Vergara-Araya, M., Lehn, H., & Poganietz, W.-R. (2020). Integrated water, waste and energy management systems – A case study from Curauma, Chile. *Resources, Conservation & Recycling, 156*.

Wang, C., Hu, X., Chen, M.-L., & Wu, Y.-H. (2005). Total concentrations and fractions of Cd, Cr, Pb, Cu, Ni and Zn in sewage sludge from municipal and industrial wastewater treatment plants. *Journal of Hazardous Materials, 119*, 245-249.

Water Environment Federation. (2012). *Solids Process Design and Management*. Europe: McGraw-Hill Education.

Wolny, L., Wolski, P., & Zawieja, I. (2008). Rheological parameters of dewatered sewage sludge after conditioning. *Desalination, 222*(1), 382-387.

Wunderlich, M., Trampnau, P., Lopes, E. F., Büchs, J., & Regestein, L. (2006). Online in situ viscosity determination in stirred tank reactors by measurement of the heat transfer capacity. *Chemical Engineering Science, 152*, 116-126.

Xu, C., & Lancaster, J. (2009). Treatment of Secondary Sludge for Energy Recovery. *Treatment of Secondary Pulp and Paper Sludge for Energy Recovery*.

Yang, J. T. (1961). The Viscosity of Macromolecules in Relation to Molecular Conformation. *Advances in protein chemistry, 16*, 323-400.

Yokoyama, S., Kuriyagawa, M., Ogi, T., Kobayashi, H., Minowa, T., Inoue, S., & Tenma, K. (1997). 5,681,449. Japan.

Zhang, Q., Hu, J., Lee, D. J., Chang, Y., & Lee, Y. J. (2017). Sludge treatment: Current research trends. *Bioresour Technol, 243*, 1159-1172. doi: 10.1016/j.biortech.2017.07.070

Chapter 3:

The influence of feedstock characteristics on processability of biosolid slurries for conversion to renewable crude oil via hydrothermal liquefaction

Statement of Authorship

Title of Paper	The influence of feedstock characteristics on processability of biosolid slurries for conversion to renewable crude oil via hydrothermal liquefaction
Publication Status	☑ Published ☐ Accepted for Publication ☐ Submitted for Publication ☐ Unpublished and Unsubmitted w ork w ritten in manuscript style
Publication Details	Edifor, S. Y., Van Eyk, P., Biller, P., & Lewis, D. M. (2020). The influence of feedstock characteristics on processability of biosolid slurries for conversion to renewable crude oil via hydrothermal liquefaction. Chemical Engineering Research and Design, 162, 284-294.

Principal Author

Name of Principal Author (Candidate)	Sylvia Yawa Edifor		
Contribution to the Paper	Designed Experiments Conducted experiments Data analysis and interpretation Drafted the manuscript and acted as corresponding author		
Overall percentage (%)	80		
Certification:	This paper reports on original research I conducted during the period of my Higher Degree by Research candidature and is not subject to any obligations or contractual agreements with a third party that would constrain its inclusion in this thesis. I am the primary author of this paper.		
Signature		Date	22/01/2021

Co-Author Contributions

By signing the Statement of Authorship, each author certifies that:

i. the candidate's stated contribution to the publication is accurate (as detailed above);
ii. permission is granted for the candidate in include the publication in the thesis; and
iii. the sum of all co-author contributions is equal to 100% less the candidate's stated contribution.

Name of Co-Author	Philip van Eyk		
Contribution to the Paper	Concept development Supervised development of work Assistance with interpretation, drafting and review of manuscript		
Signature		Date	28/1/2021

Name of Co-Author	Patrick Biller		
Contribution to the Paper	Assistance with interpretation and presentation of data Evaluating, editing and reviewing of manuscript		
Signature		Date	22.01.2021

Please cut and paste additional co-author panels here as required.

Name of Co-Author	David M. Lewis		
Contribution to the Paper	Concept development Supervised development of work Assistance with interpretation, drafting and reviewing manuscript		
Signature		Date	28/01/2021

Chemical Engineering Research and Design 162 (2020) 284–294

Contents lists available at ScienceDirect

Chemical Engineering Research and Design

journal homepage: www.elsevier.com/locate/cherd

The influence of feedstock characteristics on processability of biosolid slurries for conversion to renewable crude oil via hydrothermal liquefaction

Sylvia Y. Edifor[a,*], Philip van Eyk[a], Patrick Biller[b], David M. Lewis[a]

[a] School of Chemical Engineering & Advanced Materials, The University of Adelaide, 5005 Adelaide, SA, Australia
[b] Department of Engineering-Biological and Chemical Engineering, Aarhus University, 8200 Aarhus, Denmark

ARTICLE INFO

Article history:
Received 16 April 2020
Received in revised form 23 July 2020
Accepted 18 August 2020
Available online 24 August 2020

Keywords:
Hydrothermal liquefaction
Biosolids
Settling ability
Pumpability
Reactor design

ABSTRACT

Hydrothermal Liquefaction (HTL) is a moderate temperature-high pressure depolymerisation process that converts organics in wet biomass into crude-like oil. HTL feedstock properties and characteristics will influence the conversion of organics into crude-like oil and other by-products. The aim of the investigation is to quantify specific feedstock (biosolids) parameters to determine optimal feedstock properties for converting biosolids into crude-like oil. The properties of the feedstock which included moisture content, ash content, particle density, bulk density, porosity and particle size were analytically determined which are useful data for reactor design. The data presented in this study analyses the behaviour of biosolids using batch settling experiments and pumping studies. The influence of particle size and solid concentration of biosolid slurries on the processability in terms of stability and pumpability of the feedstock slurry was assessed. Biosolid slurries with 60 w/w% dry solids were determined to be the minimum solid concentration that demonstrated no visible settling characteristics within an observation period of 30 min. Pumpability was achieved with slurries between 30 w/w% to 60 w/w% dry biosolids using a laboratory scale peristaltic pump. Pumping power required to transport biosolid slurries increased exponentially with an increase in solid concentration.

1. Introduction

Hydrothermal liquefaction (HTL) offers the opportunity to produce an organic phase crude-like oil product that can be upgraded into liquid transportation fuels. HTL is a thermal decomposition process which exploits the properties of water at sub and super critical conditions (Jazrawi et al., 2013; Yin et al., 2010;Zhang et al., 2010) as a reactant, a medium for the reaction (Shakya et al., 2015;Zhang, 2010) and as a catalyst (Guo et al., 2010; Toor et al., 2011) by lowering the activation energy for specific reactions to occur (Biller and Ross, 2016). The complex reactions occurring in HTL are driven by the unique properties of water under subcritical conditions to break down complex organic molecules in biomass, reform intermediate products and rearrange single molecules under elevated temperatures and pressures to yield renewable crude oil, solids, gaseous and aqueous products. Renewable crude-like oil production via HTL under subcritical conditions has the potential to enhance energy security by producing fossil-like derived fuels (Biller and Ross, 2016), whilst offering sustainable management options for wet organic rich waste streams.

Municipal sewage sludge is a potential sustainable feedstock for renewable crude-like oil production via HTL due to its nutrient rich organic content. Sewage sludge in Waste Water Treatment Plants (WWTP) is further treated to reduce the moisture content and pathogen content to levels that can be safely applied to the environment with minimal environmental impacts. Treated sludge are also known as biosolids. Biosolids are obtained from the stabilisation of primary and secondary sludge from wastewater treatment

* Corresponding author.
E-mail address: sylvia.edifor@adelaide.edu.au (S.Y. Edifor).
https://doi.org/10.1016/j.cherd.2020.08.016

processes (Leonie and Graeme, 2009). Over the years, the production of stockpiled biosolids in WWTPs increases with an increase in population and urbanisation (Torri and Cabrera, 2017). Stockpiled biosolids do not only occupy land space but they also have the potential to release high amounts of greenhouse gases under anaerobic conditions (Darvodelsky, 2011). In countries like Australia, the cost of treating biosolids (dewatering, stabilisation and storage) is approximately $215 million of dry biosolids per annum (Darvodelsky, 2011). The wastewater industry is investigating inexpensive solutions to manage stockpiled biosolids using a cost effective solution. One solution to reduce the cost of waste management is by hydrothermal liquefaction. HTL of biosolids can be a suitable alternative to reduce large volumes of biosolid waste from WWTPs as opposed to the conventional management processes which includes land application, agricultural purposes, irrigation and incineration (Qian et al., 2017). HTL of biosolids is not only advantageous in the waste management industry through the reduction of about 50% sludge mass (Mulchandani and Westerhoff, 2016; Wang, 2011) while recovering >50% carbon (Marrone, 2016) but it is also promising for the energy sector through the production of renewable crude-like oil. However, there is very little information in scientific literature about the physical processing for biosolids for HTL applications.

Biosolid slurries are sand/clay-water like slurries which have great potentials of settling with time. Gravity settling of a reacting biosolid slurry during feedstock transportation and HTL process is greatly influenced by the nature and behaviour of the biosolids in a biosolid/water mixture. The settling characteristics and flow properties of biosolids are poorly understood and are yet to be assessed to determine the homogeneity and stability during transportation and reaction of biosolids in an HTL reactor. A detailed assessment of the behaviour of biosolid slurries for HTL applications has not been reported in scientific literature. In view of this, it is imperative to study the behaviour of biosolid slurries to be able to specify an optimal concentration as this data is needed to carry out an informed design of a HTL process. The optimal concentration should be stable during pumping through a piping system that connects the feedstock preparation unit to the reactor as well as through plug-flow reactors with the potential of maximising the conversion of renewable crude oil and maintaining a homogenous system. The optimal solid concentration will be that which improves slurry processability, slurry transportation and heat transfer processes in a plug-flow reactor.

The conversion of wet biomass feedstock into renewable crude-like oil via HTL provides an energetically advantageous option compared with other thermochemical processes such as pyrolysis and gasification as HTL negates an energy intensive drying process. Even though bypassing the drying process saves energy with HTL, the water handling requirement expends energy when the solid mass of the slurry is increased. Pumping of slurries require significant energy to overcome the frictional force and elevation, increase the fluid flow velocity and prevent clogging of pipelines during transportation (Shammas and Wang, 2008). Pumpability of a slurry is affected by solid concentration of the feedstock, bulk density and feedstock slurry viscosity which are functions of the particle size. Optimum particle size in reaction processes enhances solubility of reactants (Akhtar and Amin, 2011) and increase the contact area that increases the rate of chemical reactions. Size reduction is however costly and energy intensive, hence this may only be necessary depending on the type of feedstock (Elliott et al., 2015). The optimum concentration of biosolid slurry that is suitable for hydrothermal liquefaction is the specific concentration of biosolid slurries which is pumpable at a suitable viscosity, density and particle size that provides maximum yield and conversion during HTL. Hence there is a need to determine the optimum properties of the biosolids that simultaneously enhance processability in terms of transportation of the biosolids.

Pumping energy is vital for material transportation of the feedstock. Highly efficient pumps will be required to transport binary phase mixtures from a feedstock preparation unit to the HTL reactor during a continuous HTL process. Nonetheless, the energy consumed during pumping cannot be overlooked as it accounts for a significant percentage of the overall operational cost for renewable crude-like oil production via HTL of biosolid slurries. Hence the overall energy consumed and power required for slurry transportation needs to be estimated as it directly affects the cost of production, operations and maintenance in an HTL plant.

Given that organic-rich freshly treated sludge which yields high conversions and increased crude-like oil yields during HTL are readily pumpable in WWTP, aged biosolids are likely to be the poorest feedstock with challenges during slurry transport. Hence this study is based on biosolids, obtained at the last stage of the waste water treatment process which are likely difficult to transport in a slurry form. The investigation reported in this paper focuses on the quantification of the physical properties of the binary slurry of biosolids and water, in particular, quantifying the behaviour of the biosolid slurries in terms of slurry stability and pumpability. The physical and flow properties of biosolids is determined and the settling behaviour is analysed. The influence of particle size and solid concentration on the stability of the slurries is quantified and the pumping energy requirement for a standard pre-treatment method is discussed.

2. Materials and methods

2.1. *Feedstock characterisation*

Stockpiled biosolids were collected from SA Water in Bolivar, WWTP South Australia. The Bolivar WWTP treats about 135 million litres of industrial and residential wastewater on a daily basis (WSAA, 2012). The collected samples were derived from the end of the wastewater treatment process following anaerobic digestion of primary and secondary sludge and then stabilised in a lagoon for up to two years. The moisture content of the biosolids was quantified using the standard methodology prescribed in ASTM D 2216–98. The ash content of the collected samples was determined using the ISO 18122:2015(E) methodology in a LABEC muffle furnace at 550 °C for 5 h. The organic content was determined by subtracting the mass of the ash content from the original mass of the dry feedstock.

In this study, biosolids as received are termed wet biosolids. Prior to the commencement of experiments, as received biosolids were oven dried at 105 °C for 24 h, milled and classified into four particle size ranges depending on the average particle diameter using sieves with mesh sizes of 750 μm, 380 μm, 195 μm and 115 μm. These dried and milled samples are termed dry biosolids. The biosolids were dried purposely for studying the effect of different particle sizes on the settling

properties of biosolids. In the real case, wet biosolids would be processed via HTL without drying. The particle sizes of both wet and dry biosolids were analysed using a particle size analyser (Malvern Mastersizer 2000) which measures particle sizes up to 2000 μm applying the principle of light scattering and the Mie theory. The biosolid sample with a refractive index of 1.52 was dispersed in water with a refractive index of 1.33. The particle size analyser captured the scattering pattern in its optical bench and estimated the sizes of the particles using the Mie theorem (Malvern Instruments, 2010). The shape and size of the biosolid particles were viewed under an optical microscope (Olympus optical microscope IX50/IX70) with a magnification of 40 ×. The bulk density of biosolid samples were determined by measuring the mass of biosolids in a known volume. Particle density was determined using the Archimedean principle of fluid displacement for the volume measurement where a pre-weighed mass of the biosolid was added to a known volume of water in a measuring cylinder without agitation. The volume of water displaced in the cylinder was equivalent to the volume of the added biosolids. The recorded mass and determined volume of the biosolids were used to estimate the particle density of biosolids. Porosity was determined from the bulk density of the slurry and the particle density.

2.2. Determination of the nature of biosolids

A batch settling experiment was conducted to assess the nature of biosolid slurries. To determine the settling ability and stability of biosolids in a biosolid/water mixture, both wet and classified dry biosolids were weighed on a dry basis and added to specific amounts of distilled water at known solid concentrations and mixed at 90 rpm for 5 min. The wet biosolid/water mixture was placed in a sonication bath (Soniclean 250 H T, Australia) for 3 min to agitate the flocculated particles, segregate particles and enhance particle dispersion in the solution for even distribution and homogenisation during the mixing process. Settling rate of the particles was observed in a Duran glass cylinder (Diameter: 4.9 cm, Capacity: 500 mL and Height of 500 mL mark: 26.3 cm) for a period of 30 min. The settling rate was estimated by correlating the decrease in volume of the suspended solids in the cylinder to the decrease in distance from the initial height of the suspension to the height of the interface of the settling suspended solids. Settling ability was estimated from the ratio of the height of the settling interface to the total height of the slurry in the cylinder.

2.3. Pumpability and Flow properties of biosolid slurries

The flow parameters, density and viscosity, were determined to analyse the pumpability of the stable slurries. The densities of the slurry mixtures (ρ_m) were calculated using the concentration of solids by weight in the slurry (C_w), the density of the solid particles (ρ_s) and the density of the distilled water without solids (ρ_L) in the following equation (Abulnaga, 2002):

$$\rho_m = \frac{100}{C_w/\rho_s + (100 - C_w)/\rho_L} \quad (1)$$

Rheological tests were conducted under a shear rate controlled mode using a Rheometer (AntonPaar MCR 301 Rheometer) with a pressure cell accessory (Height: 71 mm and width: 32 mm) and a 4-bladed vane impeller (Height: 40 mm and ID: 12 mm) which is similar to the cup and bob configuration. The cup and vane configuration were chosen over the plate-plate and cone-plate rheometer configurations as the vane configuration is suitable for slurries with a high tendency to settle. Viscosity was determined within a range of 1 to 40 s^{-1} at 25° C to obtain the flow index (n) and flow consistency index (k). The rheological data collected (shear rate and shear stress) were fitted into the rheological models which includes the Ostwald, Herschel-Bulkley and Bingham models to obtain yield stress, flow consistency index and flow index (Hong et al., 2016).

Pumpability of biosolid slurries was conducted using a Masterflex peristaltic pump (Model 7518–00) and a Masterfllex pump tube (L/S Tygon E-lab E-3603) with a diameter of 9.7 mm. Prepared biosolid slurries with specific solid concentrations were placed in a mixer and agitated continuously for homogeneity. The pump tube connected the mixer to the inlet of the pump and the outlet of the pump to a collecting vessel. The length of the tube from the outlet of the pump to the collection tank was 15 m. The flow rate was estimated by dividing the volume of slurry collected in the collection tank per second at a fixed roller speed. A physical observation was used to determine the settled solids along the pipeline during each experiment. Accumulation in the tube was calculated by subtracting the final volume of slurry in the collection tank and the residual slurry in the mixer from the initial volume of the pumped slurry in the mixer. The transportation of the homogenous slurry in this case will represent the transportation of biosolid slurries from the feedstock preparation unit to the reactors on a bigger scale.

2.4. Pumping power requirement

Power requirement (P) for pumping biosolid feedstock slurry under laminar flow conditions was calculated using the following equation (Wileman et al., 2012):

$$P = 2f\rho\frac{\dot{V}^3 L}{AD} \quad (2)$$

Where ρ is the slurry density, $\dot{V}$ is the volumetric flow rate of the slurry, L is the length of the pipe and A is the cross-sectional area of a pipe with diameter, D. Power requirement for pumping biosolid slurry was estimated based on a real case where a HTL refinery processes 1 t/hr biosolid slurry through a 15 m long pipe with an internal diameter of 50 mm. The Fanning friction factor (f) was given by Wileman et al. (2012):

$$f = \frac{16}{Re_{MR}} \quad (3)$$

The flow index (n) and consistency index (k) obtained from the rheological models of the biosolid slurry as a power law fluid are used in estimating the Reynolds number. Reynolds number for non-Newtonian fluids was determined using the Metzner and Reed method which is a function on the fluid velocity, slurry density and pipe diameter (Chhabra and Richardson, 2008):

$$Re_{MR} = \frac{\rho_x \bar{u}^{(2-n)} D^n}{8^{(n-1)} K} \quad (4)$$

The critical transport velocity was estimated as a function of the Durand's factor (D_L), internal diameter of the pipe (D),

Table 1 – Physical properties of biosolid particles.

Property	Wet biosolids	Dry biosolids
Porosity, %	52	43
Sphericity	0.03 - 1	0.03–1
Aspect length	1 – 4.34	1–4.34
d_{50}, μm	190	102
Particle density, kg/m^3	2000	2000
Bulk density, kg/m^3		
< 750 μm	951	1140
< 380 μm	[1]n/a	1040
< 195 μm	[1]n/a	880
< 115 μm	[1]n/a	850

'n/a' no experiments conducted.

acceleration due to gravity (g), solid density (ρ_s) and the density of the liquid (ρ_L) in an equation proposed by Durand and Condolios (Roitto, 2014):

$$V_c = F_L \sqrt{2gD\frac{(\rho_s - \rho_L)}{\rho_L}} \quad (5)$$

where the Durand factor was determined from the volume concentration of the solids (C_v) and the mean particle size of the biosolid samples (d_{50}) in the equation (Roitto, 2014):

$$F_L = \left(1.3C_v^{0.125}\right)\left[1 - e^{-6.9d_{50}}\right] \quad (6)$$

2.5. *Statistical analysis*

Statistical analysis was conducted using a one-way ANOVA followed by a post-hoc test, Tukey Honestly Significant Difference (HSD), to determine the statistical difference between each pair of data sets.

3. Results and discussion

3.1. *Physical properties of biosolids*

The stockpile biosolids as received had a black colour with a moisture content of ~32%. The organic matter content and ash content of the collected samples were determined to be approximately 17% and 83% respectively.

The particle shape and size of wet and dry biosolids were determined to be non-uniform with a wide range of sphericity ranging from 0.03 to 1 and aspect lengths from 1 to 4.34 (Table 1). Although the particle densities of dry and wet biosolids were similar, the bulk density of dry biosolids was higher than that of the wet biosolids due to its low porosity. Bulk density of dry biosolids decreased with a decrease in particle size in the hundreds of micron range.

From the particle size distribution shown in Fig. 1, the particulates of the wet biosolids had a maximum size around 320 μm while dry biosolid particles peaked at 140 μm. Particulates of the fresh stockpiled biosolids as shown in Fig. 2a are larger compared to milled wet biosolids (Fig. 2b) and dry biosolids (Fig. 2c). The large particles in the fresh stockpiled biosolids is a result of the moisture in the sample which creates a strong adhesion between the solids and water molecules causing the particles to stick together and form bigger flocs. Milling the fresh stockpiled biosolids breaks the bigger flocs to form smaller particles. These smaller particles of the wet biosolids are still bigger than the particles in the dry biosolids due to presence of water molecules in the wet biosolids. The larger

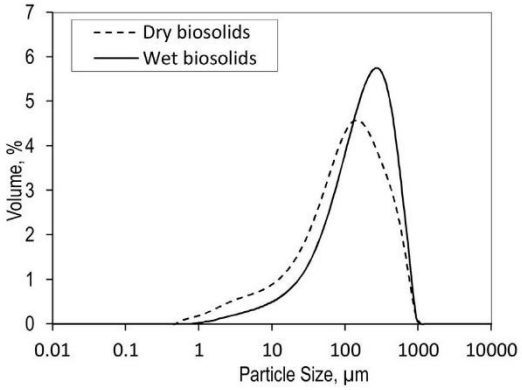

Fig. 1 – Particle size distribution of biosolids.

flocs of the wet biosolids are formed from smaller particles coalescing with other particles. Drying the biosolid particles reduces the moisture content thereby reducing the adhesion between the particulates.

The one-way ANOVA test conducted showed a significant difference in the percentage volume of wet and dry biosolids with the particle size ($F(2) = 8.14$, $p = 0.000855$) as $p < 0.05$ and $F > 3.179$ (F_{crit}). Hence, the null hypothesis was rejected. A post-hoc Tukey HSD test conducted showed a significant difference between the percentage volume of both wet and dry biosolids on the particle size where the absolute difference between the pairwise set was greater than the critical range (Supplementary Information Table 1 s – 3 s).

3.2. *Effects of solid concentration and particle size on settling property of biosolids*

To assess the influence of particle size on feedstock preparation, the behaviour of the classified particles when mixed with water at different concentrations were determined by a batch settling test. A settling test was conducted to determine the behaviour and stability of biosolid slurries at different concentrations.

During the settling rate tests, stratification was observed in each cylinder such that the high concentrations of the denser particles with particle size <750 μm settled at the bottom of the cylinder and the less dense particles with a particle size <115 μm remained on top of the denser sediment. The denser particles settled out in the areas of higher concentrations. Most particles remained in suspension in the region of hindered settling as water (supernatant) with a few suspended particles floated on the top of the slurry. Each sediment separated out in distinct layers due to non-uniform packing morphologies and the spatial arrangement of the particles during gravity separation. The zonal settling of the particles observed was in accordance to the Kynch (1952) theory of sedimentation which describes the settling of flocculated suspensions under gravity with the settling entities possessing the same size and shape at a constant concentration.

For the less concentrated solid slurries, that is, for solid concentrations below 20% w/w solids, the visibility of the distinct interface between the suspended solid zones and the supernatant was poor. Particles in less concentrated slurries settle independently when they are distant from each other. The settling characteristic of the individual particles is characterised by the properties of the solid particles and that of the

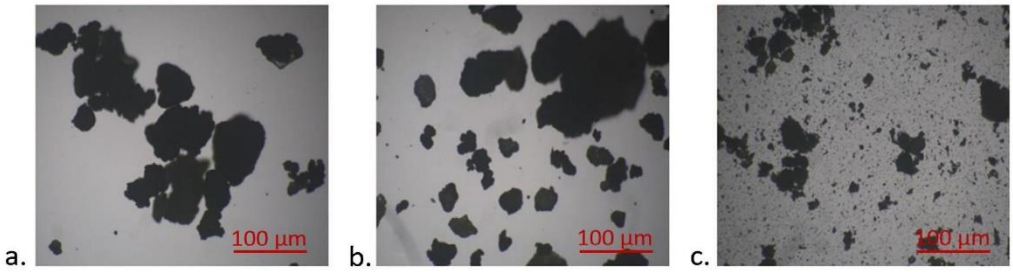

Fig. 2 – Microscopic view of biosolids under a magnification of 40x a. Fresh stockpiled biosolids (as received) b. wet biosolids c. dry biosolids.

fluid (Renko, 1998). The distance between these particles and their independent settling characteristic directly affects the settling velocity of the individual particles and hence the poor visibility of the various settling zones. For highly concentrated solutions where the distance between particles is so small, there are interactions between particles that causes them to move together and that creates a distinct layer separating the settling suspension from the supernatant. According to Koo (2009), particles in highly concentrated multi-particulate systems will experience low settling rates due to the presence of other particles that hinder the free fall of these particles. Consequently, biosolid slurries with high solid concentrations settle slower than those with low solid concentrations. The property of low settling velocity is desirable especially during transportation of slurries as low settling velocity guarantees that particles remain suspended in the slurry for a longer time reducing the chances of pipe blockage. High settling velocity depicts that the slurry is unstable and non-homogeneous with more solids settling at the bottom of the containing vessel which will easily block pipelines and clog pumps when the particles accumulate with time hence obstructing flow of the feedstock slurry.

Settling of particles in a slurry can be influenced by particle shape, particle size, gravity, solid concentration and particle densities (Gillies, 1993; Miedema, 2016). Particle size distribution affects zonal stratification of particles and this was unique for each solid concentration tested. For solid concentrations less than 60% w/w, four distinct layers of variable solid concentration including the supernatant was observed for dry biosolids with particle sizes <750 µm (Fig. 3a). The number of distinct layers reduced with a reduction in particle size range. The distinctions may be due to the dynamics of settling which is dependent on the individual particle densities (Mrokowska, 2018). The distinct layers were dependent on the particle size distribution such that, a decrease in particle size decreased the number of stratified layers in the cylinder. At 60% solid concentration, the slurries of different particle sizes all exhibited a homogeneous behaviour with almost no observable stratification even after 30 min (Fig. 3b). Contrary to the settling characteristics of biosolid slurries, slurries prepared from fresh sewage sludge may remain suspended for a longer time exhibiting a less visible settling layer. Sewage sludge from different parts of the wastewater treatment plant may settle differently especially due to their water holding capacities, presence of coagulants and the properties of the solid particles. Sewage sludge containing higher organic contents, higher moisture contents and high amounts of EPS are anticipated to remain continuously suspended in solution with a cloudy settling region making visibility between the settling layers less visible as compared to biosolids. Sewage

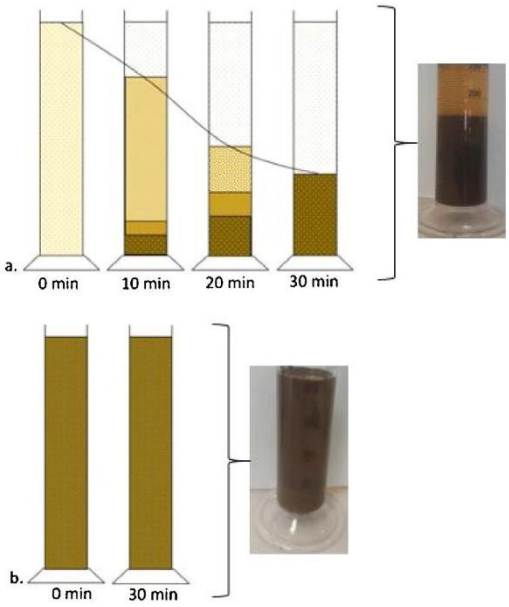

Fig. 3 – Experimental observation for batch settling experiment obtained from preparing biosolid slurries with solid concentrations of a) 15 w/w% biosolids (least stable slurry) and b) 60 w/w% biosolids (Completely stable slurry).

sludge with rich organic contents and high moisture have higher amounts of particles in the colloidal range making them behave more like a colloid. On the other hand, sewage sludge with less organics and low moisture contents such as biosolids behave more like suspensions with relatively large solid particles.

The effects of solid concentration on settling characteristic of dry biosolid slurries with particle size <750 µm was similar to the effects observed from biosolid slurries prepared with particle sizes in the range <380 µm, <195 µm and <115 µm (Fig. 4a). Settling velocity decreases as solid concentration increases from 10% to 60% dry biosolids. According to Galvin and Iveson (2013), denser fluids and high fluid viscosities have lesser particle settling velocity. Highly concentrated biosolid slurries are expected to be denser and viscous than dilute biosolid slurries due to an increase in solid content. Hence, settling velocity of biosolid slurries decreases with an increase in solid concentration irrespective of the particle size. Particle size of biosolids in the hundreds of micron range as used in this study has minimal effect on the settling velocities of the of biosolid slurries at various solid concentrations. This may be because the size range of the particles used lies within a

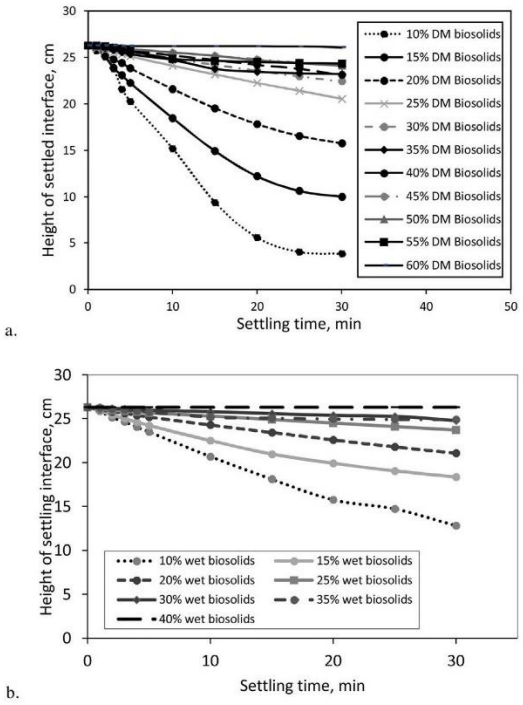

Fig. 4 – Settling velocity of variable concentration of a. dry biosolids, b. wet biosolids with particle size <750microns.

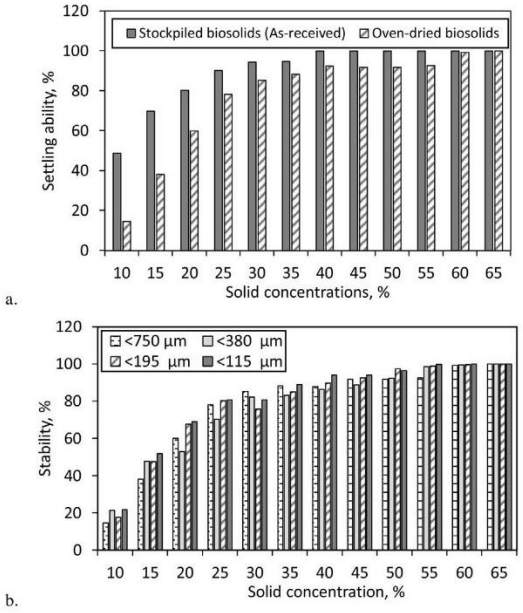

Fig. 5 – Effects of variable particle sizes and feedstock compositions on stability of biosolids after 30 min observation a. The comparison of the settling abilities of oven-dry and stockpiled biosolids slurries over a range of particle sizes <750microns and b. Stability of dry biosolid slurry with variable feedstock composition and particle sizes.

narrow range. Due to the minimal effects of solid concentrations in the hundreds of micron range on the settling ability of biosolid slurries, there may be no need for further particle size reduction below 750 µm to obtain a stable slurry.

From the plotted data shown in Fig. 4b, wet biosolid slurry remains in suspension and attains homogeneity within 30 min of close monitoring when the solid loading is increased to 40 w/w% dry biosolids. This observation is similar to that observed in dry biosolid slurries with 60 w/w% solid concentration under 30 min observation. This implies that the settling characteristics of biosolid slurries reduces when the feedstock has residual amount of moisture inherent at higher solid concentrations. The consistency of the slurry mixtures of wet biosolids at 40% w/w dry solid concentration and that of dry biosolids 60% w/w dry solid concentration are desirable and suitable for transportation of the slurry through pipelines with less settling rates and for constant heat transfer in HTL reactors during HTL due to its homogeneity.

The stability of the biosolids slurries were characterised by quantifying the settling ability over an observation period of 30 min. The term 'stability' used in this paper is defined as the ability of the particles to continuously remain suspended in the slurry. Generally, biosolid slurries are stable at higher solid concentrations. The data presented in Fig. 5a shows the gradual increase in the stability of biosolid/water mixtures which indicates that stability increases with an increase in solid loading for slurries prepared from both wet and dry solids. Stability improves at higher solid concentration because increasing solid loading increases the slurry density and hence, the settling rate of the solids reduces. Fig. 5b shows a comparison of the stability of dry biosolid slurries prepared with different particle sizes. Again, the stability of biosolid slurries increases with solid concentration for all particle sizes tested in the hundreds of micron ranges.

A one-way ANOVA test conducted showed a significant difference in the settling ability of wet and dry biosolids with solid concentration ($F(2) = 20.88$, $p = 0.000001$) as $p < 0.05$ and $F > 3.28$ (F_{crit}). Hence, the null hypothesis was rejected. A post-hoc Tukey HSD test conducted showed a significant difference between the settling ability of both wet and dry biosolids with solid concentration where the absolute difference between the pairwise set was greater than the critical range (Supplementary Information Table 4 s–6 s.)

A one-way ANOVA test conducted showed a significant difference in the stability of different particle size ranges of dry biosolids slurries with solid concentration ($F(4) = 7.34$, $p = 0.000082$) as $p < 0.05$ and $F > 2.54$ (F_{crit}). Hence, the null hypothesis was rejected. A post-hoc Tukey HSD test conducted showed a significant difference between the stability of each particle size range of dry biosolids slurry with solid concentration where the absolute difference between the pairwise set was greater than the critical range (Supplementary Information Table 7 s –9 s.). However, there was no statistical difference between pairwise data set comparing the stability of one particle size range to the other.

3.3. *Effects of settling on flow velocity in pipelines*

The transportation of settling slurries can be detrimental to pipelines, pumps and plug flow reactors during continuous HTL operations. The settling characteristics of particles in slurries that have tendency to settle out during transportation can affect the flow of the slurry in pipelines and heat transfer in plug flow reactors. Slurry density, solid concentration, slurry viscosity and flow velocity can influence the rate of particle settling during transportation in pipelines.

Transporting settling slurries can block pipelines, clog pumps and lead to pressure losses in pipes and fittings. This occurs when the flow velocity of the slurry in the pipeline is lesser than the critical transport velocity (Lea et al., 2008). The calculated critical transport velocities of biosolid slurries with solid concentrations between 30 w/w% to 60 w/w% ranges from 0.93 m/s to 1.04 m/s. Transporting slurries at flow velocities lower than the critical transport velocities can gradually create a layer of fixed or moving bed of solids close to the walls of the pipes due to gradual deposition of solids at the base of the pipe (Clayton, 2005; Water Environment Federation, 2012). As the thickness of the solid layer increases, the friction head losses also increases (Gillies, 1993). Continuous deposition of the solids will decrease the pipe diameter which will lead to a complete blockage of the pipeline and increase the pressure required for the fluid to be pumped. On the other hand, if the flow velocity is much higher than the critical transport velocity, the friction losses in the pipe will be too high causing an increase in power consumption and excessive wear and tear of pipelines and pumps (Thakur, 2017). It is important to determine the critical transport velocity which is also termed the limiting solids settling velocity, optimum safe transport velocity or the critical deposit velocity (Robinson and Graf, 1972). Pumping velocity can be set at least 10% higher than the estimated limiting velocity to prevent settling or high power consumption issues (Grzina et al., 2002).

3.4. *Pumpability of biosolid slurries*

An increase in solid loading of biosolids can potentially increase the yield and conversion of organics in biosolids to renewable crude oil. However, increasing solid loading may affect the transportation and pumpability of the slurry as well as the heat transfer processes which enhances HTL reactions and increases yield. To specify pumps, design pipelines and reactors, it is essential to know the flow and rheological properties of the feedstock. Typically, slurries with solid concentrations used for hydrothermal liquefaction processes are less than 30% wt solids. Pumping issues which includes clogging of pump shafts and blocking of pipelines may arise when solid concentration is increased above 15% resulting from large particle size of the feedstock (Anastasakis et al., 2018). Slurries with high solid concentrations, poor dewatering properties and large particle sizes have less tendency of being pumped (Berglin et al., 2012; Daraban et al., 2015). The ability of a slurry to be pumped can be determined from its flow properties and rheological characteristics which includes the slurry density and viscosity. This information can be used in the specification and design of pipelines and pumps.

The slurry density of biosolid mixtures increases with particle sizes as the bulk densities of the dry feedstock (Table 1) increases with an increase in particle size. Similarly, biosolid slurry density (Fig. 6a) increases with solid concentration. The density of biosolid slurries gradually approaches that of water at lower solid concentrations as expected. The density of the 60% solid concentration of biosolid slurry was measured to be about 1.45 times denser than water. Apparent viscosity of biosolid slurries as shown in Fig. 6b also increases with an increase in solid concentration. This may be as a result of the binary-phase (solid/liquid) nature of the slurry which makes it difficult for the slurry to deform at lower speeds (Daraban et al., 2015) hence the apparent viscosity is higher at lower shear rates. The settling characteristics of the slurries may have led to instability of slurries during the viscosity measurement which could lead to poor viscosity measurements at lower shear rates hence viscosity reading <10 s^{-1} was not captured in the data analysis. The increase in apparent viscosity with solid concentration is similar to the increase in apparent viscosity with an increase in volume fraction at a constant shear rate as illustrated in Fig. 6c. When flocs are concentrated in a slurry, they fill a large volume which increases the force needed to displace them in the dispersion (Brookfield, 2017). Hence an increased in this force is synonymous to an increase in the shear stress at a constant shear rate and this increases the apparent porosity of the slurry.

From the flow curves of dry biosolids shown in Fig. 6d, biosolid slurries within the measured range are Non-Newtonian fluids with yield stresses at concentrations >30% dry solids. The yield stress at each solid concentration represents the minimum amount of force required for the slurry to initiate motion. As the solid concentration of dry biosolids increase, the fluid deviates from Newtonian behaviour to become highly non-Newtonian. Modelling the viscosity data obtained experimentally into the Ostwald, Herschel-Bulkley and Bingham model helps to fully understand the rheological behaviour of the biosolid slurries. An example of the model fitting has been illustrated in Fig. 6d. The constants of the curve fitting viscosity models which includes the flow consistency constant, flow index constants and yield stresses can be used in calculating the Reynolds number and consequently, the friction factor when sizing pipelines.

The verification and validation of the rheological models were conducted from a histogram and a normal probability plot of the residuals in Fig. 1-4 s on the Supplementary data sheet. The histograms of the residuals for the three models used on different solid concentrations did not give a clear indication of the normality of the plots. A further graph was plotted (the normal probability plot) to predict the normality of the distribution of data. From the probability plots shown in Figs. 1-4 s on the Supplementary sheets, the Bingham model and Herschel-Bulkley model best fits the data obtained from 30 w/w% biosolid slurries (Fig. 1s). All three models displayed normal distribution from data obtained from slurries prepared from 40 w/w% biosolids (Fig. 2s). Statistically, samples prepared from 50 w/w% (Fig. 5s) and 60 w/w% (Fig. 4s) biosolid slurries display a random distribution which indicates that the models do not perfectly fit the experimental data.

According to scientific literature, transporting fluids at flow velocities above the critical transport velocity would improve the flow of the slurry. To elucidate the effect of the settling characteristics of the feedstock on the pumpability of the slurry, the pumpability test of the biosolid slurry was conducted under a flow velocity which was 15 times lower than the critical settling velocity. The pumpability of biosolid slurries were tested using a laboratory scale peristaltic pump. Pumping tests was conducted on biosolid slurries with >80% stability. Pumpability in this study was determined by the ease with which biosolid slurries can be pumped and transported from an inlet tank into an outlet tank. The terms in Table 2 were used as a measure of the pumpability of the slurries in addition to the slurry viscosity and density. The accumulation term in Table 2 is a prediction of how much of the slurry was unable to be successfully transported between the inlet and outlet tanks. The pumpable term gives an indication of transfer of slurry just by observation without clogging or blocking of the pipeline. Visible settling of solids in the tube was measured by observing if there was a stationary bed of

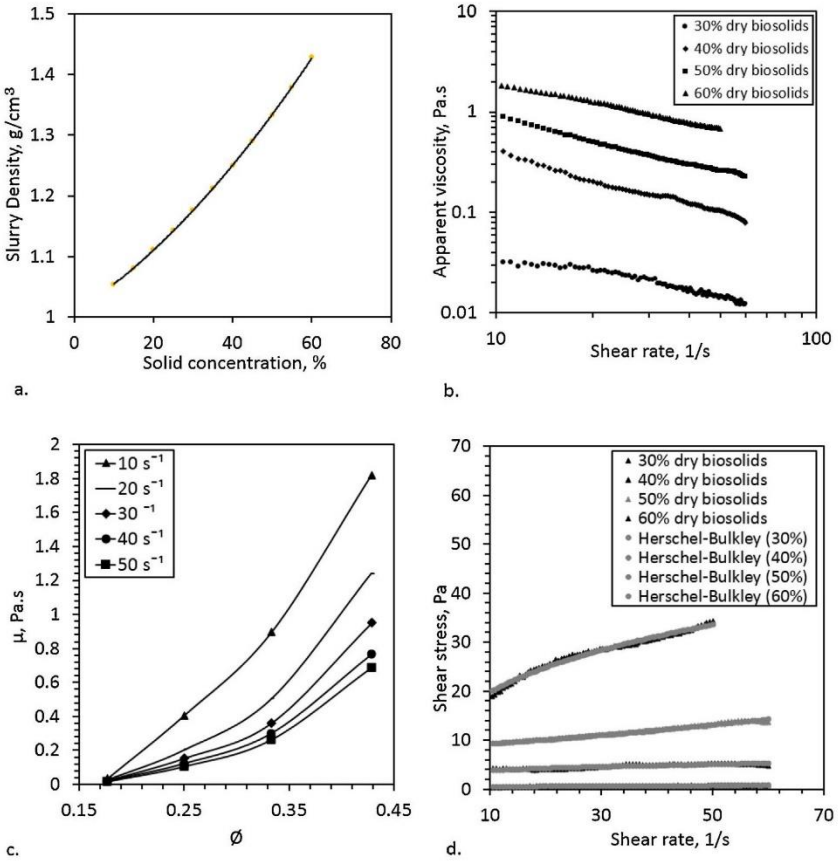

Fig. 6 – Flow properties of biosolid slurries prepared with particle sizes < 750 microns a. Slurry density b. Apparent viscosity c. Apparent viscosity as a function of volume fraction d. Flow curve with model fitting.

Table 2 – Pumping test for biosolid feedstock slurries.

Solid concentration, %	Accumulation, %	Pumpable	Visible settled solid
30	52	√	√
40	41	√	√
50	38	√	×
60	16	√	×

sediment occupying at least 5% of the cross-sectional area of the pipe after the pumping test which lasted for 5 min per test. From the data presented in Table 2, the tested biosolids slurries can be pumped. However, the settling characteristic of the slurries greatly affect the free flow of the fluid in the pipeline.

At the same roller speed, the average flow velocity of the biosolid slurries was determined to be 0.15 m/s which was lower than the critical transport velocity hence accumulation was expected in the pumping test. However, it is highly expected that when the flow speed is increased and approaches the critical transport velocity, the accumulation of solids in the pipe will decrease with time. Biosolids with solid concentrations of 30% dry solids had more than 50% solids settling in the tubing after 3 min of flow time. The deposition of the solids in the tubing started after 0.1 m travel through the tubing. Due to the settling property of the slurry, the denser solids settled quickly and the supernatant which was less concentrated with solid particles flowed through freely.

Pumping issues (blockages of pipelines and clogging of pumps) that arise from particle size, solid concentrations and particle shape of biosolids on a laboratory scale may not be anticipated when the system is scaled-up due to bigger pipe diameters and higher flow rates on pilot and demonstration plants. Nonetheless, the pumping ability of biosolid slurries still needs to be validated for commercial operations as pumping slurries with high solid concentrations and high densities can be problematic (Elliott et al., 2015) and increase pumping energy during commercial operations. On commercial scales, pumping issues may be reduced by increasing flow rate of the feedstock and employing high pressure pumps using reciprocating plunger pumps together with ball check valves (Elliott et al., 2015).

A comprehensive assessment conducted by Berglin et al. (2012) outlined options for feeding and pumping feedstock slurries for HTL. According to Berglin et al. (2012), dilute biomass slurries with solid concentrations <15% and particle sizes ranging from 2 mm to 6 mm could be pumped with less issues. A few pump options were recommended for pumping feedstock slurries for HTL and analysis between the different types of pumps were made. The diaphragm hose pump (Feluwa) and solids piston pump are capable of handling highly viscous slurries with the rotary pump having exceptional qualities of pumping higher solid concentrations. The Feluwa diaphragm pump is capable of pumping viscosities <5 Pa.s. The apparent viscosity of biosolid slurries tested were determined to be pumpable even though the tested slurries

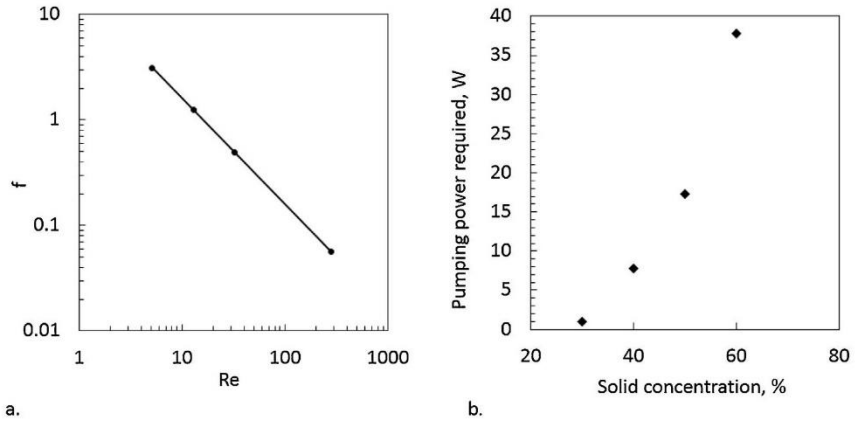

Fig. 7 – Power requirement for pumping biosolid slurries a. Friction factors in a pipe, b. Pumping power at different solid concentrations.

were prepared with solid concentration >15%. The concentrated biosolid slurries with solid concentrations >60 w/w% dry solids can be pumpable as their viscosities at shear rates >10 s^{-1} are below 5 Pa.s. Additional features which includes force-controlled valves and a screw feeder can be installed to enhance the pumpability of these slurries (Berglin et al., 2012). As per the settling test conducted in this paper, biosolid slurries with solid loading <60 w/w% dry solids have the tendency to sediment with time. The application of a screw feeder will reduce accumulation and settling of biosolid particles during transportation. The pumpability of such slurries can also be enhanced by the addition of polymers like Carboxymethyl cellulose, CMC (Lappa et al., 2016). Blending the feedstock with CMC helps to homogenise the slurry, reduces the settling rate of particles and improve upon the stability of the slurry.

3.5. *Pumping energy and power requirement*

Transportation and pumping of a binary-phase feedstock slurry can be energy intensive. Solid concentration, particle size, slurry viscosity, slurry density, pipe diameter and pipeline velocity can affect pressure drop and energy consumption during slurry transportation (Abd Al Aziz and Mohamed, 2013). Pumping energy and pumping efficiency of slurries depend on the particle size range of the solids, particle specific density, settling characteristics of the feedstock and the impeller diameter of the pump. The energy required to pump slurries can be estimated mechanically using a relation between pump power, volumetric flow rate of the slurry, slurry density and the pumping head. The energy consumed during slurry pumping can greatly increase capital cost and operational cost due to friction losses and pressure gradients, pipe blockage, pump performance and pump wear.

Friction factors calculated in the laminar flow regime as shown in Fig. 7a can be used to estimate the head loss per unit length of the pipe at a specified Reynolds number. Biosolid slurries flowing at low velocities through a pipe will yield high frictional losses especially when highly concentrated. High frictional losses increase the pumping energy and hence operational cost. According to the data presented in Fig. 7b, power required for pumping biosolid feedstock slurry at a flow rate of 1 t/hr in a pipe with an internal diameter of 50 mm increases significantly with an increase in dry matter. As expected, an increase in solid concentration increased the slurry density and viscosity. Consequently, an increase in solid loading increases the amount of energy input required to transport the slurry through a pipeline.

The accumulation of multiple layers of settled solids can obstruct the flow of the slurry during transportation. In view of this, the use of high-pressure pumps to forcefully push the slurry through the pipeline is required. Pump wear in a slurry pump can be caused by the abrasiveness of the solid particles in the slurry and corrosion of the material of construction when materials with low chemical resistivity are used (Bbosa et al., 2017). The wetted parts of a pump which includes the casing, suction liner and impeller, may need to be replaced when it wears. Replacement of wetted pump parts can increase the operational cost of pumping on an industrial plant.

4. Conclusion

Solid concentration, particle size, slurry density and viscosity greatly affect the stability and transportation of biosolid slurries prior to renewable crude-like oil production via HTL. Particle size in the hundreds of micron range has little effect of the stability of the slurry. Hence, further size reduction below < 750 μm will be unnecessary. This saves energy on grinding and size reduction. Unlike particle size, solid concentration of biosolid slurries does affect the stability of biosolid slurry. Hence, increasing the solid concentration of HTL feedstock can potentially increase yields and conversion of biosolid slurries to renewable crude oil. However, this benefit comes with transportation issues. Pipe blockage and pump clogging may occur with biosolid feedstock slurries below 60 w/w% dry solid concentration due to the high settling characteristics of the slurries. Nonetheless, using high pressure pumps with force-controlled valves and screw feeders can reduce such pumping issues. High pumping energy is required to transport biosolid slurries with higher solid concentrations. Hence, the transportation of concentrated biosolid slurries can potentially increase capital and operational costs.

Funding

This work was supported by Southern Oil Refining and the Australian Research Council's Linkage Projects funding scheme [Project LP150101241].

Conflict of interests

The authors declare that they have no known competing financial interests or personal relationships that could have appeared to influence the work reported in this paper.

Acknowledgements

The authors wish to acknowledge SA Water, in particular Mr Nick Swain for providing the feedstock; and Dr. Quihong Hu and Dr. Tony Hall for their expertise in analytical work at the University of Adelaide.

References

Abd Al Aziz, A.I., Mohamed, H.I., 2013. A study of the factors affecting transporting solid— liquid suspension through pipelines. Open J. Fluid Dyn. 3, 152–162, Retrieved from https://doi.org/10.4236/ojfd.2013.33020.

Abulnaga, B.E., 2002. In: Hager, L.S. (Ed.), Slurry Systems Handbook. McGraw-Hill, USA.

Akhtar, J., Amin, N.A.S., 2011. A review on process conditions for optimum bio-oil yield in hydrothermal liquefaction of biomass. Renewable Sustainable Energy Rev. 15, 1615–1624.

Anastasakis, K., Biller, P., Madsen, R.B., Glasius, M., Johannsen, I., 2018. Continuous hydrothermal liquefaction of biomass in a novel pilot plant with heat recovery and hydraulic oscillation. Energies 11 (2695), 1–23.

Bbosa, B., DelleCase, E., Volk, M., Ozbayoglu, E., 2017. A comprehensive deposition velocity model for slurry transport in horizontal pipelines. J Petrol Explor Prod Technol 7, 303–310, doi:0.1007/s13202-016-0259-1.

Berglin, E.J., Enderlin, C.W., Schmidt, A.J., 2012. Review and Assessment of Commercial Vendors/Options for Feeding and Pumping Biomass Slurries for Hydrothermal Liquefaction. (PNNL-21981). Pacific Northwest National Laboratory, U.S.

Biller, P., Ross, A.B., 2016. In: Luque, R., Lin, C.S.K., Wilson, K., Clark, J. (Eds.), Production of Biofuels via Hydrothermal Conversion. , second ed. Handbook of Biofuels Production, pp. 509–547.

Brookfield, A., 2017. In: Brookfield, A. (Ed.), More Solutions to Sticky Problems. Middleboro, USA, p. 16.

Chhabra, R.P., Richardson, J.F., 2008. Flow in pipes and in conduits of non-circular cross-sections. In: Non-Newtonian Flow and Applied Rheology, 2nd ed. Elsevier, pp. 110–205.

Clayton, C.T., 2005. Multiphase Flow Handbook, Vol. 59. CRC Press.

Daraban, I.M., Rosendahl, L.A., Pedersen, T.H., Iversen, B.S., 2015. Pretreatment methods to obtain pumpable high solid loading woodewater slurries for continuous hydrothermal liquefaction systems. Biomass Bioenergy 81, 437–443.

Darvodelsky, P., 2011. Biosolids Snapshot. New South Wales.

Elliott, D.C., Biller, P., Schmidt, A.J., Jones, S.B., 2015. Hydrothermal liquefaction of biomass: developments from batch to continuous process. Bioresour. Technol. 178, 147–156.

Galvin, K.P., Iveson, S.M., 2013. Cleaning of coarse and small coal. In: Osborne, D. (Ed.), The Coal Handbook: Towards Cleaner Production, Vol. 1. Woodhead Publishing, pp. 263–300.

Gillies, R.G., 1993. Pipeline Flow of Coarse Particle Slurries. (Doctor of Philosophy). University of Saskatchewan, Saskatoon.

Grzina, A., Roudnev, A., Burgess, K.E., 2002. Slurry Pumping Manual, 1st ed. In W. I. Ltd. (Ed.), pp. 66.

Guo, Y., Wang, S.Z., Xu, D.H., Gong, Y.M., Ma, H.H., Tang, X.Y., 2010. Review of catalytic supercritical water gasification for hydrogen production from biomass. Renewable Sustainable Energy Rev. 14 (1), 334–343, http://dx.doi.org/10.1016/j.rser.2009.08.012.

Hong, E., Yeneneh, A.M., Kayaalp, A., Sen, T.K., Ang, H.M., Kayaalp, M., 2016. Rheological Characteristics of Municipal Thickened Excess Activated Sludge (TEAS): Impacts of pH, Temperature, Solid Concentration and Polymer Dose. Res. Chem. Intermed. 42 (8), 6567–6585.

Jazrawi, C., Biller, P., Ross, A.B., Montoya, A., Maschmeyer, T., Haynes, B.S., 2013. Pilot plant testing of continuous hydrothermal liquefaction of microalgae. Algal Res., 268–277.

Koo, S., 2009. Estimation of hindered settling velocity of suspensions. J. Ind. Eng. Chem. 15, 45–49.

Kynch, G.J., 1952. A theory of sedimentation. Trans. Farad. Soc. 48, 166–175.

Lappa, E., Christensen, P.S., Klemmer, M., Becker, J., Iversen, B.B., 2016. Hydrothermal liquefaction of Miscanthus giganteus: preparation of the ideal feedstock. Biomass Bioenergy 87, 17–25.

Lea, J.F., Nickens, H.V., Wells, M.R., 2008. Progressing cavity pumps. In: Gas Well Deliquification, 2nd edition ed. Gulf Professional Publishing, Amsterdam; Boston, pp. 608.

Leonie, M., Graeme, K., 2009. Use of Biosolids in Agriculture. New South Wales.

Malvern Instruments, 2010. Mastersizer 2000 User Manual. In M. I. Ltd (Ed.), UK.

Marrone, P., 2016. Genifuel Hydrothermal Procesing Bench-scale Technology Evaluation Project. Retrieved From USA.

Miedema, S.A., 2016. In: Ramsdell, R.C. (Ed.), Slurry Transport: Fundamentals, a Historical Overview and the Delft Head Loss & Limit Deposit Velocity Framework. , 1st ed. SA Miedema/ Delft University of Technology, Delft, The Netherlands.

Mrokowska, M.M., 2018. Stratification-induced Reorientation of Disk Settling through Ambient Density Transition. Retrieved From Poland., http://dx.doi.org/10.1038/s41598-017-18654-7.

Mulchandani, A., Westerhoff, P., 2016. Recovery opportunities for metals and energy from sewage sludges. Bioresour. Technol. 215, 215–226, http://dx.doi.org/10.1016/j.biortech.2016.03.075.

Qian, L., Wang, S., Savage, P.E., 2017. Hydrothermal liquefaction of sewage sludge under isothermal and fast conditions. Bioresour. Technol. 232, 27–34, http://dx.doi.org/10.1016/j.biortech.2017.02.017.

Renko, E.K., 1998. Modelling hindered batch settling Part II: a model for computing solids profile of calcium carbonate slurry. Water SA 24 (4).

Robinson, M.P., Graf, W.H., 1972. Critical Deposit Velocities for Low-concentration Sand-water Mixtures. Retrieved from Atlanta, Georgia. ASCE National Water Resources.

Roitto, V., 2014. Slurry Flows in Metallurgical Process Engineering- Development of Tools and Guidelines. (Master of Science). Aalto University, Finland.

Shakya, R., Whelen, J., Adhikari, S., Mahadevan, R., Neupane, S., 2015. Effect of temperature and Na_2CO_3 catalyst on hydrothermal liquefaction of algae. Algal Res. 12, 80–90, http://dx.doi.org/10.1016/j.algal.2015.08.006.

Shammas, N.K., Wang, L., 2008. Transport and pumping of sewage sludge and biosolids. In: Wang, L.K., Shammas, N.K., Hung, Y.T. (Eds.), Handbook of Environmental Engineering, Vol. 7. The Humana Press, Totowa, NJ.

Thakur, P., 2017. Fluid flow in pipes and boreholes. In: Thakur, P. (Ed.), Advanced Reservoir and Production Engineering for Coal Bed Methane. Gulf Professional Publishing, pp. 91–104.

Toor, S.S., Rosendahl, L., Rudolf, A., 2011. Hydrothermal liquefaction of biomass: A review of subcritical water technologies. Energy 36 (5), 2328–2342, http://dx.doi.org/10.1016/j.energy.2011.03.013.

Torri, S., Cabrera, M., 2017. Environmental impact of biosolids land application. In: Collins, M. (Ed.), Organic Waste: Management Strategies, Environmental Impact and Emerging Regulations. Nova Science Publishers, Inc, Hauppauge, NY, pp. 185–208.

Wang, Z., 2011. Reaction Mechanisms of Hydrothermal Liquefaction of Model Compounds and Biowaste Feedstocks.

Water Environment Federation, 2012. Solids Process Design and Management. McGraw-Hill Education, Europe.

Wileman, A., Ozkan, A., Berberoglu, H., 2012. Rheological properties of algae slurries for minimizing harvesting energy

requirements in biofuel production. Bioresour. Technol. 104, 432–439.
Water Services Association of AustraliaWSAA, 2012. Bolivar Wastewater Treatment Plant Energy Use Case Study. Retrieved From Australia. SA Water.
Yin, S., Dolan, R., Harris, M., Tan, Z., 2010. Subcritical hydrothermal liquefaction of cattle manure to bio-oil: effects of conversion parameters on bio-oil yield and characterization of bio-oil. Bioresour. Technol. 101 (10), 3657–3664, http://dx.doi.org/10.1016/j.biortech.2009.12.058.
Zhang, Y., 2010. Hydrothermal liquefaction to convert. Biomass into crude oil. Biofuels from Agricultural Wastes and Bioproducts.
Zhang, L., Xu, C., Champagne, P., 2010. Overview of recent advances in thermo-chemical conversion of biomass. Energy Convers. Manage. 51, 969–982.

Chapter 4:

Rheological studies of municipal sewage sludge slurries for hydrothermal liquefaction biorefinery applications

Statement of Authorship

Title of Paper	Rheological studies of municipal sewage sludge slurries for hydrothermal liquefaction biorefinery applications
Publication Status	☑ Published ☐ Accepted for Publication ☐ Submitted for Publication ☐ Unpublished and Unsubmitted w ork w ritten in manuscript style
Publication Details	Edifor, S. Y.; Nguyen, Q. D.; van Eyk, P.; Biller, P.; Lewis, D. M., Rheological studies of municipal sewage sludge slurries for hydrothermal liquefaction biorefinery applications. Chemical Engineering Research and Design 2021, 166, 148-157.

Principal Author

Name of Principal Author (Candidate)	Sylvia Yawa Edifor		
Contribution to the Paper	Designed Experiments Conducted experiments Data analysis and interpretation Wrote manuscript and acted as corresponding author		
Overall percentage (%)	80		
Certification:	This paper reports on original research I conducted during the period of my Higher Degree by Research candidature and is not subject to any obligations or contractual agreements with a third party that would constrain its inclusion in this thesis. I am the primary author of this paper.		
Signature		Date	22/01/2021

Co-Author Contributions

By signing the Statement of Authorship, each author certifies that:

i. the candidate's stated contribution to the publication is accurate (as detailed above);
ii. permission is granted for the candidate in include the publication in the thesis; and
iii. the sum of all co-author contributions is equal to 100% less the candidate's stated contribution.

Name of Co-Author	Quoc Dzuy Nguyen		
Contribution to the Paper	Assistance with interpretation Drafting and review of manuscript		
Signature		Date	29-01-2021

Name of Co-Author	Philip van Eyk		
Contribution to the Paper	Concept development Supervised development of work Assistance with interpretation Drafting and review of manuscript		
Signature		Date	28/1/2021

Please cut and paste additional co-author panels here as required.

Name of Co-Author	Patrick Biller		
Contribution to the Paper	Assistance with interpretation and presentation of data Drafting and review of manuscript		
Signature		Date	22.01.2021

Name of Co-Author	David M. Lewis		
Contribution to the Paper	Concept development Supervised development of work Assistance with interpretation Drafting and review of manuscript		
Signature		Date	28/01/2021

Contents lists available at ScienceDirect

Chemical Engineering Research and Design

journal homepage: www.elsevier.com/locate/cherd

Rheological studies of municipal sewage sludge slurries for hydrothermal liquefaction biorefinery applications

Sylvia Y. Edifor[a,*], Quoc D. Nguyen[a], Philip van Eyk[a], Patrick Biller[b], David M. Lewis[a]

[a] School of Chemical Engineering and Advanced Materials, The University of Adelaide, 5005 Adelaide, SA, Australia
[b] Department of Engineering-Biological and Chemical Engineering, Aarhus University, 8200 Aarhus, Denmark

ARTICLE INFO

Article history:
Received 4 September 2020
Received in revised form 4 December 2020
Accepted 7 December 2020
Available online 11 December 2020

Keywords:
Hydrothermal liquefaction
Rheological properties
Rheological models
Pumping power
Transportation system design

ABSTRACT

Hydrothermal liquefaction (HTL) is a thermochemical process that can convert organic materials in sewage sludge into crude-like oil. Knowledge of the rheology of sewage sludge as a feedstock is important for the design of a HTL Biorefinery as it provides essential information for pumping, pipeline design and heat transfer processes. This study aims at elucidating the rheological behaviour of sewage sludge slurries. Rheological parameters of sludge obtained from different stages in Wastewater Treatment Plants were estimated and used to calculate the pumping power required for slurry transportation in pipelines as part of the front-end engineering design stage for a biorefinery. Sludge slurries were determined to be Non-Newtonian with shear thickening characteristics. Statistically, the Herschel-Bulkley rheological model best fitted the experimental data with a yield stress. The apparent viscosity of municipal sewage sludge slurries measured within a shear rate range from 10 s^{-1} to 300 s^{-1} were determined to be between 0.008–0.05 Pa.s for stockpiled biosolids, 0.04–0.11 Pa.s for sludge without polymer dosage and 0.1–0.2 Pa.s for dewatered sludge with polymer. Power requirement for pumping sludge slurries were in the order: Stockpiled biosolid < Sludge without polymer dosage < Sludge with polymer dosage.

1. Introduction

There is an increased global interest in generating electricity, producing solid fuel, transportation liquid fuel and gas from municipal and industrial waste to provide cost-effective alternatives for waste management and disposal processes. Hydrothermal liquefaction (HTL) is a thermochemical depolymerisation process that converts organics in wet biomass under subcritical conditions of about 350 °C and 22 MPa (Elliott et al., 2013) to yield renewable crude oil, gas phase, solids and an aqueous phase. Municipal sewage sludge which includes biosolids are organic rich solid waste residues obtained from the primary and secondary treatment of municipal sewage at waste water treatment facilities (Leonie and Graeme, 2009; Shammas and Wang, 2008; Torri and Cabrera, 2017). Scientific research has proven that HTL of municipal sewage sludge can be viable for commercialisation (Anastasakis et al., 2018; Berglin et al., 2012; Billing et al., 2017; Skaggs et al., 2018). However, one major challenge with scaling up to an industrial level is the efficient transportation of the sludge slurries which can signficantly affect the operational cost and plant design of a biorefinery. Pumping slurries especially with high solid contents can lead to pumping and pipeline issues such as abbrasion, clogging of pumps and blockages of transportation pipelines. Knowledge of the feedstock properties is essential for designing the material transportation sytems and providing sufficient data for reactor design for industrial applications.

Upstream processes in biorefineries, particularly material transportation (pumping of slurries) and midstream processes

* Corresponding author.
E-mail address: sylvia.edifor@adelaide.edu.au (S.Y. Edifor).
https://doi.org/10.1016/j.cherd.2020.12.004

including heat transfer processes, are affected by the slurry solid composition and concentration, characteristics of solid particles, slurry density and the rheological properties of the slurry which significantly influences pump selection, pumping specification and pipeline design. Rheological parameters such as shear stress, shear rate, viscosity, yield stress and settling rate of particles in the slurry (He et al., 2009) are specific to the type of biomass slurry due to their unique compositions, characteristics and behaviour when mixed with solvents. These rheological parameters depend on size of the particles, degree of dispersion, solid concentration, thermal properties, chemical composition and characteristics of the sludge (Wolny et al., 2008), type of sludge used and type of wastewater and sludge treatment processes (Cao et al., 2016). Hence it is important to elucidate the rheological parameters of municipal sewage sludge to ease processeability and provide required design parameters for pipeline, fittings, pump selection and reactor design.

Municipal sewage sludge are binary phase mixtures whose rheological properties can be complex and difficult to evaluate due to its unknown and unpredictable characteristics especially when the sludge is concentrated (Cao et al., 2016; Lotito et al., 1997) and thickened (Wolny et al., 2008). As sludge thickens, the viscosity increases and the sludge behaves as a non-Newtonian fluid (Forster, 2002) which increases its inability to be pumped. Rheology of sludge is greatly influenced by the solid concentration, sludge composition which includes compounds in the organic and inorganic fractions, the interparticle interactions and the changes in the structure of the sludge during flow (Wolny et al., 2008). Sludge derived from different sections in wastewater treatment plants have variable particulate concentrations and hence tend to behave differently. The rheology of municipal sludge from different stages in the WWTPs has been widely investigated to obtain optimal properties, design parameters for transportation during operations and storage of sludge. Some researchers have discovered that sludge behaves as a Non-Newtonian fluid in suspension form, visco-elastic properties in dewatered cake form (Zhang et al., 2017) and thixotropic behaviour using a rotating rheometer (Yen et al., 2002). Other research contradicts these finding by demonstrating that sludge, specifically activated sludge, behaves more like a Newtonian fluid (Dick and Ewing, 1967; Noguchi et al., 2011; Yen et al., 2002) which implies that the viscosity of sludge is a constant irrespective of the shear rate. However, this information on the rheology of sludge is limited to the WWTP application only. This is particularly relevant as a HTL biorefinery application differs to traditional handling requirements in WWTP by desiring higher solid concentration, requiring high pressures and high temperatures through heat exchange. The rheological properties of slurries prepared from fresh sludge, dewatered sludge and stockpiled biosolids are yet to be investigated for HTL processes and applications.

In scientific literature, the rheological parameters of sludge which includes the shear rate, shear stress and viscosity have been determined experimentally to ascertain the flow properties of the sludge for the WWTP applications. The experimental data were fitted into mathematical models that relates shear rate to shear stress and shear rate to viscosity depending on the model used (Seyssiecq et al., 2003). The Ostwald de Vaele, Herschel-Bulkley, Bingham, Sisko, Carreau and Cross models (Hong et al., 2016) have been widely used to characterise municipal sewage sludge samples. These rheological models were used to determine the yield stress, high shear limiting viscosity, flow index, consistency index, infinite-rate apparent viscosity, zero-shear apparent viscosity, time constant and the cross rate constant from the shear stress, shear rate and viscosity data. A similar rheological study on concentrated sludge for HTL application is yet to be investigated, which will differ from previous work as the aim is to obtain high dry matter slurries and achieve much higher pressure. It is important to fit the experimental data obtained after the rheological characterisation of sludge slurries for HTL applications into a rheological model to fully characterise and understand the sludge slurries prior to conversion via HTL. Fitting the experimental data into the rheological model is essential for plant design purposes and calculating pumping requirement. Additionally, rheological models can be used to predict the flow and heating properties of the slurry for HTL applications which is important for heat exchanger and piping design as well as overall expected performance of a future HTL biorefinery.

The reported investigation focuses on understanding the rheological characterisation of sewage slurries prior to HTL. This study aims at elucidating the rheological properties of slurries prepared from dewatered sewage sludge and stockpiled biosolids at ambient conditions to determine parameters that result in pumping issues and increase processability prior to the HTL process in a biorefinery. Unlike sludge slurries used in WWTPs application which are mostly dilute, slurries used in HTL processes are prepared from concentrated and dewatered sludge rich in carbon and organic matter. The experimental data are fitted into a model to describe the relationship between shear stress, shear rate and apparent viscosity of the sludge. The rheological parameters from the viscosity model will be used to estimate the pumping power required in transporting the sludge slurries through pipelines and the heating requirement in a biorefinery.

2. Materials and methods

2.1. *Sample collection*

Sludge samples were collected from different WWTPs where they had undergone unique waste water treatment processes. The first sample (S1) was obtained after anaerobic digestion and stabilisation of primary and secondary treatment processes of municipal sewage sludge and stockpiled for two years at the SA Water Plant, Bolivar, South Australia. The second sample (S2) was collected from the Melbourne Water Western Treatment Plant, Victoria, Australia after aerobic digestion, anaerobic digestion and dewatering processes. The third sample (S3) was obtained from dewatered municipal sewage sludge that had been dosed with polymer (Ferric chloride) and centrifuged after primary and secondary treatment processes in Queensland Urban Utilities, Australia. Sample (S4) was obtained from dewatering S3 samples by partially drying large masses of the collected sludge in a drying oven at 45°C for 36 h and milling the dried samples.

2.2. *Sludge characterisation*

Particle size distribution of the sewage sludge samples was conducted in a particle size analyser which estimated the size of particles by scattering light at different angles and applying the Mie theory (Malvern Mastersizer 2000). The refractive index of sludge and water used for particle anal-

ysis were 1.52 and 1.33 respectively. The moisture content of all three samples were determined by the loss on drying the sludge in a drying oven at 40°C till a stable mass was obtained. Micrographic images of sludge samples were taken with a microscope (Zeiss AXIO) at a magnification of 10×.

Organic matter was determined using ISO 18122:2015 Standard (International Organization for Standardization, 2015). Pre-dried sludge sample was placed in a cold furnace and incinerated at 550°C for 5 h. The organic matter content was determined by the difference in weight before and after incineration over the weight of dry sludge.

CHNS analysis was conducted on dry S1, S2 and S3 sludge samples. An elemental analyser (Perkin Elmer 2400 series II CHNS/O Elemental Analyzer) was used to determine the CHN and S mass concentrations in the given sample using an analytical standard of Cystine (formula: $(SCH_2CH(NH_2)CO_2H)_2$) with known abundances of carbon (30%), hydrogen (5.1%), nitrogen (11.7%) and sulphur (26.7%). Oxygen was obtained by subtraction.

2.3. Rheological measurements

To study the viscosity of different types of sludge samples, slurries with different concentrations were prepared from S1, S2 and S3 using distilled water. The slurries were mixed with a Heidolph mixer at 90 rpm for 5 min. Rheological properties of the prepared slurries were measured at 25°C using a rotational rheometer (AntonPaar MCR301) with a cup and bob-like configuration which detects torque values as small as 1 nNm. A pressure cell configuration with a vane accessory was used as the cup and bob configuration. The vane configuration unlike the bob configuration is suitable for measuring the viscosity of settling slurries. The pressure cell configuration was equipped with a pressure cup (ID: 32 mm, Height: 71 mm) and a four-bladed vane impeller accessory (ID: 12 mm, Height: 40 mm) that was purchased from Anton Paar. To determine the universality, validity and repeatability of viscosity measurements with the selected rheometer configuration, the viscosity of a standard fluid was determined in triplicates with acceptable errors of <10%. The standard fluid which was manufactured in accordance with ISO 17025/ISO Guide 34 was purchased from Anton Paar. Viscosity measurements of sludge samples were conducted in four stages: (a) pre-shearing at 300 s^{-1} for 180 s at 25°C, (b) equilibration phase for 60 s, (c) linear ramp up of shear rate from 0 to 300 s^{-1} and (d) linear ramp down of shear rate from 300 to 0 s^{-1}. The cycle was repeated three other times and the average shear rate, shear stress and viscosity were plotted to determine the type of the fluid, yield stress and flow curve of the fluid. Viscosity measurements with errors <10% were accepted.

To study the effects of solid concentration on the viscosity of dewatered sludge, slurries of different solid concentrations were prepared from specific amounts of S4 using distilled water. Rheological tests were conducted using the Anton Paar MCR301 with similar accessories in four stages.

2.4. Rheological modelling and data analysis

The rheological behaviour of the slurries was characterised by fitting the experimental data into rheological models to show the dependency of shear stress on shear rate. Three rheological models including Ostwald de Vaele, Herschel-Bulkley and Bingham models (Hong et al., 2016) were used to characterise the slurries prepared from municipal sewage sludge samples using the following equations

$$\tau = K\dot{\gamma}^n \tag{1}$$

$$\tau = \tau_y + K\dot{\gamma}^n \tag{2}$$

$$\tau = \tau_y + \eta_B\dot{\gamma} \tag{3}$$

The rheological models were used to determine the yield stress τ_y (Pa), high shear limiting viscosity η_B (Pa.s), flow index n and flow consistency index K (Pa.s^n) from the shear stress τ (Pa) and shear rate γ (s^{-1}) data. A suitable rheological model will be estimated from a comparable correlation using the regression coefficient of each model.

2.5. Power requirement for pumping sludge slurries

Pumping power was calculated based on a pipeline with a flow rate of 1000 kg/hr and a pipe length of 15 m. Pumping power (P) required was estimated as a function of the slurry density (ρ), pipe length (L), pipe diameter (D), volumetric flow rate $\left(\dot{V}\right)$ and Reynolds number (Re_{MR}) in the equation (Wileman et al., 2012):

$$P = 128\rho\frac{\dot{V}^3 L}{\pi D^3 Re_{MR}} \tag{4}$$

The Reynolds number was determined in the laminar region using the Metzner and Reed method in the following equation (Metzner and Reed, 1955; Wileman et al., 2012):

$$Re_{MR} = \frac{\rho v^{(2-n)} D^n}{8^{(n-1)} K} \tag{5}$$

where n represents in power law index, v is the velocity of the slurry and K is the consistency index.

3. Results and discussion

3.1. Physical properties of sludge

The micrographs of sludge are shown in Fig. 1. As shown in Fig. 1a, sample S1 contains crystalline particles with relatively larger diameters compared to S2 in Fig. 1b. Sample S2 in Fig. 1b contains multiple tiny particles unlike sample S3 in Fig. 1c which contains larger flocs most likely due to the addition of the flocculation polymer in this sample. As shown in Fig. 2, the average particle sizes, d (50) of S1, S2 and S3 were determined to be 190 μm, 72 μm and 345 μm respectively. The differences in peak, average diameter and particle size range would be due to the different sources of feedstock, treatment processes, storage methods and biodegradability of the sludge samples, which affects the structure and form of the sludge particles (Houghton and Stephenson, 2002). The particle size distribution of sludge samples S1, S2 and S3 contained particles >1 μm. For all three samples, no particle with a size <0.4 μm was detected by the instrument. S1 showed a common peak between the particle size ranges of 200–400 μm. S2 and S3 indicated major peaks within a size range of 70–90 μm and 500–700 μm respectively. S3 appears to have the largest particle sizes, which is because of the addition of flocculants and coagulants which causes particulates to clump together to form bigger flocs. S2 was the freshest

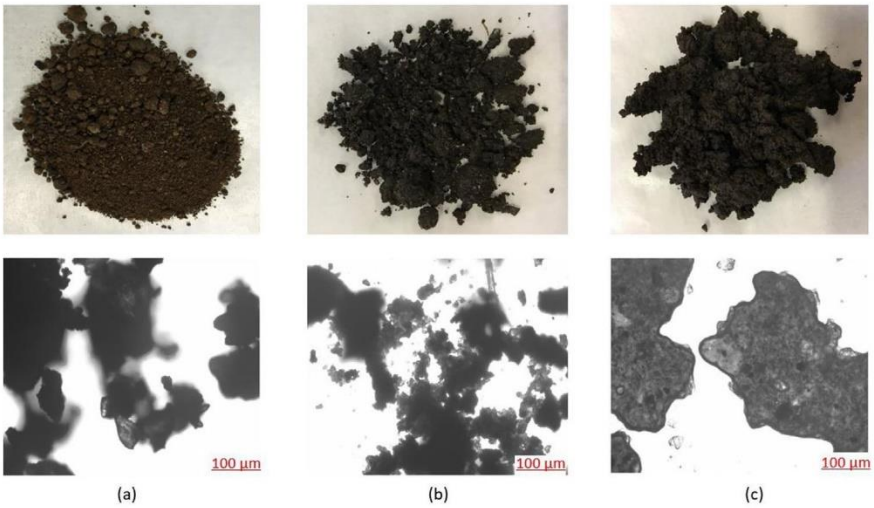

Fig. 1 – Micrograms of (a) S1, (b) S2, and (c) S3 sludge samples.

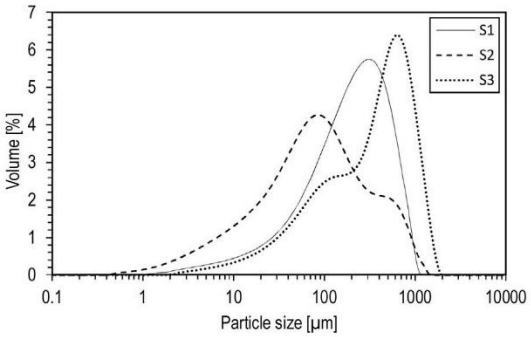

Fig. 2 – Average particle size distribution of S1, S2 and S3 sludge samples.

Table 1 – Characterisation of municipal sewage sludge.

Parameter, %	S1	S2	S3
Moisture content	32	52	82
Organic content (dry)	17	36	77
Ash Content (dry)	83	64	23
Carbon, afdw	34	60	49
Hydrogen, afdw	5	9	8
Nitrogen, afdw	4	7	8
Sulphur, afdw	5	6	4
Oxygen, afdw	52	18	31

sludge sample which has been less flocculated and coagulated hence the smaller particle sizes as compared to S1 which had undergone all the treatment processes till they were stabilised.

Particle size and particle size distribution affects the rheological behaviour of slurries. At a constant volume fraction, a decrease in particle size leads to an increase in the number of small particles in the fluid. An increase in the number of small particles increases the strength of the inter-particulate forces between the particles and increases the flow resistance of the fluid. Hence, a larger number of small particles increases the viscosity of the fluid. An increase in particle size distribution of particulates in a sample increases the packing fraction and the random dispersion of closely packed particulates. Large packing density decreases the viscosity of the slurry. Consequently, the viscosity of the slurries prepared from particles with a large particle size distribution are relatively lower than slurries prepared from particles with a smaller size distribution. (Luckham and Ukeje, 1999). According to the data shown in Fig. 2, the differences in the particle size distribution of the sludge samples increases in the order of S1 < S2 < S3 where S1 has the smallest particle size range and S3 has the largest particle size range. Consequently, the apparent viscosity of the sludge slurries is in the increasing order of S3 < S2 < S1. Particle size distribution may be insufficient to fully describe the rheological behaviour of sewage sludge slurries as the rheological behaviour is dependent on other factors which includes chemical compositions.

Municipal sewage sludge are semi-solid materials that consist of dispersed, soluble and insoluble particles with a wide range of sizes. The presence and interaction of these particles have a great influence on the properties of the sludge (Gregory, 1983). Samples of S3 possessed a high moisture content of 82% as S3 was freshly obtained from the drying pans after primary and secondary treatment of the sludge. Due to the high moisture content of 82%, S3 may require further dewatering to obtain higher solid concentrations (>18%w/w dry solids) during slurry preparations for HTL applications. Conversely, S1 contained low moisture content of 32% as shown in Table 1 as it was UV stabilised and stockpiled for several months. As shown in Table 1, S2 and S3 contain high amounts of carbon and organic materials that are suitable for renewable crude-like oil production via HTL. Sample S1 has the least amount of organic matter and carbon content which implies that it would produce less crude-like oil with low carbon recovery. Preferred feedstock for renewable crude oil production via HTL process should be organic rich with high carbon content. From the different types of sludge used in this study, the suitability of HTL feedstock based on the organic and carbon content are in the increasing order of S1 < S2 < S3. Nonetheless, the carbon content in each type of sludge especially stockpiled biosolids, S1 can be recovered by mixing it with other types of sludge obtained from other parts of the WWTPs to increase the conversion of sludge to renewable crude oil while reducing solid waste simultaneously.

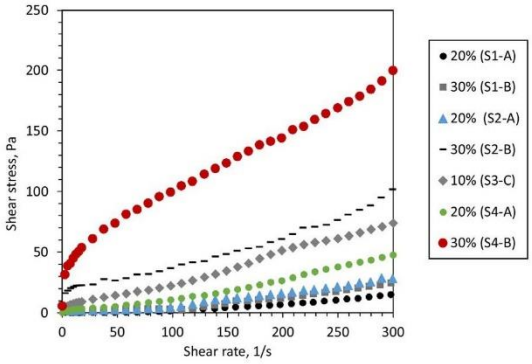

Fig. 3 – Rheograms of stockpiled biosolids and dewatered sludge at 25°C obtained from the average shear stress and shear rate data with an average standard error of 0.64%.

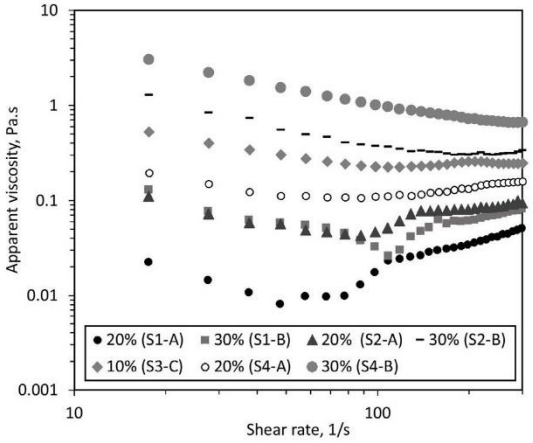

Fig. 4 – Flow curves of S1, S2, S3 and S4 sludge samples at 25 °C obtained from the average apparent viscosity and shear rate data with an average standard error of 0.64%.

3.2. *Rheological measurements*

3.2.1. *Shear stress and shear rate*

The viscosity of the Newtonian standard fluid was determined to be 0.726 ± 0.004 Pa.s. This indicates the validity and accuracy of the method for viscosity measurement. As shown in Fig. 3, the shear stress-shear rate curves for municipal sewage sludge slurries are non-linear. Consequently, municipal sewage sludge slurries exhibits non-Newtonian characteristics at 25°C. The rheological behaviour of sludge slurries is due to the dispersed particles in sludge which is dependent on the pH, solid content and presence of flocculants in each sample (Sanin, 2002). Municipal sewage sludge consists of a mixture of particles with different sizes and shapes. When these particles are in motion, they collide against one another with a certain force which is dependent on their shape, size and cohesiveness of the particles. Hence, the amount of force (stress) at each shear rate will vary per sample (Brookfield, 2017). This variable force translates as variable viscosities at different shear rates which makes sludge a non-Newtonian slurry. The rheological parameters of shear stress and shear rate were fitted into rheological models to characterise the non-Newtonian behaviour of the slurries as the plotted rheograms in Fig. 3 does not fully describe the slurry behaviour.

All sludge samples shown in Fig. 3 do not exhibit yield stress with the exception of S2-B which exhibits Bingham plastic characteristics with a yield stress at 30 w/w% dry solid concentration. The yield stress refers to the minimum force that needs to be overcome before the fluid can just begin to flow. The yield stress requirement for flow of S2 is mainly due to the strong bonds of forming the larger flocs in S2. When the bonds between the flocs are extremely strong, a stronger force is required to break these bonds before the slurry can begin to move freely (Brookfield, 2017).

Slurries prepared from S3 and S4 samples exhibited a similar rheological effect as S2 samples. Both S3 and S4 which have the same composition, but different moisture contents were non-Newtonian. At lower solid concentrations, these slurries behave close to Newtonian fluids and deviate from Newtonian behaviour with an increase in solid concentration. Slurries prepared from 20 w/w% S2 solid concentrations behaved like Newtonian fluids. As the solid concentration of the slurry increased, the fluid becomes more non-Newtonian. This is similar to the investigation on the rheological characterisation of municipal sewage sludge conducted by Eshtiaghi et al. (2013) where they stated that sewage sludge slurries with solid concentration >3% deviate from Newtonian behaviour. At lower shear rates, the shear applied on the samples deform the flocs. As the shear rate is increased, these flocs break into smaller particles, increasing the friction between the particles, the shear stress and apparent viscosity (Brookfield, 2017). Hence the shear stress and apparent viscosity of sludge increases with an increase in solid concentration.

3.2.2. *Effects of shear rates on apparent viscosity of slurries prepared from different types of sludge*

Each type of sludge from different parts of the WWTP is chemically, biologically and physically different from another. The rheological properties of municipal sewage sludge can be complex due to the continuous ageing and microbial activity in the sludge. The rheological properties of municipal sewage sludge for HTL applications were analysed from the log apparent viscosity-log shear rate plots of all samples obtained after experimental analysis. As shown in Fig. 4, the apparent viscosity of sludge at lower shear rates decrease with an increase in shear rate which indicates that the fluids are non-Newtonian. This is in agreement with other investigations conducted on fresh sludge characteristics in the WWTPs applications as viscosity is dependent on shear rate (Cao et al., 2016). High viscosity at lower shear rates signifies that sludge is viscous when at rest and its viscosity gradually reduces and thins out at high shear rates. However, above a shear rate of 80 s^{-1}, the apparent viscosity of S1 and 20 wt% of S2 slurries begin to increase with an increase in shear rate. This effect may be due to the instability of the slurry after a critical shear rate. The point at which the apparent viscosity of sludge increases signifies the critical shear rate for flow instability. The apparent viscosity above this critical shear rate does not show the real properties of the slurry. The addition of ferric chloride as a coagulant to sludge in WWTP affects the apparent viscosity of S3 sludge. According to Zengeni (2016), the presence of coagulants and flocculants increases the strength on the bonds binding the flocs and agglomerates in the sludge thereby increasing yield stress which relates to an increase in the apparent viscosity of the sludge. Consequently, sludge slurries with polymer dosages (S3 and S4) will have relatively higher viscosities compared to slurries without polymer. Hence the addition of polymer dosages presents a trade off in the context of a HTL

biorefinery in being able to dewater sludges easier to a desired dry matter content and increase pumping energy requirement due to the higher viscosities.

Comparing the flow curves of the lowest solid concentration prepared from S1, S2 and S3 as displayed in Fig. 4, S1 samples have the least apparent viscosities. The presence of organic materials that are rich in polysaccharides and proteins significantly contribute to the inter-particulate interractions and viscosity of sludge (Li et al., 2014). According to Li et al. (2014), both organic and inorganic contents of sludge which includes mineral salts, suspended particles and metal ions contribute to sludge viscosity by altering the adhesive and cohesive characteristics of the sludge in the process of forming agglomerates. Moisture content, water holding capacity and the presence of polymeric materials enhance the formation of these agglomerates and this increases the adhesive and cohesive forces in the particles. This explains why S1, with the least amount of organic materials, low moisture content and highest amount of inorganic materials as shown in Table 1 has the lowest viscosity range (Fig. 4). Even though the lowest solid concentration of S3 used in this study is 50% less than the amount of solids used to prepare the lowest concentration of S1 and S2, S3 still records a high range of apparent viscosity within the measured shear rate range. This is mainly due to the high organic contents of the sludge which is possibly rich in proteins and polyssacharides as well as the presence of coagulants which possibly improves the viscosity of the slurry.

The changes in the apparent viscosity of sludge with an increase in shear rate may be due to presence and properties of the particulate in the suspension. According to Eshtiaghi et al. (2013), sludge comprises of colloids and organic materials, flocs and extra polymeric substances (EPS). The EPS are gel-like polymeric structures that are held together by electrostatic and hydrogen bonds (Markis et al., 2016; Nazari et al., 2017). Strengthening of these bonds by increasing solid concentration which increases the hydrodynamic and non-hydrodynamic interactions between flocs can increase the apparent viscosity. Sludge from different parts of the processing plants contains different concentrations of soluble EPS which plays a vital role in holding large amounts of bound water by adsorption, chemical hydration, crystallisation and osmotic effect. Consequently, larger amounts of EPS decrease the dewaterability of the sludge. Sludge may contain extra cellulosic polymeric materials that possess high-molar mass and high viscosity that bind sludge particles together. Hence, an increase in the amount of EPS can increase the apparent viscosity of sludge as the presence of such polymeric materials in sludge greatly affects the viscosity of the sludge (Sanin, 2002).

3.2.3. *Influence of solid concentration on the apparent viscosity of dewatered sludge*

Solid concentration of dewatered sludge (S4) has significant impact on apparent viscosity. As shown in the flow curves in Fig. 5, the apparent viscosity of sludge increases with an increase in solid concentration at constant temperatures as expected. At lower solid concentration of 15%w/w and 20%w/w, the apparent viscosity of S4 decreases with an increase in shear rate until a critical shear rate and then the curve gradually increases with increasing shear rate. This indicates that lower solid concentration of dewatered sludge exhibits a shear thinning behaviour at lower shear rates. Above shear rates of 105 s^{-1}, dewatered sludge begins to behave as a non-Newtonian fluid with shear thickening characteristics. Dilute slurries prepared from dewatered sludge deviate from shear thinning behaviour at higher shear rates.

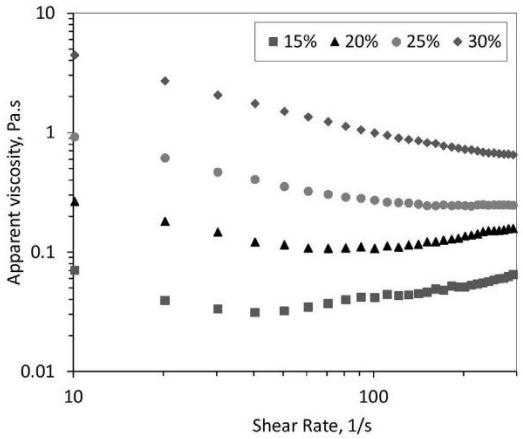

Fig. 5 – Flow curves of dewatered sludge indicating the effects of solid concentration on the apparent viscosity and shear rates at 25 °C obtained from the average apparent viscosity and shear rate data with an average standard error of 0.68%.

The findings from studying the influence of solid concentration on apparent viscosity of dewatered sludge show that solid concentration is directly proportional to the apparent viscosity of sludge. At higher solid concentrations, particles interract more with each other forming a network of particles that influences the apparent viscosity of the sludge (Cao et al., 2016). The apparent viscosity of highly concentrated slurries are higher than dilute slurries due to entanglement and intermolecular forces joining the particles together. In highly concentrated slurries where flocs occupy larger volumes in the dispersion medium, the force required to disperse the solids in the dispersion medium increases. This increased force translates as an increase in apparent viscosity of the sludge (Brookfield, 2017).

3.3. *Rheological models and data analysis*

The shear rate-shear stress data were fitted into Ostwald, Bingham and Herschel-Bulkley models at specific temperatures as shown in Fig. 6. One-way ANOVA coupled with a Tukey HSD post hoc test was used to validate the models to predict the best model that fits the rheological data. From the ANOVA test conducted, there was a significant difference between all three models used on the samples containing 20 wt% solids; S1-A [$F(4, 145) = 83.04$, $p < 0.05$], S2-A [$F(4, 145) = 73.76$, $p < 0.05$] and S3-C [$F(4, 145) = 42.11$, $p < 0.05$] as shown in Table S1, Table S3 and Table S5 respectively on the Supplementary Information. The ANOVA test was insufficient to specify exactly what the cause of these differences were, hence, a post hoc test was conducted. The Tukey HSD post hoc test revealed a significant difference between the shear rate and shear stress values as expected. There was no significant difference between the experimental values of shear stress and the modelled shear stress values using all three rheological models as the absolute mean differences as shown in Table S2, Table S4 and Table S6 of the Supplementary Information sheet were less than the critical range. No significant difference between the models implies that all three models fit the experimental data and are in agreement with one another. However, a comparison

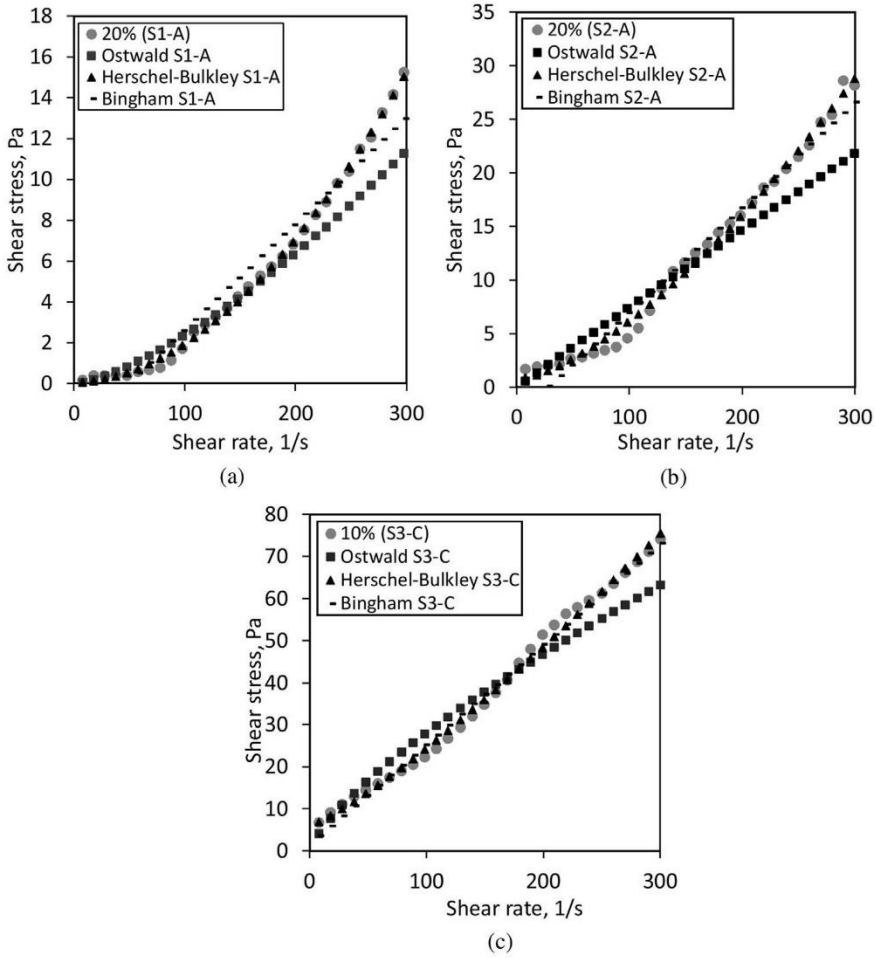

Fig. 6 – Shear stress-shear rate data with rheological models of (a) 20 w/w% S1, (b) 20 w/w% S2, and (c) 10 w/w% S3.

made between the absolute mean differences of individual pairs (each rheological model and experimental data) reveals that the Herschel-Bulkley model best fits the experimental data as it yields the least mean difference of 0.0001, 0.0004 and 0.0001 for S1-A, S2-A and S3-C respectively.

The flow index, n for Herschel-Bulkley model was determined to be greater than unity ($n > 1$) for all samples which clearly indicates and confirms that the slurries are non-Newtonian with shear thickening behaviour. The degree of shear thickening was in the order of S3 < S2 < S1. Shear thickening behaviour increases with an increase in solid concentration. As solid concentration in S4 increases, the fluid exhibits more of a shear thickening behaviour.

Increasing the concentration of solids in the slurries increased the value of the Herschel-Bulkley consistency index for stockpiled biosolids and sewage sludge. An increase in the value of k corresponds to an increase in the apparent viscosity of the fluid as it represents the cohesiveness of the fluid (Pollice et al., 2006). Consequently, the apparent viscosity of each tested slurry increased with an increase in solid concentration as expected.

According to Seyssiecq et al. (2003), yield stress is the minimum amount of stress that needs to be overcome to break the cohesive Van der-Waals forces existing in the network of flocs. Yield stress can interfere with mass flow and heat transfer processes of slurries during the HTL process. The Herschel-Bulkley yield stress increases with solid concentration for all sludge types. Yield stresses are low at lower solid concentrations and increase with solid concentration. For sludge samples, yield stress increases in the order S1 < S2 < S3. The yield stress of 10 w/w% of S3 was higher than the yield stresses for S1 and S2 at their lowest solid concentrations of 20 w/w%. High yield stress in S3 is mainly due to the polymer dose (Wang et al., 2011) as the presence of flocculants (Ferric chloride) will increase the strength of the bonds between agglomerates and hence increase the yield stress of the slurry (Zengeni, 2016).

3.4. *HTL-Biorefinery application of rheological data*

Rheological characterisation of sludge slurries and the prediction of a suitable rheological model is essential for accurate calculation of the friction loss and head loss that influence pipeline and pump selections (Walmsley et al., 2014). The parameters of the sludge slurries obtained from the rheological model were used to estimate the friction loss in the laminar flow regimes which was determined using the Reynolds number. Reynolds number is inversely proportional to the viscosity of a Newtonian fluid as its viscosity is constant (Water Environment Federation, 2012). Since the sewage sludge slurries were non-Newtonian fluids whose viscosities are not constant as they are dependent on shear rate, a different approach was used to estimate the Reynolds number

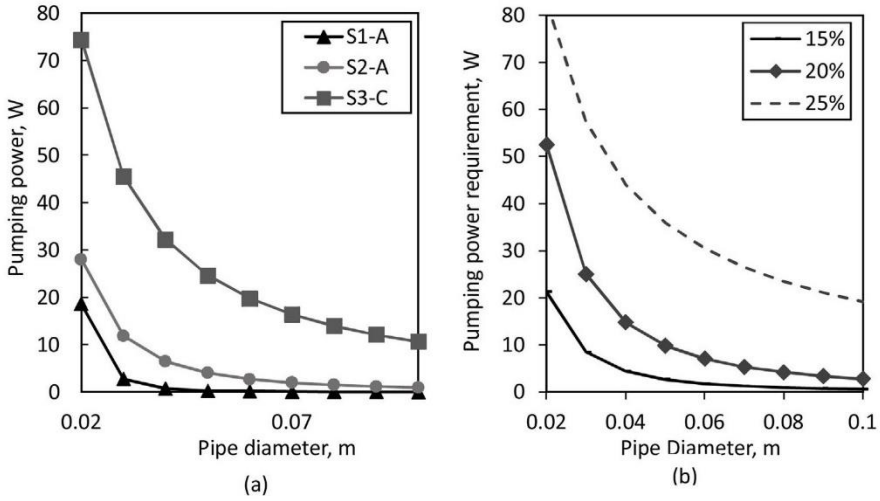

Fig. 7 – Pumping power requirements under laminar flow regime (a) Power requirements for different types of sludge, (b) Power requirement for different solid concentrations of dewatered sludge, S4.

and head loss for Non-Newtonian fluids. The type of non-Newtonian fluid (pseudoplastic, Bingham or shear thickening) greatly affects the constants used in calculating the Reynolds number as the constants, especially the yield stress and flow consistency index, vary per each type of fluid. The shear rate used was directly proportional to the fluids velocity in the pipeline.

Pumping power was calculated based on a plant with an assumed flow rate of 1000 kg/hr using the average values of the rheological parameters after rheological measurements with an average standard error of 0.64%. Pumping power of sludge slurries decreases with an increase in pipe diameter as expected. In designing a HTL system, it is important to choose the size of pipelines carefully as it greatly affects capital cost. Increasing the diameters of a pipe increases the cost of the pipe. Large pipe diameters decrease the pressure drop along the pipeline. Lower pressure drops in pipelines reduce the power required to pump the slurry and eventually decrease the daily energy consumption and operational cost in transporting the slurry (Aspiration Energy, 2019). Pipe sizing and selection is critical for maximum pump efficiency at a minimal cost. The minimum total cost is calculated as the sum of the investment cost which is dependent on the size of the pipe diameter and the operation cost which is derived from the cost incurred whiles pumping the slurry (Lotito and Lotito, 2014). As shown in Fig. 7a, pump power requirement of different sludge slurries was in an increasing order of S1 < S2 < S3. The increase in pump power for the sludge slurries is synonymous to the increase in apparent viscosity of these slurries and an increase in yield stress. An increase in the viscosity and yield stress of sludge decreases the pump efficiency which increases the power required to pump the fluid (Wilson et al., 2006). The pump power required for S2 is larger than S1 due to the higher apparent viscosity and the presence of the yield stress implies that the force required to pump S2 needs to be greater than the minimum force (yield stress) required to be overcome before the fluid begins to move. Hence, the yield stress increases the pumping power required for S2 slurry to continue in motion. During pump selection, it is important to choose a pump that can overcome the yield stress of the slurry as yield stress affects pump performance. The pumping power for S3 shown in Fig. 7a is mainly as a result of the high apparent viscosity recorded due to its high moisture content and the positive effects of the added coagulants in the sludge.

As shown in Fig. 7b, the pumping power requirement increases with an increase in solid concentration in dewatered sludge slurries (S4). This result is anticipated as increasing the solid loading in the slurry will increase the resistance of the slurry to flow freely hence a higher energy input will be required for the slurry to move at a desired velocity. The presence of solids in a slurry increases the slurry viscosity. An increase in the apparent viscosity of the slurry consequently increases the pump power required to transport the slurry (Wilson et al., 2006).

4. Conclusion

The rheological properties of sludge and stockpiled biosolids vary from different sources and different sampling points from the WWTP. The shear rate-shear stress data indicated that stockpiled biosolids and sludge were non-Newtonian fluids with shear thickening behaviour. Solid concentration between 15 wt% and 30 wt% significantly influenced the apparent viscosity of sludge and stockpiled biosolids such that an increase in solid concentration increases the apparent viscosity of sludge. The apparent viscosity of sewage sludge was determined to be in the increasing order of stockpiled biosolids (0.008–0.05 Pa.s) < Sludge without polymer dosage (0.04–0.11 Pa.s) < dewatered sludge with polymer dosage (0.1–0.2 Pa.s). The Herschel-Bulkley viscosity model best fitted the experimental data from statistical analysis. The parameters obtained from the Herschel-Bulkley model of the sludge slurries, specifically the yield stress and the flow consistency index, can be used in estimating various factors such as the friction factor and the Reynolds number required for designing pipelines. Elucidating the rheological behaviour of sludge helps in specifying design parameters for feedstock transportation during HTL process. Accurate prediction of the rheological properties of sludge can help in the specifying the economic pipe diameter during sizing of pipelines and fittings. The power requirement for pumping sludge are in the increasing order of stockpiled biosolids < Sludge without polymer dosage < Sludge with polymer dosage which is similar to an increase in apparent viscosity of the sludge slurries.

Conflict of interests

The authors declare that they have no known competing financial interests or personal relationships that could have appeared to influence the work reported in this paper.

Declaration of Competing Interest

The authors report no declarations of interest.

Acknowledgements

The authors wish to acknowledge SA Water, Melbourne Water and Queensland Urban Utilities in particular Mr. Nick Swain and Mr Bill Pemberton for providing the feedstock.

Funding: This work was supported by Southern Oil Refining and the Australian Research Council's Linkage Projectsfunding scheme [Project LP150101241].

Appendix A. Supplementary data

Supplementary material related to this article can be found, in the online version, at doi:https://doi.org/10.1016/j.cherd.2020.12.004.

References

Anastasakis, K., Biller, P., Madsen, R.B., Glasius, M., Johannsen, I., 2018. Continuous hydrothermal liquefaction of biomass in a novel pilot plant with heat recovery and hydraulic oscillation. Energies 11 (2695), 1–23.

Aspiration Energy, from 2019. Why Pipe Sizing and Flow Rate Is Important? https://aspirationenergy.com/why-pipe-sizing-and-flow-rate-is-important/.

Berglin, E.J., Enderlin, C.W., Schmidt, A.J., 2012. Review and Assessment of Commercial Vendors/Options for Feeding and Pumping Biomass Slurries for Hydrothermal Liquefaction. (PNNL-21981). Pacific Northwest National Laboratory, U.S.

Billing, J., Hallen, R., Schmidt, A., Snowden-Swan, L., 2017. Hydrothermal Processing of Biomass. 2017 Project Peer Review. DOE Bioenergy Technologies Office (BETO). Pacific Northwest National Laboratory.

Brookfield, A., 2017. In: Brookfield, A. (Ed.), More Solutions to Sticky Problems. Middleboro, USA, p. 16.

Cao, X., Jiang, Z., Cui, W., Wang, Y., Yang, P., 2016. Rheological properties of municipal sewage sludge: dependency on solid concentration and temperature. Procedia Environ. Sci. 31, 113–121.

Dick, R.I., Ewing, B.B., 1967. The rheology of activated sludge. Water Pollution Control Federation 39, 543–560.

Elliott, D.C., Hart, T.R., Schmidt, A., Neuenschwander, G.G., Rotness, L.J., Olarte, M.V., Zacher, A.H., Albrecht, K., Hallen, R.T., Holladay, J.E., 2013. Process development for hydrothermal liquefaction of algae feedstocks in a continuous-flow reactor. Algal Res. 2, 445–454.

Eshtiaghi, N., Markis, F., Yap, S.D., Baudez, J.-C., Slatter, P., 2013. Rheological characterisation of municipal sludge: a review. Water Res. 47, 5493–5510.

Forster, C.F., 2002. The rheological and physico-chemical characteristics of sewage sludges. Enzyme Microb. Technol. 30, 340–345.

Gregory, J., 1983. Physical properties. In: Carberry, J.B., Englande, A.J.J. (Eds.), Sludge Characteristics and Behavior, 66. Martinus Nijhoff Publishers, Hague.

He, W., Park, C.S., Norbeck, J.M., 2009. Rheological study of comingled biomass and coal slurries with hydrothermal pretreatment†. Energy Fuels 23 (10), 4763–4767, http://dx.doi.org/10.1021/ef9000852.

Hong, E., Yeneneh, A.M., Kayaalp, A., Sen, T.K., Ang, H.M., Kayaalp, M., 2016. Rheological characteristics of municipal thickened excess activated sludge (TEAS): impacts of pH, temperature, solid concentration and polymer dose. Res. Chem. Intermed. 42 (8), 6567–6585.

Houghton, J.I., Stephenson, T., 2002. Particle size analysis of digested sludge. Water Res. 36 (18), 4643–4647.

International Organization for Standardization, I, 2015. Solid biofuels — determination of ash content. In: ISO 18122 Solid Biofuels — Determination of Ash Content. International Organization for Standardization, Switzerland.

Leonie, M., Graeme, K., 2009. *Use of biosolids in agriculture*. New South Wales.

Li, B., Wang, F., Chi, Y., Yan, J.H., 2014. Adhesion and cohesion characteristics of sewage sludge during drying. Dry. Technol. 32 (13), 1598–1607, http://dx.doi.org/10.1080/07373937.2014.910522.

Lotito, V., Lotito, A.M., 2014. Rheological measurements on different types of sewage sludge for pumping design. J. Environ. Manage. 137, 189–196.

Lotito, V., Sinosa, L., Mininni, G., Antonacci, R., 1997. The rheology of sewage sludge. Water Sci. Technol. 36 (11), 79–85.

Luckham, P.F., Ukeje, M.A., 1999. Effect of particle size distribution on the rheology of dispersed systems. J. Colloid Interface Sci. 220, 347–356.

Markis, F., Baudez, J.C., Parthasarathy, R., Slatter, P., Eshtiaghi, N., 2016. Predicting the apparent viscosity and yield stress of mixtures of primary, secondary and anaerobically digested sewage sludge: simulating anaerobic digesters. Water Res. 100, 568–579.

Metzner, A.B., Reed, J.C., 1955. Flow of non-newtonian fluids-correlation of the laminar, transition, and turbulent-flow regions. Aiche J., 434–440.

Nazari, L., Yuan, Z., Santoro, D., Sarathy, S., Ho, D., Batstone, Xu, C., Ray, M.B., 2017. Low-temperature thermal pre-treatment of municipal wastewater sludge: process optimization and effects on solubilization and anaerobic degradation. Water Res. 113, 111–123.

Noguchi, T., Noda, Y., Yamasaki, Y., Inoue, S., Matsumura, Y., Kawai, Y., Shimizu, Y., Minowa, T., 2011. The rheological characteristics of biomass slurry under high pressure and high temperature. J. Jpn. Inst. Energy 90.

Pollice, A., Giordano, C., Laera, G., Saturno, D., Mininni, G., 2006. Rheology of sludge in a complete retention membrane bioreactor. Environ. Technol. 27, 723–732.

Sanin, F.D., 2002. Effect of solution physical chemistry on the rheological properties of activated sludge. Water SA 28 (2).

Seyssiecq, I., Ferrasse, J.-H., Roche, N., 2003. State-of-the-art: rheological characterisation ofwastewater treatment sludge. Biochem. Eng. J. 16, 41–56.

Shammas, N.K., Wang, L., 2008. Transport and pumping of sewage sludge and biosolids. In: Wang, L.K., Shammas, N.K., Hung, Y.T. (Eds.), Handbook ofEnvironmental Engineering, 7. The Humana Press, Totowa, NJ.

Skaggs, R.L., Coleman, A.M., Seiple, T.E., Milbrandt, A.R., 2018. Waste-to-Energy biofuel production potential for selected feedstocks in the conterminous United States. Renew. Sustain. Energy Rev. 82, 2640–2651.

Torri, S., Cabrera, M., 2017. Environmental impact of biosolids land application. In: Collins, M. (Ed.), Organic Waste: Management Strategies, Environmental Impact and Emerging Regulations. Nova Science Publishers, Inc, Hauppauge, NY, pp. 185–208.

Walmsley, H., Modulon, G., Schmiedte, W., Taylor, D., 2014. Going the Distance: Primary Sludge Pumping. GHD Pty Ltd and 4Malabar Alliance, NSW, Australia.

Wang, Y., Dieude-Fauvel, E., Dentel, S.K., 2011. Physical characteristics of conditioned anaerobic digested sludge – a fractal, transient and dynamic rheological viewpoint. J. Environ. Sci. 23 (8), 1266–1273.

Water Environment Federation, 2012. Solids Process Design and Management. McGraw-Hill Education, Europe.
Wileman, A., Ozkan, A., Berberoglu, H., 2012. Rheological properties of algae slurries for minimizing harvesting energy requirements in biofuel production. Bioresour. Technol. 104, 432–439.
Wilson, K.C., Addie, G.R., Sellgren, A., Clift, R., 2006. Effect of solids on pump performance. In: Slurry Transport Using Centrifugal Pumps, 3rd ed. Springer, Boston, MA, pp. 227–248.
Wolny, L., Wolski, P., Zawieja, I., 2008. Rheological parameters of dewatered sewage sludge after conditioning. Desalination 222 (1), 382–387.
Yen, P.S., Chen, L.C., Chien, C.Y., R.M., W, Lee, D.J., 2002. Network strength and dewaterability of flocculated sludge. Water Res., 539–550.
Zengeni, B.T., 2016. Bingham Yield Stress and Bingham Plastic Viscosity of Homogenous Non-newtonian Slurries. Masters of Technology Mechanical Engineering), Cape Peninsula University of Technology, Cape Town, South Africa.
Zhang, Q., Hu, J., Lee, D.J., Chang, Y., Lee, Y.J., 2017. Sludge treatment: current research trends. Bioresour. Technol. 243, 1159–1172, http://dx.doi.org/10.1016/j.biortech.2017.07.070.

SUPPLEMENATRY INFORMATION SHEET

Rheological studies of municipal sewage sludge slurries for hydrothermal liquefaction biorefinery applications

Sylvia Y. Edifor*[, a], Quoc D. Nguyen[a], Philip van Eyk[a], Patrick Biller[b] and David M. Lewis[a]

[a]School of Chemical Engineering and Advanced Materials, The University of Adelaide, 5005 Adelaide, SA

[b]Department of Engineering-Biological and Chemical Engineering, Aarhus University, 8200 Aarhus, Denmark

*Corresponding Author's email: sylvia.edifor@adelaide.edu.au

Table 1s. ANOVA results for 20% S1-A

Source of Variation	SS	df	MS	F	P-value	F crit
Between Groups	521352	4	130338	83.04	1.62E-36	2.43
Within Groups	227601.6	145	1569.67			
Total	748953.6	149				

Table 2s. Tukey HSD test for 20% S1-A

Comparison	Absolute mean difference	Critical range	Results
Shear rate-Shear stress	147.23	27.92	Means significantly different
Shear rate-Ostwald	147.87	27.92	Means significantly different
Shear rate-HB	147.23	27.92	Means significantly different
Shear rate-Bingham	147.22	27.92	Means significantly different
Shear stress-Ostwald	0.63	27.92	Not Significantly different
Shear stress-HB	0.0001	27.92	Not Significantly different
Shear stress-Bingham	0.008	27.92	Not Significantly different
Ostwald-HB	0.63	27.92	Not Significantly different
Ostwald-Bingham	0.64	27.92	Not Significantly different
HB-Bingham	0.008	27.92	Not Significantly different

Table 3s. ANOVA results for 20% S2-A

Source of Variation	SS	df	MS	F	P-value	F crit
Between Groups	479012.9	4	119753.2	73.76	5.52E-34	2.43
Within Groups	235418	145	1623.57			
Total	714430.9	149				

Table 4s. Tukey HSD test to 20% S2-A

Comparison	Absolute mean difference	Critical range	Results
Shear rate-Shear stress	141.01	28.4	Means significantly different
Shear rate-Ostwald	142.05	28.4	Means significantly different
Shear rate-HB	141.01	28.4	Means significantly different
Shear rate-Bingham	141.02	28.4	Means significantly different
Shear stress-Ostwald	1.04	28.4	Not Significantly different
Shear stress-HB	0.0004	28.4	Not Significantly different
Shear stress-Bingham	0.003	28.4	Not Significantly different
Ostwald-HB	1.04	28.4	Not Significantly different
Ostwald-Bingham	1.03	28.4	Not Significantly different
HB-Bingham	0.003	28.4	Not Significantly different

Table 5s. ANOVA results for 20% S3-C

Source of Variation	SS	df	MS	F	P-value	F crit
Between Groups	321076.4	4	80269.11	42.11	2.14E-23	2.43
Within Groups	276396.3	145	1906.18			
Total	597472.7	149				

Table 6s. Tukey HSD test for 20% S3-C

Comparison	Absolute mean difference	Critical range	Results
Shear rate-Shear stress	115.3337	30.76867	Means significantly different
Shear rate-Ostwald	116.5684	30.76867	Means significantly different
Shear rate-HB	115.3338	30.76867	Means significantly different
Shear rate-Bingham	115.3966	30.76867	Means significantly different
Shear stress-Ostwald	1.2347	30.76867	Not Significantly different
Shear stress-HB	0.000124	30.76867	Not Significantly different
Shear stress-Bingham	0.062977	30.76867	Not Significantly different
Ostwald-HB	1.234576	30.76867	Not Significantly different
Ostwald-Bingham	1.171723	30.76867	Not Significantly different
HB-Bingham	0.062853	30.76867	Not Significantly different

Chapter 5:

Viscosity variation of model compounds during hydrothermal liquefaction under subcritical conditions of water

Statement of Authorship

Title of Paper	Viscosity variation of model compounds during hydrothermal liquefaction under subcritical conditions of water
Publication Status	☑ Published ☐ Accepted for Publication ☐ Submitted for Publication ☐ Unpublished and Unsubmitted w ork w ritten in manuscript style
Publication Details	Edifor, S. Y.; Nguyen, Q. D.; Van Eyk, P.; Biller, P.; Lewis, D. M., Viscosity variation of model compounds during hydrothermal liquefaction under subcritical conditions of water. Industrial & Engineering Chemistry Research 2021, 60, 980-989.

Principal Author

Name of Principal Author (Candidate)	Sylvia Yawa Edifor		
Contribution to the Paper	Designed Experiments Conducted experiments Data analysis and interpretation Drafted the manuscript and acted as corresponding author		
Overall percentage (%)	80		
Certification:	This paper reports on original research I conducted during the period of my Higher Degree by Research candidature and is not subject to any obligations or contractual agreements with a third party that would constrain its inclusion in this thesis. I am the primary author of this paper.		
Signature		Date	22/01/2021

Co-Author Contributions

By signing the Statement of Authorship, each author certifies that:

i. the candidate's stated contribution to the publication is accurate (as detailed above);
ii. permission is granted for the candidate in include the publication in the thesis; and
iii. the sum of all co-author contributions is equal to 100% less the candidate's stated contribution.

Name of Co-Author	Quoc Dzuy Nguyen		
Contribution to the Paper	Assistance with interpretation and presentation of data Evaluating, editing and reviewing of manuscript		
Signature		Date	29-01-2021

Name of Co-Author	Philip van Eyk		
Contribution to the Paper	Concept development Supervised development of work Assistance with interpretation, drafting and review of manuscript		
Signature		Date	28/1/2021

Please cut and paste additional co-author panels here as required.

Name of Co-Author	Patrick Biller		
Contribution to the Paper	Assistance with interpretation and presentation of data Drafting and review of manuscript		
Signature		Date	22.01.2021

Name of Co-Author	Tony Hall		
Contribution to the Paper	Assistance with interpretation and presentation of data Drafting and review of manuscript		
Signature		Date	24.01.2021

Name of Co-Author	David M. Lewis		
Contribution to the Paper	Assistance with interpretation and presentation of data Drafting and review of manuscript		
Signature		Date	28/01/2021

I&EC research
Industrial & Engineering Chemistry Research
pubs.acs.org/IECR
Article

Viscosity Variation of Model Compounds during Hydrothermal Liquefaction under Subcritical Conditions of Water

Sylvia Y. Edifor,* Quoc D. Nguyen, Philip van Eyk, Patrick Biller, Tony Hall, and David M. Lewis

Cite This: *Ind. Eng. Chem. Res.* 2021, 60, 980−989
Read Online
ACCESS | Metrics & More | Article Recommendations | Supporting Information

ABSTRACT: Recent assessments in waste-to-energy technologies highlight hydrothermal liquefaction (HTL) as a suitable process for converting organic-rich waste with high moisture content into a useful resource. Organic waste materials, including sewage sludge, food, and agricultural waste residues, typically contain lipids, carbohydrates, proteins, and lignin with varying compositions depending on their origin. Fluid properties of reacting HTL slurries under subcritical water conditions, particularly viscosity and density, affect material flow and heat transfer in both batch and continuous HTL process systems. Real-time viscosity variations of 20 wt % water slurries of model compounds, sunflower oil, sucrose, and soy protein were determined in a stirred tank batch reactor using the Metzner−Otto method. Measured torque on the impeller shaft at a fixed impeller speed was used to determine the changes in the viscosity of the reacting slurry at different reaction temperatures. Changes in the viscosity of the sunflower oil mixture were insignificant as compared to viscosity variations with sugar- and soy protein-derived feedstock. The viscosity of the soy protein solution decreased rapidly with the temperature during hydrolysis of polypeptides into amino acids between 25 and 100 °C. Further increase in the temperature led to minimal changes in viscosity as more soluble compounds were produced above 100 °C. The viscosity of the sucrose solution changed significantly above 250 °C when carbon compounds precipitated from the solution. Viscosity variations of mixtures of model compounds were determined to predict viscosity changes in biomass.

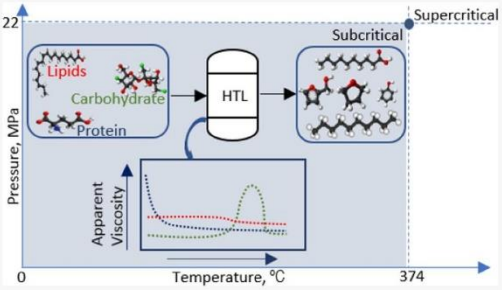

1. INTRODUCTION

There is a global need to develop a sustainable solid waste disposal solution to manage food waste, agricultural waste residues, and municipal sewage sludge in a more sustainable fashion. A global shift to thermal conversion technologies and processes is one effective way to convert large amounts of solid waste into useful products rather than landfilling and combustion for energy. Hydrothermal liquefaction (HTL) is a thermochemical depolymerization process that converts single-phase (liquids such as pure lipids/water mixture) and binary-phase (solids and liquids from biomass/water mixtures) feedstock into multiphase products (solid, liquid, and gas). HTL uses pressurized water to convert macromolecules in biomass including solid waste materials into crude like oil, aqueous, solid, and gas phase products under near critical conditions of elevated temperatures between 280 and 370 °C and pressures between 10 and 25 MPa.[1−3] During the HTL process, a series of complex reactions, which include depolymerization, dehydration, deamination, condensation, decarboxylation, and recombination reactions,[2,4] occur to produce intermediate and final products. The macromolecules in biomass comprise lipids, proteins, carbohydrates, and lignin in different variations and proportions.[5,6] Under HTL conditions, the elevated temperatures and pressures greatly influence the transformation of these macromolecules into different intermediate and final products. The presence and composition of each organic macromolecule in biomass additionally affect the properties of the products produced during HTL.[7]

Viscosity is one important rheological property of biomass slurries that affects the transportation behavior and heat transfer required during the HTL process. The presence of proteins and polysaccharides contained in biomass such as municipal sewage sludge can greatly influence the viscosity of the biomass feedstock.[8] However, there is limited information reported in the scientific literature on how the presence of each macromolecule type in biomass affects the viscosity variation of biomass during HTL. The rheological properties of binary-phase biomass feedstock which changes from the beginning of an HTL reaction through to the final formation of the three

Received: October 1, 2020
Revised: December 8, 2020
Accepted: December 23, 2020
Published: January 5, 2021

https://dx.doi.org/10.1021/acs.iecr.0c04845
Ind. Eng. Chem. Res. 2021, 60, 980−989

phase products (solids, liquids, and gas) are elucidated and reported in this paper.

Possible factors that can cause changes in viscosity include phase transition, changes in chemical composition, molecularity of the products, compressive volume change, and the intensity, normal stresses, and duration of external stress such as shear forces, temperature, and pressure.[9−11] The formation of intermediates and HTL products during the application of heat can affect the viscosity of the final products formed due to the changes in the physicochemical composition of the compounds. Additionally, products obtained from the HTL of mixtures of macromolecules adversely affect the slurry viscosity due to the synergistic and antagonistic effects of the mixtures, which affect biocrude yield under HTL conditions.[12,13] Agitation of the biomass slurry during HTL increases the shearing force on the reacting slurry and this can greatly influence the viscosity of the HTL product.[14] The changes in viscosity may differ from one macromolecule to the other due to the difference in the compositions and molecularity of the compounds. To fundamentally understand how these viscosity changes occur in the reacting biomass, it would be necessary to elucidate the thermal degradation of each macromolecule in the biomass feedstock. The thermal degradation and the effect of temperature and pressure on the viscosity variation of the various macromolecules in biomass under HTL conditions have not been reported in the current scientific literature.

The dynamic viscosity of fluids can be measured from the shear stress (τ)−shear rate (γ) data during agitation of a fluid in an HTL stirred tank batch reactor. This implies that the real-time viscosity of an HTL reacting fluid can be estimated by directly measuring the speed and torque on the rotating impeller. Typically, close clearance impellers, which include anchor and helical impellers, are recommended for highly viscous fluids to achieve uniform viscosity.[15] The anchor and helical impellers are energy-efficient impellers that promote homogeneity and enhance heat transfer in reactors. The anchor impeller is a U-shaped impeller that allows a tangential flow throughout the fluid and improves mixing, especially at the walls of the vessel, hence making it suitable for mixing viscous fluids.[16] The measured speed (N) and torque (M) on an impeller shaft can be directly related to the HTL reacting fluid's viscosity (η) using the Metzner and Otto method.[17] The Metzner−Otto method compares the power requirements for mixing a non-Newtonian fluid to the mixing power for a Newtonian fluid in a specific mixing system. The Metzner−Otto constant is used to determine the average shear rate from the impeller speed data of the fluid.

The main aim of this study was to investigate the fundamental rheological changes of macromolecules in biomass to better understand their impact on rheological changes in biomass feedstock as a whole. This study focuses on the viscosity variation of model compounds as a function of temperature and pressure. Sunflower oil, soy protein, and sucrose from granulated sugar model compounds were used to represent lipids, proteins, and carbohydrates, respectively. These model compounds were selected as they have been widely studied in the scientific literature and are easily sourced. Hydrothermal liquefaction was conducted with each macromolecule and the changes in the impeller speed−torque data at fixed impeller speeds were converted into apparent viscosity using the Metzner−Otto method. The HTL products were separated and analyzed. Viscosity variations of binary and ternary mixtures comprising the organic fractions of model compounds were determined as a function of temperature and pressure under subcritical conditions to predict the viscosity profile of biomass in the absence of lignin and inorganics.

2. METHODOLOGY

2.1. Real-Time Viscosity Measurement. *2.1.1. Experimental Setup.* A 1 L Model 4577 Parr steel reactor with a 4848 controller, a torque sensor (2 ± 0.01 Nm), and an anchor impeller for agitation manufactured by Parr Instrument Co., Moline, IL was used for the real-time viscosity measurement. A custom-made digital acquisition device was used in conjunction with the torque sensor to measure torque with an accuracy of 1 μm. The experiment was set up as shown in the diagram in Figure 1.

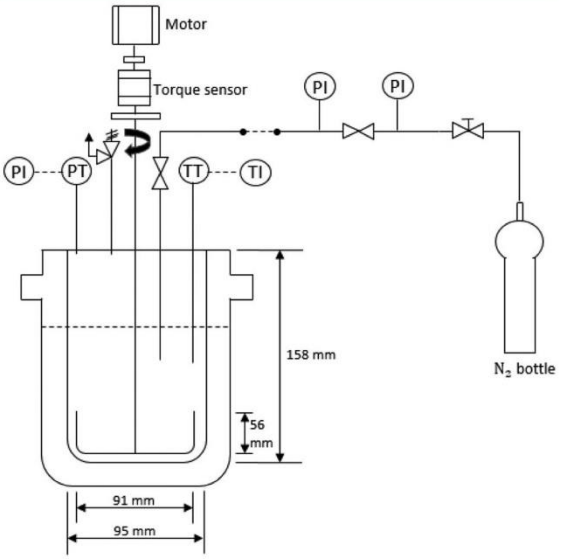

Figure 1. Experimental setup for real-time viscosity measurement.

2.1.2. Determination of Rheological Constants. The Metzner−Otto method was used to determine rheological constants for viscosity measurement as proposed by Metzner and Otto.[17] The silicon oil viscosity standard was purchased from Ametek Brookfield and used as a Newtonian fluid. Carboxymethyl cellulose (CMC) was purchased locally in Australia. A 2 wt % CMC solution was prepared and used as a non-Newtonian fluid during the determination of rheological constants. The consistency index and flow behavior index of the non-Newtonian fluid were determined using the strain-controlled mode on a rheometer (Rheometer SR5, TA Instrument) with a cone and plate configuration. Properties of the Newtonian and non-Newtonian fluid are described in previous research.[18] Both Newtonian and non-Newtonian fluids were used to determine the Metzner−Otto constant k_s^{MO}.[17] The shear stress constant k_τ was determined using the method proposed by Bbosa et al.[19] Shear stress was determined as a product of the shear stress constant and the torque on the impeller shaft, while the shear rate was determined as a product of the Metzner−Otto constant and the impeller rotational speed under each reaction condition. The ratio of shear stress to shear rate is the apparent shear

https://dx.doi.org/10.1021/acs.iecr.0c04845
Ind. Eng. Chem. Res. 2021, 60, 980−989

viscosity, which varies with the shear rate for non-Newtonian fluids.

2.1.3. Validation of the Apparent Viscosity Measurement. The validation and verification of the Metzner−Otto method were conducted using the purchased silicon oil with a viscosity of 12.3 Pa·s at 25 °C and a low-viscosity silicon oil viscosity standard (purchased from Anton Paar, Europe) with a viscosity of 0.7 Pa·s at 25 °C. The 2 wt % CMC solution was used as a power law fluid to validate the method for non-Newtonian fluids. The predetermined rheological constants were used to convert the torque and speed values into the viscosity of the silicon oils and 2 wt % CMC solutions at variable temperatures. The maximum errors in viscosity measurements were less than ±10%.

2.1.4. Real-Time Viscosity Measurement of Model Compounds during HTL. Model compounds were used to represent the macromolecules in biomass. Sunflower oil and household granulated sugar (sucrose) were purchased from the local markets in Adelaide, South Australia, and assumed to be representative samples for pure lipids and carbohydrate macromolecules, respectively. Soy protein was purchased from Bulk Nutrients, Australia, and used as a model for pure protein.

HTL experiments were conducted in the batch reactor. Each model compound was mixed with distilled water to obtain a desired dry matter concentration of 20 wt %. Model compounds were mixed in equal amounts for mixtures of model compounds. Prepared slurries were transferred into the batch reactor vessel. The reactor was sealed completely to hold pressure and purged thrice with nitrogen. An initial amount of nitrogen was charged into the reactor vessel.

The speed of the impeller was set to 120 rpm while the vessel was heated up to 350 °C. One impeller rotational speed (shear rate) was used due to design limitations of the equipment. First, the torque range (0−2 Nm) was selected to measure a wide range of viscosities of both dilute and concentrated slurries. However, the wide range reduces the sensitivity of the equipment for the viscosity measurement of slurries, which increases the errors of viscosity at lower rotational speeds. Below the shear rate of 370 s^{-1}, the viscosity measurement of model compounds using the reactor configuration as shown in Figure 1 falls below the limits of detection for the equipment. Due to the limitations of using the Metzner−Otto method, which is valid in the laminar flow regime only, viscosity could not be measured at higher rotational speeds where turbulence flow exists. Second, a single rotational speed was used to serve as a basis of comparison. A fixed impeller speed was used as the basis for comparing the changes in apparent viscosity with temperature and pressure. Unlike Newtonian fluids, whose viscosity is independent of the shear rate, the apparent viscosity of non-Newtonian fluids strongly depends on the shear rate. Hence, a comparison between changes in the apparent viscosity of the reacting slurry can only be conducted at a fixed shear rate and impeller speed over a range of temperatures and pressures.

As the temperature increased from room temperature to 350 ± 10 °C, the pressure increased from the initial pressure to 200 ± 10 bar. The changes in torque on the impeller shaft at a fixed impeller speed were logged on labview software. Impeller speed and torque values were converted into apparent viscosity values using the Metzner−Otto constant. The reactor was cooled to room temperature and the gas was released under an extraction hood. HTL products (solids, aqueous, and organic crudelike oil) were collected for analysis from experiments conducted at 200, 250, 300, and 350 °C in duplicate.

2.2. Product Separation. Solid products obtained after the HTL of sucrose were separated from the aqueous phase using vacuum filtration and dried at 40 °C in a drying oven until no change in mass was observed. The hydrocarbons in the solid fraction were determined using a source rock analyzer via pyrolysis and oxidation of the dry solids at 300 and 650 °C.[20] Renewable crude like oil produced after HTL of sunflower oil was separated from the aqueous phase using gravity separation in a Buchner funnel. The mass of the gas produced was calculated by subtracting the mass of products in the reactor vessel from the mass of the reactants. The organic yield of each model compound was estimated by the quantity of organics in the product (renewable crude like oil, gas, and solids) as a percentage of the organics in the feedstock. The organic yield of the aqueous phase was determined by subtraction. The mass yields of the products after HTL of each model compound were determined from the mass of the physically separated renewable crude like oil, aqueous, and solid products collected over the total feedstock. The mass yield of the gas phase was determined by subtraction.

2.3. Product Analysis. The functional groups of renewable crude like oil produced from sunflower oil and soy protein were characterized using a Fourier transform infrared spectrophotometer (FT-IR) from PerkinElmer. The FT-IR spectrophotometer was used to collect FT-IR spectra in a range of 400−4000 cm^{-1} with 40 scans.

A gas chromatograph−mass spectrometer (GC−MS, SQ8, PerkinElmer) was used to identify the different organic components in the liquid products. Hydrocarbons in the solid products were detected using a Fisons MD800 mass spectrometer with an Agilent 7980 gas chromatograph. Details of the columns and the mass spectroscopy of the liquid and solid products are outlined in previous work by Obeid et al.[21] The chemical compounds were identified using PerkinElmer TurboMass 6.0 software and were compared to the NIST14 Library Database.

3. RESULTS AND DISCUSSION

3.1. Validation of Viscosity Measurement. The consistency and power law indices of the 2 wt % CMC were determined to be 26.3 ± 0.6 and 0.4 ± 0.02, respectively. The k_s^{MO} was 28.7 ± 0.2 and k_τ was 1349 ± 4 Pa/Nm. The Metzner−Otto method was valid for measuring the viscosity of the high-viscosity standard fluid with an error of ±0.5% and the low-viscosity standard fluid with an error of ±2%. As shown in Figure 2, the effective shear stress and effective shear rate calculated from experimental data on the rheometer coincide with the shear rate and shear stress data of the non-Newtonian fluid obtained from the standard rheometer. Hence, the Metzner−Otto viscosity method is valid for non-Newtonian fluids as the experimental data agrees with the viscosity data obtained from the standard conventional rheometer.

3.2. Apparent Viscosity Variation of Individual Model Compounds. *3.2.1. Lipids.* Apparent viscosity changes of lipid feedstock against temperature and pressure were observed during HTL of a 20 wt % sunflower oil/water mixture. As shown in Figure 3, the torque and apparent viscosity of the reacting slurry decrease by 0.01 Nm and 0.03 Pa·s as the temperature and pressure increased from 25 °C, 45 bar to 280 °C, 90 bar at a shear rate of 372 s^{-1} and a heating rate of 9 °C.

https://dx.doi.org/10.1021/acs.iecr.0c04845
Ind. Eng. Chem. Res. 2021, 60, 980−989

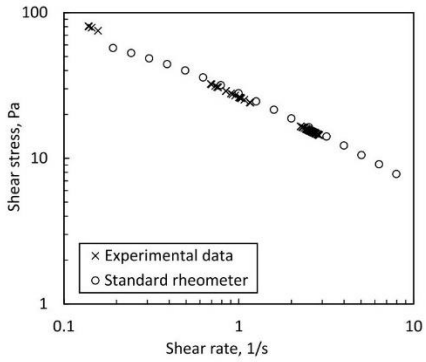

Figure 2. Validation of viscosity measurement using non-Newtonian fluid.

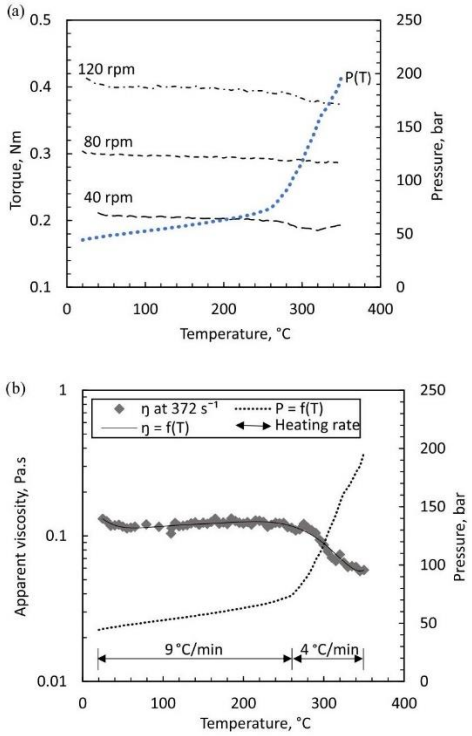

Figure 3. (a) Changes in torque at different rotational speeds and (b) apparent viscosity variations during HTL of 20 wt % sunflower oil/water.

As the temperature increased from 280 to 350 °C, the pressure in the headspace increased exponentially from 90 bar to 200 bar at a reduced heating rate of 4 °C/min and the apparent viscosity of the reacting slurry decreased from 0.12 to 0.06 Pa·s. Apparent viscosity decreased with a decrease in the heating rate from 9 to 4 °C.

The viscosity of the purchased sunflower oil (0.068 Pa·s) was determined to be higher than the viscosity of water (0.001 Pa·s) at 25 °C and exhibited a Newtonian behavior. A mixture of sunflower oil and water is predictably more viscous than water and tentatively less viscous than sunflower oil. The sunflower oil/water solution, which is a mixture of two Newtonian fluids, can deviate from Newtonian behavior due to the mixing properties and conditions of the final solution. The apparent viscosity of the mixture may be higher than the viscosity of the individual fluids if the fluids are reactive at a given temperature and pressure, exhibit a change in the molecular structure due to the fluid−structure interaction of the mixture, and change their shear-rate dependency. The apparent viscosity of non-Newtonian fluid cannot be directly compared to the viscosity of the individual Newtonian fluids due to the shear-rate dependency of non-Newtonian fluids. Hence, the higher the concentration and yield of oil in the feed, the higher the apparent viscosity of the combined mixture.

HTL of 20 wt % sunflower oil/water starts as two immiscible liquid phases (80% water phase and 20% oil phase) at the beginning of the reaction process. As the temperature increases, the polarity and solubility of the oil-rich phase increase, making the reacting feedstock miscible in the pressurized water at higher temperatures.[22] Produced aldehydes in reacting slurries of lipid feedstock degrade into fatty acids under hydrothermal conditions. As presented in Table 1, the number of free fatty acids produced at higher temperatures with increasing water solubilities increases with decreasing number of aldehydes. Hence, the solubility of reacting lipid slurries in water increases with increasing hydrothermal conditions.

During heating, the interaction of the aqueous and oil phase results in the production of gas under different reaction conditions. According to the reaction pathway proposed by Obeid et al.,[7] HTL lipid feedstock reacts to produce renewable crude like oil and soluble compounds in the aqueous products that degrade and recombine to form other products in the aqueous and crude like oil phase, respectively, under different reaction conditions. The gas products result from decarboxylation of the renewable crude like oil phase. Production of gas reduces the combined mass of the aqueous and crude like oil products.

Organic yields of renewable crude like oil were >90% at reaction temperatures between 200 and 350 °C, which agreed with other investigations on HTL of sunflower oil/water mixtures.[4,7] According to the material balance in the Supporting Information, the change in mass percentage of crude like oil over the total mass of products from 200 to 300 °C was almost insignificant (0.3%) as the apparent viscosity of the reacting slurry decreases by 0.06 Pa·s within the same temperature range. This implies that a small change in crude like oil yields resulting from the degradation and recombination of certain compounds in addition to the minimal changes in the product mass contributes to the variations in the apparent viscosity of the reacting slurry.

Sunflower oil contains polysaturated fats (linoleic acid), monosaturated fats (oleic acid), and saturated fats. Figure 4a shows the FT-IR spectra displaying the main peaks and functional groups in the oil-rich phase produced from HTL of the 20% sunflower oil/water mixture. The intensity of the peaks of the spectral band at 1160 and 1750 cm^{-1} decreases with increasing temperature, while spectral bands at 940, 1290, 1420, and 1700 cm^{-1} increase with increasing temperature.

Commercial sunflower oil largely contains triglycerides.[24] During HTL of sunflower oil in hot compressed water, triglycerides in the oil decompose to form free fatty acids and glycerol.[25] Glycerol is converted into a water-soluble compound, which exists in the aqueous phase.[2] These

https://dx.doi.org/10.1021/acs.iecr.0c04845
Ind. Eng. Chem. Res. 2021, 60, 980−989

Table 1. GC−MS Identified Compounds in Crudelike Oil after HTL of Sunflower Oil/Water Feedstock

Compound	Solubility at 230 °C, 15 MPa, mol/kg H_2O[a]	Peak area, 10^7			
		200 °C	250 °C	300 °C	350 °C
Octadecanoic acid	0.001	19.0	28	1847.1	1309.1
Hexadecanoic acid	0.01	-	5.7	426.3	384
Octanoic acid	1	-	6.1	10.4	8.3
Oxononanoic acid	0.15	-	-	-	8.2
Oleic acid	0.001	-	56.7	-	6.4
Tetradecanoic acid	0.01	-	-	-	5.1
Pentadecanoic acid	0.01	-	41.6	-	-
Cyclopentanecarboxylic acid	0.0015	3.8	-	-	-
Hexanal	-	4.1	7.4	11.6	-
Decadienal	-	13.9	19.3	11.5	-
Undecadienal	-	-	-	9.3	-
Nonadienal	-	22.6	10.8	-	-
Heptanal	-	2.1	-	-	-

[a]Solubility data adapted from Khuwijitjaru et al.[23]

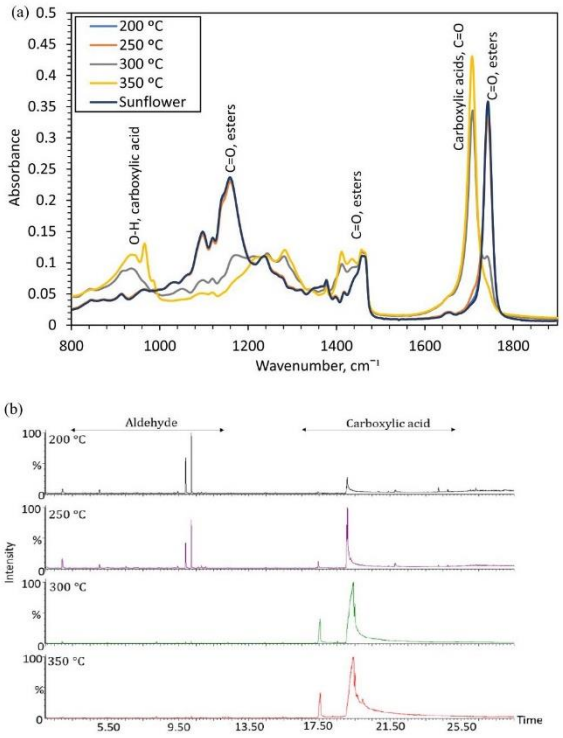

Figure 4. (a) FT-IR spectra of sunflower oil and crudelike oil after HTL of the 20 wt % sunflower oil/water mixture and (b) GC−MS spectra of crudelike oil produced at different reaction times and 200, 250, 300, and 350 °C.

triglycerides, which are represented by C═O esters at 1746 cm^{-1} as shown in Figure 4a, gradually disappear with an increase in the temperature from 200 to 350 °C. Similarly, aldehydes and other organic compounds formed in the crude like oil after HTL of sunflower oil disappear with an increase in the temperature as shown in Figure 4b. The disappearance of triglycerides leads to the simultaneous production of free fatty acids in the reacting slurry.

At 1715 cm^{-1}, as shown in the FT-IR spectra, carboxylic acid groups, which represent free fatty acids, are formed from the hydrolysis of oil above 200 °C and the quantity of these acid groups increased when the temperature was increased to 350 °C. Carboxylic acids, as presented in Table 1, include octadecanoic acids, hexadecanoic acids, octanoic acids, and oleic acids. The apparent viscosity decreases with a decrease in long-chain fatty acids and hydrocarbons. Consequently, the disappearance of triglycerides, which are long-chain hydrocarbons, contributes to the decreased apparent viscosity of the reacting slurry. FT-IR spectral bands at 1418, 1397, and 950 cm^{-1} increase with an increase in the temperature above 300 °C. These spectral bands represent CH bonds of the olefinic groups. The formation of a C−O ester at 1155 cm^{-1} decreases with an increase in the temperature. Between 1176 and 1163 cm^{-1}, the C═O represents the ester carbonyl functional group of triglycerides. Changes in the chemical speciation of the lipid feedstock and HTL products under different reaction conditions greatly affect the apparent viscosity of the reacting slurry.

3.2.2. Proteins. A 20 wt % soy protein/water mixture yields an insoluble thick slurry. Soy protein is hygroscopic at ambient temperatures; hence, when added to water, it swells up and thickens. Application of heat to a soy protein/water mixture increases the solubility of the solids in the water. As the temperature increases, protein denatures and solubilizes in the hot compressed water, thereby reducing the apparent viscosity of the reacting slurry. From the data shown in Figure 5, the apparent viscosity of the soy protein/water mixture decreases by 2.3 Pa·s from room temperature to 160 °C (48 bar) and changes insignificantly (±0.05 Pa·s) when the temperature and pressure increase from 160 °C at 48 bar to 350 °C at 200 bar. Between 25 and 100 °C, polypeptides in protein hydrolyze to produce amino acids, which dissolve in the aqueous phase.[7] HTL reactions of proteins include decomposition, decarboxylation, deamination, dehydration, deoxygenation, deamination, denitrogenation, and decomposition reactions that break down complex protein bonds into peptides and amino acids.[4,26] When heat is applied to pressurized HTL protein feedstock, the van der Waal forces holding the protein bonds break apart, thereby decreasing the bond energy and reducing the amount of force required to agitate the fluid. A decrease in this force translates to a decrease in the torque and apparent viscosity of the mixture at a fixed shear rate.[27] Above 100 °C (43 bar), most of the protein bonds would have been broken. Amino acids decompose via decarboxylation and deamination

https://dx.doi.org/10.1021/acs.iecr.0c04845
Ind. Eng. Chem. Res. 2021, 60, 980−989

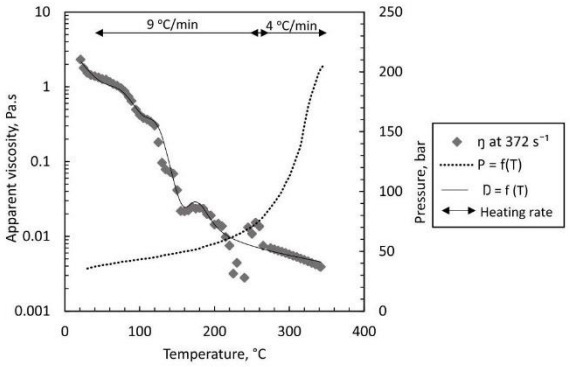

Figure 5. Apparent viscosity variations during HTL of 20 wt % soy protein.

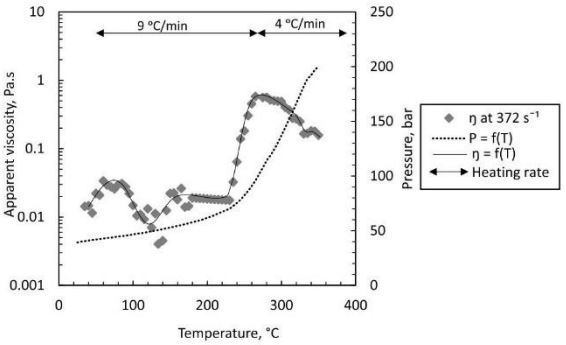

Figure 6. Apparent viscosity variations during HTL of a 20 wt % sucrose solution.

reactions,[28] and the change in apparent viscosity reduces to 0.05 Pa·s.

Solids in soy protein feedstock solubilize into the aqueous phase during heating. Organic yields of crude like oil from HTL of soy protein feedstock above 200 °C were in the range of 25−30%. This observation is in agreement with the reaction pathway proposed by Obeid et al.,[7] where the solids in HTL protein feedstock dissolve in the aqueous phase, which then reacts to form renewable crude like oil reversibly as well as the gaseous products. Above 200 °C, the aqueous phase constituted <92% of the combined product mass. The aqueous phase, which largely comprises of dissolved organics (>60% organic yield) in hot compressed water, is less viscous than the renewable crude like oil phase. High aqueous yields decrease the viscosity of the reacting slurry.

The mass percentage of crude like oil in the product significantly influences viscosity. However, the mass percentage of crude like oil produced after HTL of protein feedstock decreases insignificantly between 200 and 350 °C. Nonetheless, the crude like oil produced from the HTL of soy protein contains light and heavy oils. Heavy oil in crude like oil decreases as the temperature is increased from 200 to 350 °C. An increase in the amount of heavy oil increases the apparent viscosity as heavy oil contains high-molecular-weight compounds compared to light oil. The presence of a high amount of heavy oil in the product would increase the apparent viscosity of the pressurized slurry from 200 to 350 °C if the mass percentage of crude like oil decreased significantly.

3.2.3. Carbohydrates. At room temperature, 20 wt % granulated sugar completely dissolved in water. When pressurized HTL carbohydrate feedstock is heated to 100 °C, the physical structure of the carbohydrates disintegrates, and long-chain compounds break down to produce reduced and nonreduced sugars such as sucrose via hydrolysis.[28] Mostly, glucose, which is a reducing sugar, decomposes into furans.[2,29] Other intermediates such as furfural, organic acids, and hydrochar are produced after isomerization, depolymerization, polymerization, and condensation reactions.[30] Decomposition of carbohydrates feedstock under subcritical conditions increases with an increase in temperature and pressure.[7] The apparent viscosities of the sucrose solution during HTL under subcritical water conditions are shown in Figure 6.

During the heating period from 25 °C at 40 bar to 230 °C at 70 bar, the apparent viscosity of the reacting slurry decreased by 0.01 Pa·s. Above 200 °C (62 bar), carbon compounds in the reacting slurry begin to precipitate out of solution in a process similar to hydrothermal carbonization (HTC). At this stage, the reacting slurry undergoes several reactions including hydrolysis, depolymerization, dehydration, and decarboxylation processes that lead to structural and chemical changes in the slurry.[31] This observation corresponds to the increase in the mass percentage of solids from 200 (3%) to 250 °C (10%). Organic compounds dissolved in the aqueous phase at room temperature are converted into solid products under HTC conditions while approaching HTL conditions. The organic yield of solids increased significantly from 14% at 200 °C to 46% at 250 °C and then decreased gradually to 41% at 350 °C (Supporting Information). The formation of high-molecular-weight organic compounds in solid products, which include 1-(2-furanyl)ethanone, 2-ethyl-1*H*-benzimidazole, 2-methylfuran, and 3-methyl-2-cyclopenten-1-one, during HTL between 250 and 300 °C contributes to the changes in the apparent viscosity of the reacting slurry. An increase in the production of high-molecular-weight compounds from 200 to 300 °C increases the apparent viscosity, while a decrease in the production of lower molecular weight compounds from 300 to 350 °C decreases the apparent viscosity of the slurry.[32] The apparent viscosity of the reacting slurry increased by 0.58 Pa·s from 230 °C (70 bar) and peaked at 280 °C (114 bar), where solid formation was maximum. Above 280 °C and 114 bar, solids decomposed into the aqueous phase and recombined to form gaseous products, thereby decreasing the solid yield from 280 (114 bar) to 350 °C (200 bar) by 1%. A decrease in the mass percentage of solids in the product fraction decreases the amount of force required to agitate the reacting slurry as there is less resistance between the solid particles and the impeller. Hence, the apparent viscosity decreases at a fixed shear rate with a decrease in solid yield from 280 (114 bar) to 350 °C (200 bar).

3.3. Viscosity Variation of Mixtures of Model Compounds. The apparent viscosity variations of mixtures of model compounds with combined temperature and pressure are shown in Figure 7. Variations in the apparent viscosity of mixtures of model compounds are minimal, with binary mixtures showing a change of ±0.1 Pa·s and ternary mixtures of ±0.06 Pa·s across the reported temperature and pressure profile. Generally, the apparent viscosities of mixtures of model compounds decrease with an increase in temperature and pressure, except for lipids and carbohydrates, which indicates an increase in viscosity at 250 °C due to solid formation. These

https://dx.doi.org/10.1021/acs.iecr.0c04845
Ind. Eng. Chem. Res. 2021, 60, 980−989

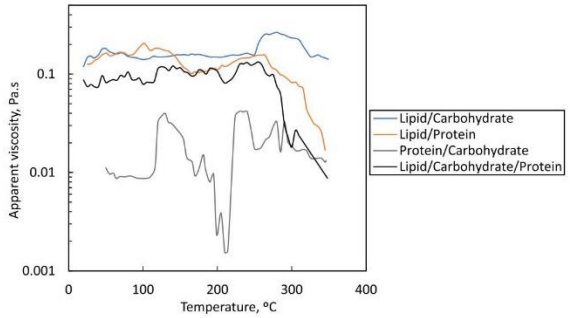

Figure 7. Apparent viscosity profile of mixtures of model compounds at 372 s^{-1}.

apparent viscosity profiles can be used to predict the viscosity variations in real biomass depending on the dominant composition of the biomass. However, the predictions using the viscosity profile of mixtures of the model compound may deviate from the viscosity profile of biomass in the presence of specific compounds in the feedstock.

Mineral elements in high-ash-containing biomass such as municipal biosolids can potentially act as catalysts and reactants to yield unique products that can alter the yields of the product and consequently contribute to the variations in apparent viscosity. Additionally, insoluble nonreactive minerals in the ash can increase the solid fraction of the product. The presence of solids in HTL products increases the resistance of the fluid to deformation, thereby increasing the internal friction as particles slide past each other in the fluid and hence an increase in the slurry's apparent viscosity. The existence of other components in biomass including lignin, especially in lignocellulosic biomass and salts from microalgae, can have an impact on the variations in the viscosity profiles depending on the effects of these elements to the chemical speciation and phase transitions of the reacting slurry.[18] These deviations may be minimal depending on the extent of the reaction and reaction pathway of the biomass sample.

The data presented in Figure 8 shows the apparent viscosity−temperature profile of mixtures of model compounds compared to the viscosity profile of the individual model compounds. Generally, the apparent viscosity of mixtures of model compounds decreases with a decrease in temperature at a constant shear rate. The apparent viscosity of mixtures of lipids and protein as shown in Figure 8a mimics the viscosity of lipids. As shown in Figure 8b, the apparent viscosity variations of a mixture of lipids and carbohydrates resemble those of the lipids between room temperature and 250 °C, where the apparent viscosity profile increases to 0.6 Pa·s due to the formation of solids in the presence of carbohydrates. Apparent viscosity changes of the carbohydrate/protein mixture, as shown in Figure 8c, mimic those of carbohydrates from room temperature to 240 °C. Above 250 °C, the apparent viscosity of the protein/carbohydrate mixture varied insignificantly compared to the apparent viscosity variation of the carbohydrate feedstock. Despite the formation of solid carbon compounds in the HTL of the carbohydrate feedstock, the apparent viscosity of the mixture remained unaffected by the presence of the carbohydrates. The decrease in the apparent viscosity of the mixture is due to the occurrence of Milliard reactions between proteins and carbohydrates, which inhibit the production of solids in these mixtures.[20] A ternary mixture

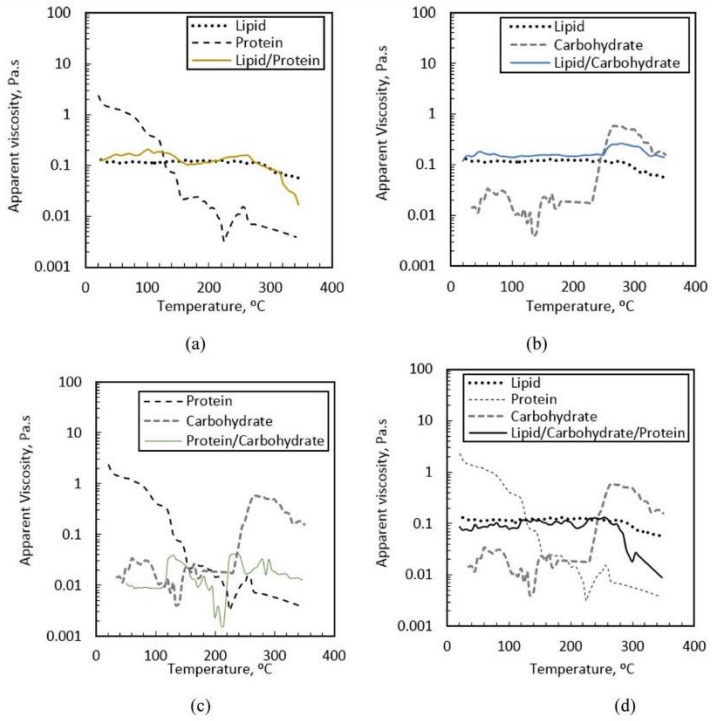

Figure 8. Apparent viscosity profile of mixtures of model compounds.

https://dx.doi.org/10.1021/acs.iecr.0c04845
Ind. Eng. Chem. Res. 2021, 60, 980−989

of proteins, carbohydrates, and lipids as shown in Figure 8d exhibited insignificant changes in the apparent viscosity from room temperature to 250 °C, after which the apparent viscosity decreased by 0.01 Pa·s.

Macromolecules including lipids, proteins, and carbohydrates can greatly influence the apparent viscosity profile of the reacting biomass slurry. The dominance of one or more macromolecules in the biomass can be used to predict the apparent viscosity profile of the reacting slurry. The apparent viscosity of biomass slurry containing mixtures of macromolecules in varying amounts would decrease with an increase in the reaction temperature.

3.4. Factors Affecting the Apparent Viscosity Change of Model Compounds during HTL. Under conventional conditions, the viscosity of liquids decreases with an increase in temperature. However, this phenomenon is not always true, especially when there is more than one substance under consideration. Mixtures of fluids, solutions, and slurries have different reaction pathways when heated at certain temperatures under specific reaction conditions. The application of a certain amount of heat causes reacting fluids to undergo phase transformations, which yields products with variable compositions. The new products, which are characterized by changes in their chemical speciation and compositions of the reacting slurries, exhibit unique rheological properties that differ from the rheological properties of the reactants. This is true for the reacting slurries of single model compounds, where compounds in the feedstock degrade and react to form high-molecular-weight compounds (HTL of the protein feedstock) and compounds in new phases (gas in all macromolecule feedstocks and formation of solids during HTL of the carbohydrate feedstock). Thus, a change in the chemical composition and phase transition changes the apparent viscosity of the reacting slurry.

The changes in the apparent viscosity of dilute slurries are expected to mimic the decreasing viscosity of water with an application of thermal energy as the solid concentration approaches zero. However, this assumption deviates from reality, especially at critical temperatures, where the applied heat does not only change the phase of the reactant into a multiphase product but also produces new compounds with different molecularities held up by various types of bonds that adversely affect viscosity. During HTL of model compounds under subcritical conditions of water, water acts as a catalyst, a reactant, and a reaction medium.[33] The presence and properties of water enhance HTL reactions such as hydrolysis, which leads to dehydration, depolymerization, decomposition, recombination, decarboxylation, and deamination reactions.[25,34,35] Under subcritical conditions of water, water behaves as an incompressible fluid and a polar solvent. As the conditions of water approach the critical point of 374 °C and 22 MPa, its properties, which include diffusivity, polarity, self-ionization, solvation power, viscosity, and surface tension, change significantly with temperature and pressure.[34,36,37] At near critical point, water behaves as a nonpolar solvent.[25] Subcritical water is able to enhance the dissociation of water at high temperatures.[35,38] Under such elevated reaction conditions, the hydrogen bonds holding water molecules weaken and this leads to reduced dielectric constants, which increases the solubility of polar molecules in the water.[39] The nonpolar nature under near critical conditions increases the ability of the water to extract useful compounds around 120−160 °C.[33] A decrease in polarity decreases fluid viscosity; hence, the viscosity of water decreases with increasing temperature.

HTL of model compounds under subcritical conditions of water occurred between 280 and 350 °C in a pressurized batch reactor. Predictably, the application of heat to the reacting slurry increased the pressure of the reacting slurry. The rate of increase in pressure with temperature was similar for all model compounds. Pressure increased gradually from room temperature to 280 °C. When HTL began at 280 °C, the pressure increased rapidly with the temperature at a reduced heating rate. The reactor is pressurized to keep the reactants in the liquid state as pressure compresses fluids to increase the intermolecular resistance between molecules.[40] An increase in intermolecular forces including attractive and repulsive forces increases the viscosity. The intermolecular resistance increased as the fluid was continuously compressed. Hence, an increase in temperature, which increases the pressure and the compression of the fluids, increases the resistance in the fluid. Consequently, an increase in pressure can increase fluid viscosity. However, the effect of pressure on the apparent viscosity of slurries below subcritical conditions is minimal and negligible.

4. CONCLUSIONS

Biomass is comprised of lipids, carbohydrates, proteins, and lignin in varying amounts. The presence and quantities of each of these components can influence the viscosity of the biomass feedstock under hydrothermal liquefaction conditions. Changes in viscosity result from differences in phase composition and phase transitions, reaction conditions under subcritical temperatures and pressures, and the influence of shearing forces from agitation. The apparent viscosity profiles of proteins, lipids, and carbohydrates vary from one another due to their thermal degradation under subcritical conditions of water. During HTL of lipids, the viscosity of the reacting slurry changes insignificantly. The viscosity variations of proteins change significantly at lower temperatures due to the thermal degradation of polypeptide bonds, which increases the solubility of the protein molecules in the solvent. Carbohydrates exhibit negligible changes in viscosity from room temperature to 250 °C, when solids precipitate in solution, thereby increasing the viscosity of the slurry. The viscosity variations of binary mixtures exhibit small changes as compared to the individual model compounds. It is expected that real biomass containing relatively high amounts of monomers of model compounds, binary, or ternary mixtures of model compounds will exhibit a similar viscosity profile as shown in the study, provided it contains little amounts of or no inorganics, lignin, and salt, which could influence the viscosity of the reacting slurry.

■ ASSOCIATED CONTENT

Supporting Information

The Supporting Information is available free of charge at https://pubs.acs.org/doi/10.1021/acs.iecr.0c04845.

Material balance of HTL products; product yield analysis; percentage composition of light and heavy oil fractions in crudelike oil and solid products; and gas chromatography-mass spectrometry results (PDF)

https://dx.doi.org/10.1021/acs.iecr.0c04845
Ind. Eng. Chem. Res. 2021, 60, 980−989

AUTHOR INFORMATION

Corresponding Author

Sylvia Y. Edifor − *School of Chemical Engineering and Advanced Materials, The University of Adelaide, Adelaide, South Australia 5005, Australia;* orcid.org/0000-0002-6265-8639; Email: sylvia.edifor@adelaide.edu.au

Authors

Quoc D. Nguyen − *School of Chemical Engineering and Advanced Materials, The University of Adelaide, Adelaide, South Australia 5005, Australia*

Philip van Eyk − *School of Chemical Engineering and Advanced Materials, The University of Adelaide, Adelaide, South Australia 5005, Australia;* orcid.org/0000-0003-3768-2044

Patrick Biller − *Department of Engineering-Biological and Chemical Engineering, Aarhus University, Aarhus 8200, Denmark;* orcid.org/0000-0003-2982-6095

Tony Hall − *Faculty of Science, The University of Adelaide, Adelaide, South Australia 5005, Australia*

David M. Lewis − *School of Chemical Engineering and Advanced Materials, The University of Adelaide, Adelaide, South Australia 5005, Australia*

Complete contact information is available at: https://pubs.acs.org/10.1021/acs.iecr.0c04845

Author Contributions

This paper was written through contributions of all authors. All authors have given approval to the final version of the paper. All authors contributed equally.

Notes

The authors declare no competing financial interest.

ACKNOWLEDGMENTS

This work was supported by Southern Oil Refining and the Australian Research Council's Linkage Projects funding scheme [Project LP150101241].

REFERENCES

(1) Xue, Y.; Chen, H.; Zhao, W.; Yang, C.; Ma, P.; Han, S. A review on the operating conditions of producing biooil from hydrothermal liquefaction of biomass. *Int. J. Energy Res.* **2016**, *40*, 865−877.

(2) Toor, S. S.; Rosendahl, L.; Rudolf, A. Hydrothermal liquefaction of biomass: A review of subcritical water technologies. *Energy* **2011**, *36*, 2328−2342.

(3) Tian, C.; Liu, Z.; Zhang, Y. Hydrothermal Liquefaction (HTL): A Promising Pathway for Biorefinery of Algae. *Algal Biofuels* **2017**, 361−391.

(4) Gollakota, A.; Savage, P. E. Hydrothermal Liquefaction of Model Food Waste Biomolecules and Ternary Mixtures under Isothermal and Fast Conditions. *ACS Sustainable Chem. Eng.* **2018**, *6*, 9018−9027.

(5) Vassilev, S. V.; Baxter, D.; Andersen, L. K.; Vassileva, C. G.; Morgan, T. J. An overview of the organic and inorganic phase composition of biomass. *Fuel* **2012**, *94*, 1−33.

(6) Tursi, A. A review on biomass: importance, chemistry, classification, and conversion. *Biofuel Res. J.* **2019**, *22*, 962−979.

(7) Obeid, R.; Lewis, D.; Smith, N.; Van Eyk, P. The elucidation of reaction kinetics for hydrothermal liquefaction of model macromolecules. *Chem. Eng. J.* **2019**, *370*, 637−645.

(8) Baroutian, S.; Eshtiaghi, N.; Gapes, D. J. Rheology of a primary and secondary sewage sludge mixture: Dependency on temperature and solid concentration. *Bioresour. Technol.* **2013**, *140*, 227−233.

(9) Ramasamy, U. S.; Bair, S.; Martini, A. Predicting Pressure−Viscosity Behavior from Ambient Viscosity and Compressibility: Challenges and Opportunities. *Tribol. Lett.* **2015**, *57*, No. 357.

(10) Muhammed, N. B. Review in causes of viscosity in fluids. *J. Bio Innovation* **2017**, *6*, 117−123.

(11) Beglan, R. What Determines the Viscosity of a Fluid?, 2017. https://sciencing.com/determines-viscosity-fluid-8702394.html.

(12) Lu, J.; Liu, Z.; Zhang, Y.; Savage, P. E. 110th Anniversary: Influence of Solvents on Biocrude from Hydrothermal Liquefaction of Soybean Oil, Soy Protein, Cellulose, Xylose, and Lignin, and Their Quinary Mixture. *Ind. Eng. Chem. Res.* **2019**, *58*, 13971−13976.

(13) Lu, J.; Liu, Z.; Zhang, Y.; Savage, P. E. Synergistic and Antagonistic Interactions during Hydrothermal Liquefaction of Soybean Oil, Soy Protein, Cellulose, Xylose, and Lignin. *ACS Sustainable Chem. Eng.* **2018**, *6*, 14501−14509.

(14) Dickey, D. S. *Tackling Difficult Mixing Problems*; American Institute of Chemical Engineers, 2015.

(15) Luan, D.; Chen, Q.; Zhou, S. Numerical Simulation and Analysis of Power Consumption and Metzner-Otto Constant for Impeller of 6PBT. *Chin. J. Mech. Eng.* **2014**, *27*, 635−640.

(16) Kamla, Y.; Ameur, H.; Karas, A.; Arab, M. I. Performance of new designed anchor impellers in stirred tanks. *Chem. Pap.* **2020**, *74*, 779−785.

(17) Metzner, A. B.; Otto, R. E. Agitation of Non-Newtonian Fluids. *AIChE J.* **1957**, *3*, 3−10.

(18) Edifor, S. Y.; Nguyen, Q. D.; Van Eyk, P.; Biller, P.; Lewis, D. M. *Real-Time Viscosity Variations of Sewage Sludge during Hydrothermal Liquefaction under Subcritical Water Conditions*; The University of Adelaide, 2020; p 23.

(19) Bbosa, B.; DelleCase, E.; Volk, M.; Ozbayoglu, E. Development of a mixer-viscometer for studying rheological behavior of settling and non-settling slurries. *J. Pet. Explor. Prod. Technol.* **2017**, *7*, 511−520.

(20) Obeid, R.; Lewis, D. M.; Smith, N.; Hall, T.; van Eyk, P. Reaction Kinetics and Characterization of Species in Renewable Crude from Hydrothermal Liquefaction of Mixtures of Polymer Compounds To Represent Organic Fractions of Biomass Feedstocks. *Energy Fuels* **2020**, *34*, 419−429.

(21) Obeid, R.; Lewis, D. M.; Smith, N.; Hall, T.; van Eyk, P. Reaction kinetics and characterisation of species in renewable crude from hydrothermal liquefaction of monomers to represent organic fractions of biomass feedstocks. *Chem. Eng. J.* **2020**, 389.

(22) Gollakota, A. R. K.; Kishore, N.; Gu, S. A review on hydrothermal liquefaction of biomass. *Renewable Sustainable Energy Rev.* **2018**, *81*, 1378−1392.

(23) Khuwijitjaru, P.; Adachi, S.; Matsuno, R. Solubility of Saturated Fatty Acids in Water at Elevated Temperatures. *Biosci., Biotechnol., Biochem.* **2002**, *66*, 1723−1726.

(24) Faba, E. M. S.; Ferrero, G. O.; Dias, J. M.; Eimer, G. A. Alternative Raw Materials to Produce Biodiesel through Alkaline Heterogeneous Catalysis. *Catalysts* **2019**, *9*, No. 690.

(25) Cheng, F.; Cui, Z.; Chen, L.; Jarvis, J.; Paz, N.; Schaub, T.; Nirmalakhandan, N.; Brewer, C. E. Hydrothermal liquefaction of high- and low-lipid algae: Bio-crude oil chemistry. *Appl. Energy* **2017**, *206*, 278−292.

(26) Teri, G.; Luo, L.; Savage, P. E. Hydrothermal Treatment of Protein, Polysaccharide, and Lipids Alone and in Mixtures. *Energy Fuels* **2014**, *28*, 7501−7509.

(27) Bacigalupe, A.; Poliszuk, A. K.; Eisenberg, P.; Escobar, M. M. Rheological behavior and bonding performance of an alkaline soy protein suspension. *Int. J. Adhes. Adhes.* **2015**, *62*, 1−6.

(28) Gai, C.; Zhang, Y.; Chen, W.-T.; Zhang, P.; Dong, Y. An investigation of reaction pathways of hydrothermal liquefaction using *Chlorella pyrenoidosa* and *Spirulina platensis*. *Energy Convers. Manage.* **2015**, *96*, 330−339.

(29) Li, F.; Liu, L.; An, Y.; He, W.; Themelis, N. J.; Li, G. Hydrothermal liquefaction of three kinds of starches into reducing sugars. *J. Cleaner Prod.* **2016**, *112*, 1049−1054.

(30) Wang, T.; Zhai, Y.; Zhu, Y.; Li, C.; Zeng, G. A review of the hydrothermal carbonization of biomass waste for hydrochar

formation: Process conditions, fundamentals, and physicochemical properties. *Renewable Sustainable Energy Rev.* **2018**, *90*, 223−247.
(31) Missaoui, A.; Bostyn, S.; Belandria, V.; Cagnon, B.; Sarh, B.; Gökalp, I. Hydrothermal carbonization of dried olive pomace: Energy potential and process performances. *J. Anal. Appl. Pyrolysis* **2017**, *128*, 281−290.
(32) Wang, Y.; Zhang, Y.; Liu, Z. Effect of Aging in Nitrogen and Air on the Properties of Biocrude Produced by Hydrothermal Liquefaction of Spirulina. *Energy Fuels* **2019**, *33*, 9870−9878.
(33) Zhang, Y. Hydrothermal Liquefaction to Convert Biomass into Crude Oil. In *Biofuels from Agricultural Wastes and Bioproducts*; Wiley, 2010.
(34) Suryawanshi, P. G.; Das, S.; Borugadda, V. B.; Goud, V. V.; Dalai, A. K. Process Improvements and TechnoEconomic Feasibility of Hydrothermal Liquefaction and Pyrolysis of Biomass for Biocrude Oil Production. In *Biorefinery of Alternative Resources: Targeting Green Fuels and Platform Chemicals*; Springer: Singapore, 2020; pp 221−248.
(35) Masoumi, S.; Borugadda, V. B.; Dalai, A. K. Biocrude Oil Production via Hydrothermal Liquefaction of Algae and Upgradation Techniques to Liquid Transportation Fuels. In *Biorefinery of Alternative Resources: Targeting Green Fuels and Platform Chemicals*; Springer: Singapore, 2020; pp 249−270.
(36) Tian, Y.; Wang, F.; Djandja, J. O.; Zhang, S.; Xu, Y.; Duan, P. Hydrothermal liquefaction of crop straws: Effect of feedstock composition. *Fuel* **2020**, 265.
(37) Gu, X.; Martinez-Fernandez, J. S.; Pang, N.; Fu, X.; Chen, S. Recent development of hydrothermal liquefaction for algal biorefinery. *Renewable Sustainable Energy Rev.* **2020**, No. 109707.
(38) Yin, S.; Dolan, R.; Harris, M.; Tan, Z. Subcritical hydrothermal liquefaction of cattle manure to bio-oil: Effects of conversion parameters on bio-oil yield and characterization of bio-oil. *Bioresour. Technol.* **2010**, *101*, 3657−3664.
(39) Guo, Y.; Yeh, T.; Song, W.; Xu, D.; Wang, S. A review of bio-oil production from hydrothermal liquefaction of algae. *Renewable Sustainable Energy Rev.* **2015**, *48*, 776−790.
(40) Ametek, B. *More Solutions to Sticky Problems*; Brookfield Engineering Laboratories, Inc., 2017; p 16.

https://dx.doi.org/10.1021/acs.iecr.0c04845
Ind. Eng. Chem. Res. 2021, 60, 980−989

Supporting Information

Viscosity variation of model compounds during hydrothermal liquefaction under subcritical conditions of water

Sylvia Y. Edifor[a]* *Quoc D. Nguyen*[a] *Philip van Eyk*[a] *Patrick Biller*[b] *Tony Hall*[c] *David M. Lewis*[a]

[a]School of Chemical Engineering and Advanced Materials, The University of Adelaide, Adelaide, South Australia 5005 Adelaide, Australia

[b]Department of Engineering-Biological and Chemical Engineering, Aarhus University, 8200 Aarhus, Denmark

[c]Faculty of Science, The University of Adelaide, Adelaide, South Australia 5005, Australia

*Corresponding Author: sylvia.edifor@adelaide.edu.au

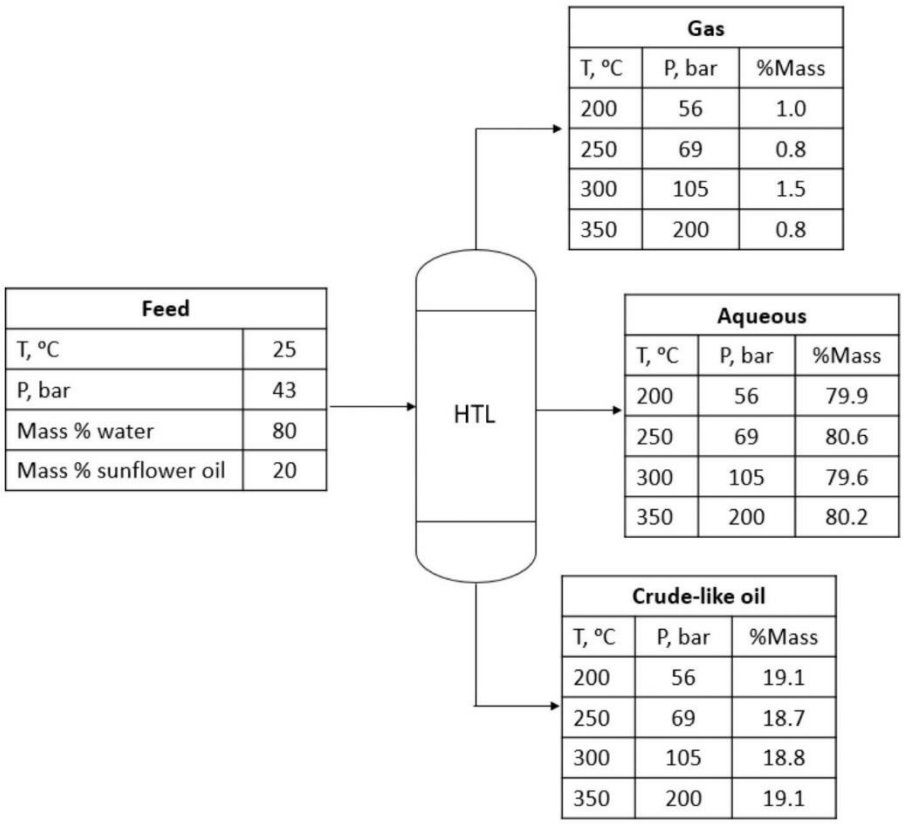

Figure S1. Material balance of products after HTL of Sunflower oil/water feedstock

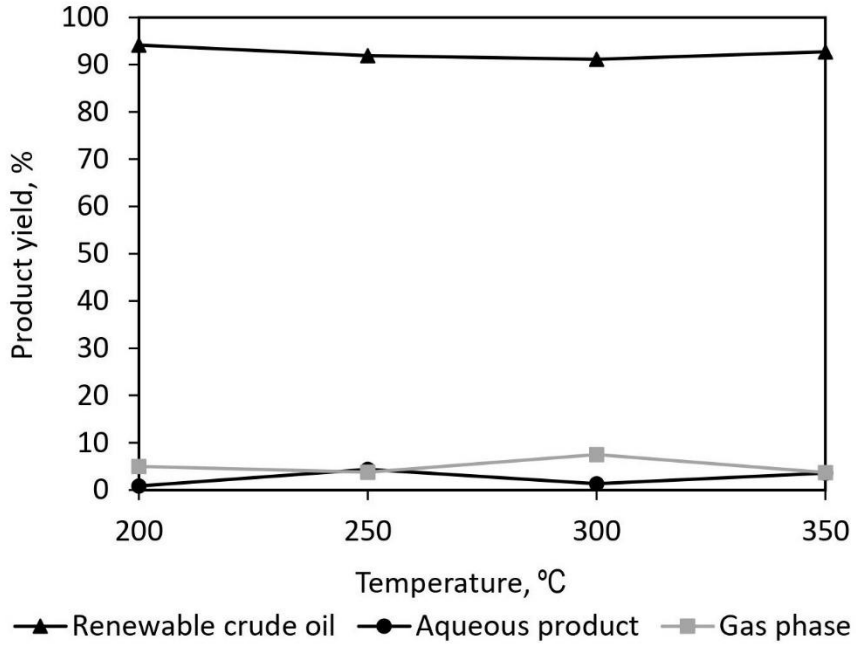

Figure S2. Organic yields of products after HTL of Sunflower oil/water feedstock

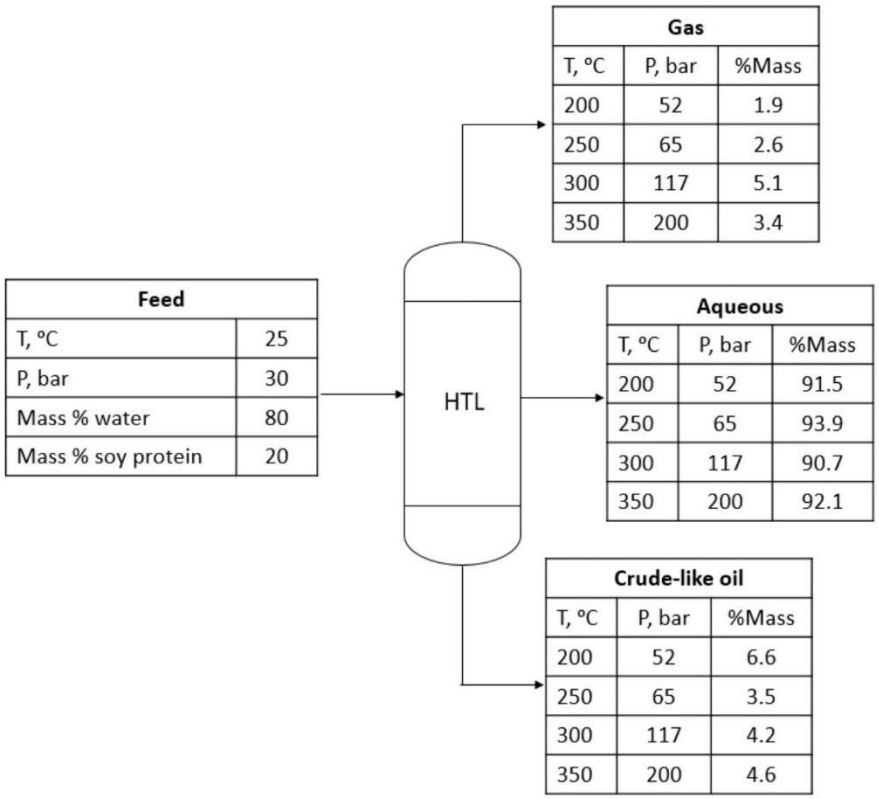

Figure S3. Material balance of products after HTL of Soy protein/water feedstock

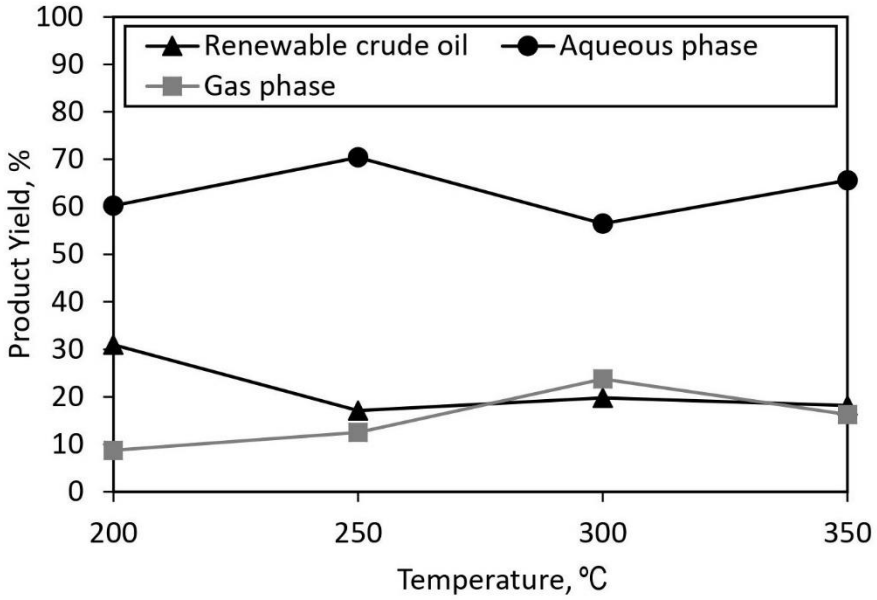

Figure S4. Organic yields of products after HTL of Soy protein/water feedstock

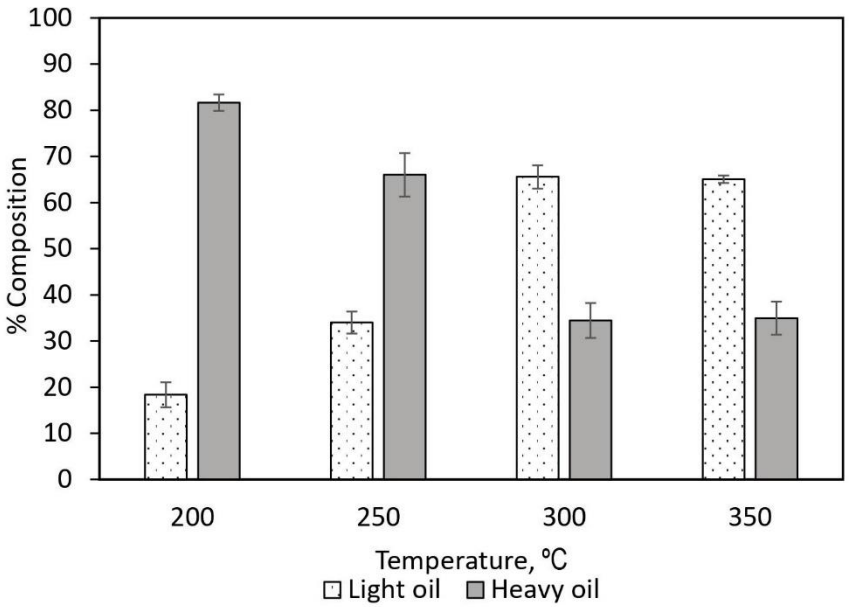

Figure S5. Light and heavy oil fractions in crude-like oil produced after HTL of soy protein

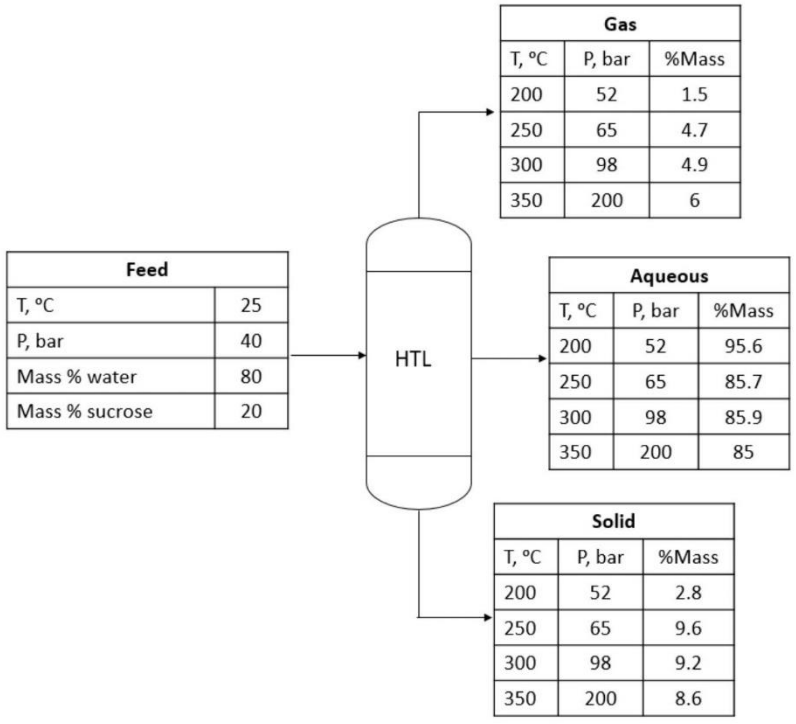

Figure S6. Material balance of products after HTL of Sucrose/water feedstock

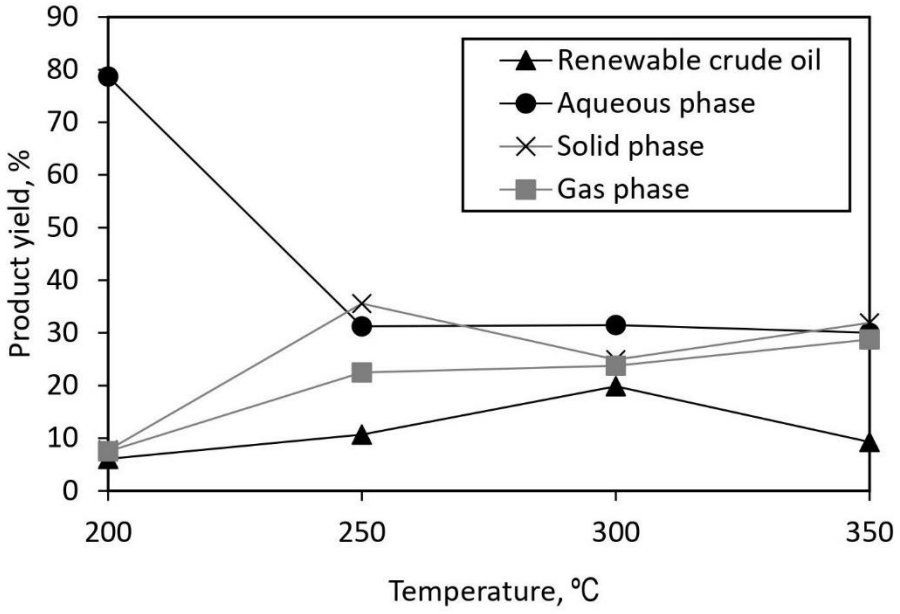

Figure S7. Organic yields of products after HTL of Sucrose/water feedstock

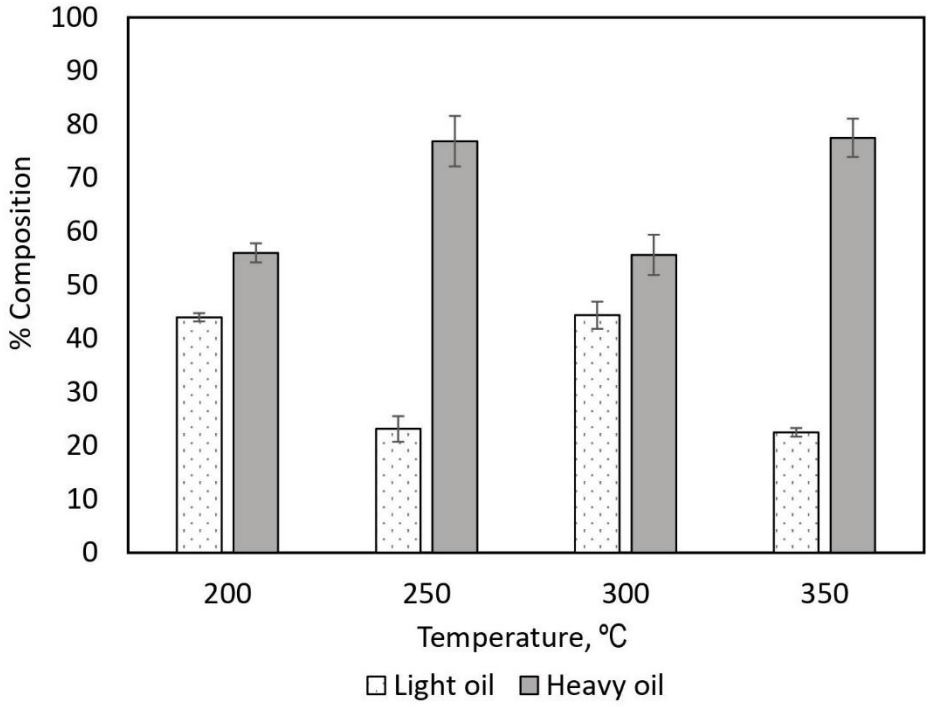

Figure S8. Light and heavy oil fractions in solid products after HTL of sugar

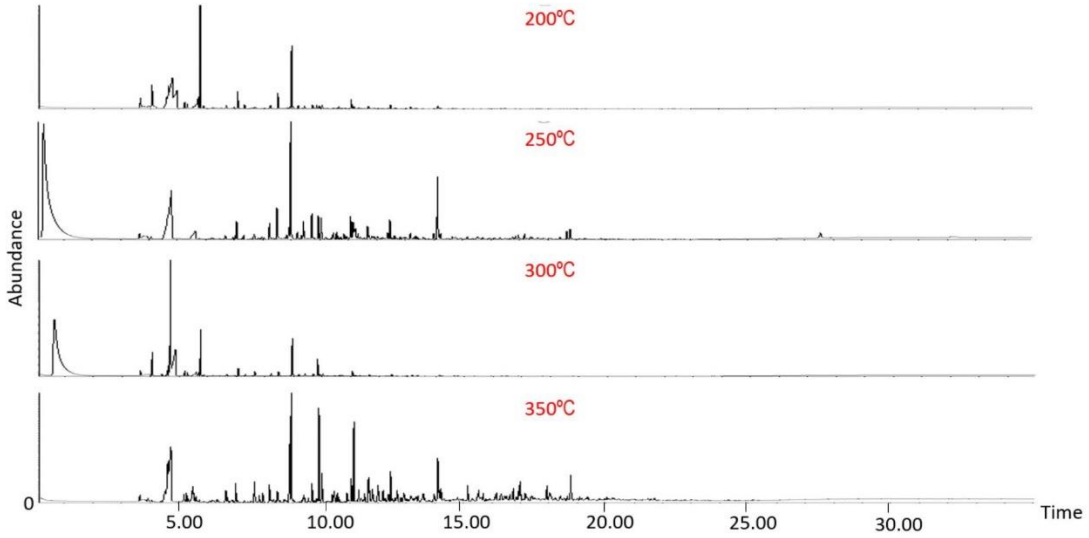

Figure S9. GCMS Spectra of solid products produced from HTL of sucrose feedstock at 200°C, 250°C, 300°C and 350°C

Table S1. GCMS data for solid products produced after HTL of sucrose feedstock at 200°C

Retention Time	Area	% by response	Name	MW
4.772	186828838	17.86438	2-pentene, (Z)	70
5.752	140359675	13.42104	2.5-dimethyl-furan	96
4.936	130293797	12.45856	3-methyl-1-butene	70
8.972	115916962	11.08386	1-(2-furanyl)-ethanone	110
4.64	68549312	6.554613	1,2-dimethyl-, trans-cyclopropane	70
4.06	66645840	6.372605	Acetone	58
4.584	41800996	3.996967	Acetic acid or 1,1-dimethyl-hydrazine	60
8.49	28607039	2.735375	cyclopent-4-ene-1,3-dione	96
7.075	28562354	2.731102	2-ethyl-5-methylfuran	110
3.656	24818126	2.373083	Carbon dioxide	44
5.679	23507264	2.24774	2-ethyl-furan	96
11.073	16604807	1.587734	2-Acetyl-5-methylfuran	124
5.612	16459146	1.573806	Benzoic acid, 4-amino-2-chloro-, 2-(diethylamino)ethyl ester	270
3.787	10160383	0.971525	Glycolaldehyde dimer	120
5.208	9872218	0.943971	3-methyl-butanal	86
3.93	9105972	0.870703	Ethanol	94
9.706	8846477	0.845891	dihydro-5-methyl-2(3H)-Furanone	100
8.231	8069634	0.77161	5-methyl-2(3H)-Furanone	98

10.043	7916191	0.756938	Phenol	94
5.305	7822358	0.747966	2-methyl-butanal	86
9.852	7353637	0.703147	5-methyl-2-Furancarboxaldehyde	110
6.676	6940613	0.663654	Toluene	92
9.942	6906630	0.660405	3-methyl-2-Cyclopenten-1-one	96
7.317	6692965	0.639974	2,3,5-trimethylfuran	110
9.418	6489876	0.620555	5-methyl-2(5H)-Furanone	98
12.454	6318299	0.604149	2-methyl-benzofuran	132
9.207	5839514	0.558368	2,5-Hexanedione	114
5.872	5288487	0.50568	2,4-Dimethylfuran	96
14.109	5176065	0.49493	1,2-dihydro-2-methyl-Cinnoline	146
5.518	4609338	0.44074	3-methyl-2-butanone	86

Table S2. GCMS data for solid products produced after HTL of sucrose feedstock at 250°C

Retention Time	Area	% by response	Name	MW
0.306	1023246052	44.73981	Carbon dioxide	44
4.787	264427982	11.56169	Acetic acid	60
8.974	157030660	6.865916	1-(2-furanyl)ethanone	110
14.122	74850445	3.272717	2-ethyl-1H-Benzimidazole	146
8.494	48371011	2.114946	1,3-dione-4-cyclopentene	96
5.623	34245003	1.497308	Propanoic acid	74
9.715	34223155	1.496353	dihydro-5-methyl-2(3H)-furanone	100
10.044	29882842	1.30658	Phenol	94
9.945	29303995	1.281271	3-methyl-2-cyclopenten-1-one	96
11.079	28843476	1.261135	2-acetyl-5-methylfuran	124
11.24	27313850	1.194255	4-oxopentanoic acid	116
11.164	26849909	1.17397	2,3-dimethyl-2-cyclopenten-1-one	110
9.42	25980593	1.13596	5-methyl-2(5H)-furanone	98
12.456	23651698	1.034133	2-methylbenzofuran	132
8.232	23252250	1.016668	5-methyl-2(3H)-furanone	98
7.082	18197039	0.795637	2-ethyl-5-methylfuran	110
11.671	17299272	0.756383	3-methylphenol	108
27.552	15157648	0.662744	Eicosane	282
8.907	15050447	0.658057	2-methyl-2-cyclopenten-1-one	96
3.814	15039229	0.657566	p-hydroxynorephedrine	167
9.209	12975247	0.567322	2,5-hexanedione	114
18.778	12807183	0.559974	4-methoxy-1-Naphthalenol	174
13.172	11138219	0.487001	4-(5-methyl-2-furanyl)-2-Butanone	152
7.689	11127237	0.486521	2-cyclopenten-1-one	82
13.987	10739661	0.469575	4,7-dimethylbenzofuran	146
18.655	10682600	0.46708	8-methoxy-2H-1-Benzopyran-2-one	176

12.38	10596347	0.463308	7-methylbenzofuran	132
10.466	10479277	0.45819	Vinyl crotonate	112
10.843	9785090	0.427838	cyclobutanone	70
11.83	8961651	0.391834	1,3-pentadiene, (Z)	68

Table S3. GCMS data for solid products produced after HTL of sucrose feedstock at 300°C

Retention Time	Area	% by response	Name	MW
0.647	944953823	51.06045	Carbon dioxide	44
4.701	216654034	11.70687	2-methylfuran	82
4.879	202473340	10.94062	Acetic acid	60
8.97	82808382	4.474539	1-(2-furanyl)ethanone	110
5.756	76869878	4.153653	2,5-dimethylfuran	96
4.067	42877316	2.31687	Acetone	58
9.856	37168084	2.008372	5-methyl-2-furancarboxaldehyde	110
4.644	20572882	1.111653	2-butanone	72
5.613	17529822	0.947221	Propanoic acid	74
3.654	15478056	0.836355	carbon dioxide	44
7.083	15122634	0.817149	2-ethyl-5-methylfuran	110
7.659	13153415	0.710743	Furfural	96
8.493	11818502	0.638611	4-cyclopentene-1, 3-dione	96
11.074	11700662	0.632244	2-acetyl-5-methylfuran	124
3.944	11369987	0.614376	Ethanol	46
4.587	10306945	0.556934	2,3-butanedione	86
5.207	9599612	0.518714	3-methylbutanal	86
3.849	8231451	0.444785	alpha.-methylbenzenepropanamine	149
8.234	7419704	0.400923	5-methyl-2(3H)-furanone	98
9.416	7306372	0.394799	5-methyl-2(5H)-furanone	98
5.687	6824972	0.368786	2-ethylfuran	96
9.706	6535411	0.35314	dihydro-5-methyl-2(3H)-furanone	100
10.037	6357600	0.343532	phenol	94
3.802	6201563	0.335101	2-amino-1-(o-hydroxyphenyl)propane	151
5.304	6158568	0.332777	2-methylbutanal	86
9.946	5269224	0.284722	3-methyl-2-cyclopenten-1-one	96
6.681	5124391	0.276896	Toluene	92
11.664	4759504	0.257179	p-cresol	108
5.522	4736272	0.255924	2-carbamyl-9-[.beta.-d-ribofuranosyl]hypoxanthine	295
9.204	4008298	0.216588	2,5-hexanedione	114

Table S4. GCMS data for solid products produced after HTL of sucrose feedstock at 350°C

Retention Time	Area	% by response	Name	MW
4.736	106916580	8.866241	Acetic acid	60
8.96	73999845	6.136564	1-(2-furanyl)ethanone	110
9.935	70285387	5.828536	3-methyl-2-cyclopenten-1-one	96
4.629	53266064	4.41718	1,2-dimethylhydrazine	60
11.159	52276128	4.335088	2,3-dimethyl-2-cyclopenten-1-one	110
14.107	42538115	3.527546	2-methyl-3-phenyl-2-propenal	146
8.897	37245065	3.088611	2-methyl-2-cyclopenten-1-one	96
11.675	30133037	2.498834	3-methylphenol	108
10.04	22720455	1.884133	Phenol	94
18.773	21195346	1.75766	1-[4-(1-methyl-2-propenyl)phenyl]ethanone	174
12.453	20612501	1.709327	2-methylbenzofuran	132
8.191	20291431	1.682702	1,3-dimethylbenzene	106
12.012	18790779	1.558258	4-methyl-1,4-hexadiene	96
5.501	18198632	1.509153	2-pentanone	86
7.668	18053286	1.4971	2-cyclopenten-1-one	82
15.538	17584355	1.458213	2-isopropyl-5-methyl-3-cyclohexen-1-one	152
11.073	16570036	1.374099	2-Acetyl-5-methylfuran	124
4.53	15326895	1.271009	1,1-dimethylhydrazine	60
17.002	14686604	1.217912	7-methylindan-1-one	146
17.938	14398784	1.194044	2,6-dimethyl-1H-Indole	145
9.693	14379392	1.192436	dihydro-5-methyl-2(3H)-furanone	100
11.813	13575487	1.125771	3-ethyl-2-cyclopenten-1-one	110
13.158	13273325	1.100713	3-ethylphenol	122
16.755	12940086	1.073079	(Z)-1-Phenylpropene	118
15.159	12767281	1.058749	2,3-dihydro-1H-Inden-1-one	132
7.013	12383351	1.026911	Cyclopentanone	84
12.185	12109888	1.004233	1-Isopropylcyclohex-1-ene	124
12.923	12084296	1.002111	2,3-dimethylphenol	122
13.601	12001085	0.995211	3,5-dimethylphenol	122

Chapter 6:

Real-time viscosity variations of sewage sludge during hydrothermal liquefaction under subcritical water conditions

Statement of Authorship

Title of Paper	Real-time viscosity variations of sewage sludge during hydrothermal liquefaction under subcritical water conditions
Publication Status	☐ Published ☐ Accepted for Publication ☐ Submitted for Publication ☑ Unpublished and Unsubmitted w ork w ritten in manuscript style
Publication Details	Edifor, S. Y.; Nguyen, Q. D.; Van Eyk, P.; Biller, P.; Lewis, D. M., Real-time viscosity variations of sewage sludge during hydrothermal liquefaction under subcritical water conditions. In The University of Adelaide: 2020; p 23.

Principal Author

Name of Principal Author (Candidate)	Sylvia Yawa Edifor
Contribution to the Paper	Designed and conducted experiments Data analysis and interpretation Drafted the manuscript and acted as corresponding author
Overall percentage (%)	80
Certification:	This paper reports on original research I conducted during the period of my Higher Degree by Research candidature and is not subject to any obligations or contractual agreements with a third party that would constrain its inclusion in this thesis. I am the primary author of this paper.
Signature	Date 22/01/2021

Co-Author Contributions

By signing the Statement of Authorship, each author certifies that:

i. the candidate's stated contribution to the publication is accurate (as detailed above);
ii. permission is granted for the candidate in include the publication in the thesis; and
iii. the sum of all co-author contributions is equal to 100% less the candidate's stated contribution.

Name of Co-Author	Quoc Dzuy Nguyen
Contribution to the Paper	Assistance with interpretation and presentation of data Drafting and review of manuscript
Signature	Date 29-01-2021

Name of Co-Author	Philip van Eyk
Contribution to the Paper	Concept development Supervised development of work Assistance with interpretation, drafting and review of manuscript
Signature	Date 28/1/2021

Please cut and paste additional co-author panels here as required.

Name of Co-Author	Patrick Biller		
Contribution to the Paper	Assistance with interpretation and presentation of data Drafting and review of manuscript		
Signature		Date	22.01.2021

Name of Co-Author	Tony Hall		
Contribution to the Paper	Assistance with interpretation and presentation of data Drafting and review of manuscript		
Signature		Date	24.01.2021

Name of Co-Author	David M. Lewis		
Contribution to the Paper	Assistance with interpretation and presentation of data Drafting and review of manuscript		
Signature		Date	28/01/2021

Real-time viscosity variations of sewage sludge during hydrothermal liquefaction under subcritical water conditions

Sylvia Y. Edifor[a]* Quoc D. Nguyen[a] Philip van Eyk[a] Patrick Biller[b] Tony Hall[c] David M. Lewis[a]

[a]School of Chemical Engineering and Advanced Materials, The University of Adelaide, South Australia 5005, Australia

[b]Department of Engineering-Biological and Chemical Engineering, Aarhus University, 8200 Aarhus, Denmark

[c]Faculty of Science, The University of Adelaide, South Australia 5005, Australia

Corresponding Author: *sylvia.edifor@adelaide.edu.au

Abstract

Hydrothermal liquefaction (HTL) of sewage sludge could be an energy efficient process to manage solid waste and produce useful fuel in the form of crude-like oil under subcritical conditions of water. In designing a continuous process for commercialisation, design parameters for pipelines and reactors such as viscosity and density are essential data needed to analyse the flow and heat transfer properties of the process. This study seeks to measure the real-time viscosity of sludge during HTL by converting the measured torque/impeller speed data from an anchor impeller in a reactor to shear stress/shear rate data using the Metzner-Otto methods and the Couette principle. Viscosity changes of sewage sludge during HTL were compared to the viscosity variations of algae and mixtures of model compounds. An increase in temperature and pressure decreases viscosity of reacting sludge slurries. The viscosity of sewage sludge can be affected by the chemical speciation of the reacting slurry. The presence

of lignin and metallic ions in ash could catalyse the HTL reaction, affect product yield and hence influence the changes in viscosity of reacting slurries.

Keywords: Hydrothermal liquefaction, Viscosity, Subcritical condition, Rheo-reactor, Reactor design

1. Introduction

The conversion of organic rich wet biomass feedstock via hydrothermal liquefaction (HTL) to produce renewable crude-like oil, aqueous phase, solids and gas below critical conditions of water of 22.1 MPa and 374°C (Wang et al., 2018) is an upcoming process of global interest. Dewatered sewage sludge from Wastewater Treatment Plants (WWTPs) is a binary phase organic slurry which is a potential feedstock for HTL. HTL involves a series of depolymerisation, condensation and polymerisation reactions that change the physicochemical properties of the feedstock (Xue et al., 2016; Yang et al., 2019). The chemical speciation and flow properties of the slurry differ after each reaction process under variable reaction conditions. Flow properties of sewage sludge feedstock such as viscosity and density gradually change from a thick slurry which are mostly Non-Newtonian fluids in real biomass (Yen et al., 2002) into a less viscous slurry. For biomass, the rheological properties of the reacting slurry differ with variable shear rates which consequently leads to a change in the viscosity of the reacting slurry at specific reaction conditions. Variations in slurry viscosity affects slurry motion and heating rate as temperature increases. In the scientific literature, there is no information on the changes in slurry viscosity during HTL under subcritical water conditions, which is required for design purposes. Knowledge of the changes in viscosity will be useful in predicting the flow properties and heating requirements of the HTL feedstock for reactor and piping design process.

Viscosity of sewage sludge can be measured ex-situ, at-line or on-line. Ex-situ viscosity measurement involves sampling the reacting sludge slurry at different reaction times, cooling down the sample to room temperature and determining the viscosity using existing rheometers. One demerit of ex-situ viscosity measurement is that the cooling process could affect the properties of the intermediate products after quenching the reaction and sampling it at a specific reaction condition. This may not capture the true viscosity value at the desired reaction conditions of temperature and pressure which can significantly affect the slurry viscosity. Contrary to ex-situ viscosity measurements, at-line measurement involves sampling a portion of the reacting slurry through a tube to measure viscosity without necessarily quenching the reaction. Pollak et al. (2017) designed a capillary rheometer as an example of at-line viscosity measurement to determine viscosity at high temperatures and high pressure. In that study, viscosity of Newtonian fluid was measured using the pressure drop in the tube by applying Hagen-Poiseuille's equation. Due to the viscosity dependency on shear rate of Non-Newtonian fluids, the apparent viscosity of Non-Newtonian fluids was estimated using the Weissenberg-Rabinowitch equation as a correction for the shear stress and using the flow rate to determine the shear rate in the Newton's law of viscosity (Pollak et al., 2017). At-line viscosity measurement unlike ex-situ may be more precise for viscosity measurement since it avoids the cooling down by sampling and measuring the viscosity immediately. However, sampling the intermediate products during the reaction can potentially alter the reaction conditions, particularly pressure, and ultimately affect the accuracy of viscosity measurement. Both ex-situ and at-line viscosity measurement gives predicted viscosity values of the reacting slurry which may not be the accurate value. On-line viscosity measurement, also known as the real-time viscosity measurement, is preferred as it gives the true and accurate viscosity data under HTL reaction conditions. Nonetheless, real-time viscosity measurements cannot be conducted in conventional existing rheometers. Existing rheometers have a design limitation on

temperature and pressure which makes them unsuitable for viscosity measurement at subcritical conditions of water of about 350°C and 20 MPa. Hence, there is a need to modify a reactor as a real-time viscosity measuring instrument which can operate under HTL conditions.

Technological advancement has led to real-time viscosity measurements during a process on both batch and continuous operations. This has led to the diverse use of mixers and reactors with additional functions and operations including rheometery. Devices that can measure rheological changes of a fluid during a specific process are known as mixer-type rheometers or rheo-reactors. Accurate prediction of real-time viscosity of a slurry using a rheo-reactor involves using physical parameters such as impeller speed and torque to estimate the rheological constants for determining the viscosity of the fluid. Unlike most conventional rheometers, mixer-type rheometers and rheo-reactor keep settling slurries homogeneous throughout the mixture and reduce errors that could arise from wall effect as a result of narrow gaps between impellers and mixers or reactor vessels. Aït-Kadi et al. (2002) studied the rheological characteristics of fluids with both mixer-type and conventional rheometers. Their viscosity–shear rate data using a double couette system, anchor impeller, vane impeller, double helical ribbon and a helical ribbon were in agreement with one another. Choplin and Marchal (2010) conducted experiments using two different impellers on a rheo-reactors: an anchor impeller and a helical ribbon impeller. A comparison drawn from their rheograms obtained from the rheo-reactors and the conventional rheometers proved excellent agreements with errors <5%. All existing rheo-reactors have been limited in their application to moderate temperatures up to 180°C and pressures as high as 400 bar. Nonetheless, there is currently no existing rheometer that can accurately measure the viscosity of fluids near critical water conditions (up to 350°C). A rheo-reactor can be modified for real-time viscosity measurement under subcritical condition of water with minimal errors.

In constructing a rheo-reactor to operate under HTL conditions, it is important to select a suitable impeller geometry and measuring method with least limitations on the reaction conditions. Most biomass samples which are hydrothermally liquefied consist of solids suspended in a solvent, typically water. One advantage of using a rheo-reactor is the ability to measure the viscosity of a homogenous binary phase biomass slurry with reduced phase separation, sedimentation and errors associated with the gap depending on the choice of impeller and its geometry during measurement. Close clearance impellers are recommended for highly viscous fluids (Luan et al., 2014) with a potential of reducing phase separations during agitation. For mixing fluids in the laminar region, the anchor and helical impellers are employed with the benefit of having a narrow gap between the impeller blades and the walls of the mixing vessel which reduces the unyielding zone over the vessel (Jo et al., 2017). The geometry and dimensions of the close-clearance impellers are carefully designed to reduce errors that could arise due to the particle size of the suspended solids in the slurry. Research has shown that the vane and helical impellers have suitable geometries to reduce errors during viscosity measurement of viscous fluids (Bbosa et al., 2017; Castell-Perez et al., 1991). However, the most challenging task in using such geometric impellers is the conversion of the measured torque-impeller speed data into a shear stress/ shear rate data for estimating the slurry viscosity. To accurately predict the viscosity of slurries in a rheo-reactor, it is important to determine the geometric and rheological constants using properties of the measuring system and standard fluids using the appropriate methods.

The Couette analogy and Metzner-Otto methods can be used to convert torque/impeller speed data into shear stress/shear rate data (Bbosa et al., 2017; Choplin & Marchal, 2010; Jo et al., 2017; Luan et al., 2014). These analogies can be adopted in any reactor configuration with two concentric cylinders where the internal cylinder or impeller is rotating at a known speed. The Couette analogy uses impeller geometries whereas the Metzner-Otto constant uses

dimensionless numbers to estimate the geometric constants for real-time viscosity estimation. Both analogies can be used for power predictions and quantifying heat requirements of agitated vessels containing non-Newtonian fluids obeying the power law model (Choplin & Marchal, 2010). Rheograms drawn from data obtained using both analogies were similar with minimal errors <5%. Derived geometric constants from these analogies have shown good agreements in rheological data using anchor, helical ribbon, double helical ribbons (Choplin & Marchal, 2010).

This study seeks to measure the viscosity of sludge before and during HTL by converting the measured torque/impeller speed data from an anchor impeller in a custom-built rheo-reactor to shear stress/shear rate data using the Metzner-Otto methods and the Couette principle. The variation in apparent viscosity of sludge slurries at different concentrations during HTL process was estimated. A comparison between the viscosity profile of sewage sludge to other types of real biomass as well mixtures of model compounds with similar organic constituents were analysed to determine the effects of inorganics and lignin to the changes in viscosity.

2. Materials and Methods

2.1.Reactor set up

The rheo-reactor set up consisted of a 1L Parr batch reactor (Model 4577, Parr Instrument Co., Moline, IL, USA) equipped with a 4848 PID controller with speed and temperature controllers, a 2 Nm torque sensor with an accuracy of 0.01 Nm and an anchor impeller (Dimensions of U-shaped Blade: 9.1 cm x 1.3 cm x 5.6 cm). The stirred tank reactor vessel has an internal diameter of 9.5 cm and a depth of 15.8 cm. The reactor was modified by attaching a more accurate torque sensing device. A data acquisition (DAQ) device was attached to the torque sensor to provide accurate torque reading up to 1µm. The reactor was set up as shown in Figure 1.

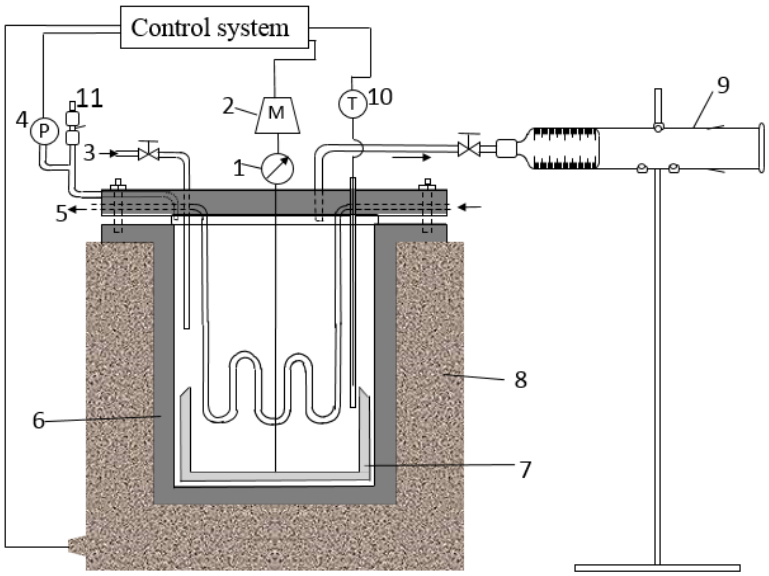

No.	Part
1	Torque sensor
2	Adjustable speed motor
3	Gas inlet tube
4	Pressure transducer
5	Cooling water tube
6	Stirred tank reactor
7	Anchor impeller
8	Electric furnace
9	Gas collection syringe
10	Thermocouple
11	Pressure relief valve

Figure 5. Rheo-reactor type rheometer set up

2.2.Determination of geometric constants

2.2.1. Couette analogy

The Couette analogy concept was used to interpret data obtained from the measurements on the speed and torque on the anchor impeller following the approach of Aït-Kadi et al. (2002). An unloaded torque on the impeller shaft in a sealed reactor vessel was measured as a function of the impeller speed at room temperature. The impeller torque and speed data were related and interpreted to obtain geometric constants after calibrating the reactor to function as a rheometer using a Newtonian fluid with known properties. A general-purpose silicone fluid viscosity standard produced by Brookfield Ametek was purchased and used as the Newtonian fluid standard. This Newtonian standard is referred to as a high viscosity silicon oil in this study (12.3 Pa.s at 25°C). The reactor vessel was loaded with the Newtonian fluid and sealed completely. Torque values at different rotational speeds were recorded at room temperature. The shear rate and shear stress constants were estimated to determine the viscosity of the fluid.

2.2.2. Metzner and Otto constants

The high viscosity silicon oil which is a Newtonian fluid was again in conjunction with 2% carboxymethyl cellulose (CMC) solution which is a power law fluid. A Universal Stress Rheometer SR5 (TA Instruments) with a cone and plate configuration was used to obtain shear rate-shear stress data of the power law fluid. The shear rate (γ)-shear stress (τ) data was fitted into the power law model to obtain its rheological constants. The Metzner –Otto constant as proposed by Metzner and Otto (1957) was used to determine the viscosity of both Newtonian and non-Newtonian fluids.

2.2.3. Validation and verification of viscosity measurement

Silicon oil with variable dynamic viscosities from 1 Pa.s to 0.02 Pa.s between 20°C to 100°C was purchased from Anton Paar. This viscosity standard will be referred to as the low viscous silicon oil in this study. The high viscosity silicon oil, low viscosity silicon oil and 2w/w% CMC solution were used to validate the viscosity measurements obtained from the rheo-reactor. The viscosity standards used as validation fluids were transferred into the reactor vessel and sealed completely. The torque values from the impeller shaft at different impeller speeds at constant temperatures were logged using labview software. The viscosities of the fluids were estimated from the torque-speed data. These values were compared to the standard values using the coefficient of regression. Tolerance in viscosity reading with errors <10% will be acceptable (Wrolstad et al., 2005). Additionally, one-way ANOVA followed by Tukey HSD post hoc was used to determine if the viscosity data collected were statistically different using the Couette analogy and Metzner-Otto method.

2.3.Rheological characterisation

The experiment was set-up as shown in Figure 1 without the cooling coils to reduce resistance from the wetted parts of the reactor. The reactor was sealed with no sample, purged three times

and pre-charged with 92 bar N_2. The initial N_2 charge is to ensure that the temperature and pressure of the N_2 gets to the operating conditions of the HTL reactor/operating conditions like that of the biomass feedstock. During heating, the temperature of the reacting slurry increased by 9ºC/min from room temperature 300ºC and 2ºC/min from 300ºC to 350ºC. The torque of the N_2 loaded reactor vessel at a constant impeller speed was recorded from room temperature to the operating conditions of 350ºC, 200 bars. At each impeller rotational speed, the measured torque value was measured as a function of temperature and this was used as the background for subsequent measurements.

Dewatered sewage sludge obtained after aerobic and anaerobic treatment from Melbourne Water Western treatment Plant, Victoria, Australia was used as the main biomass in this study. Prepared biomass slurries with different solid concentrations were loaded into the reactor vessel and sealed completely. The reactor vessel was purged three times and pre-charged with N_2. The impeller speed was set to a constant value and the torque at different temperatures were recorded while the reactor vessel was heated up to 350ºC. The absolute torque was subtracted from the background to obtain the actual data which was used to estimate the apparent viscosity across a temperature range from 25ºC to 350ºC.

2.4.Feedstock characteristics of biomass

Variations in apparent viscosity of 20%w/w dry sewage sludge slurries were compared to the changes in the apparent viscosity of 20%w/w *Tetraselmis sp*, *Spirulina sp* and mixtures of model compounds based on the organic compositions of dry samples at 124 s^{-1}, 248 s^{-1} and 372 s^{-1}. This study was conducted to predict the effects of inorganics on the viscosity variations in biomass. *Tetraselmis sp* was cultured in salt water and used as a no-lignin/high ash feedstock. *Spirulina sp* was purchased from Bulk Nutrients, Australia and used as a no-lignin/low ash biomass. The composition of the feedstock used as determined by Obeid (2020) have been

presented as stated in Table 1s on the Supplementary Information Sheet. The viscosity profile for each biomass sample was determined using the measured torque at a fixed impeller speed over a temperature/pressure range under subcritical water conditions.

2.5. Product analysis

After the HTL process, the reactor was cooled to room temperature and the gas released. The gas phase was quantified by subtracting the mass of products in the cooled reactor from the mass of reactants in reactants in the reactor prior to heating. Crude-like oil product floating on the aqueous phase was collected into a container and dried at 40ºC to evaporate any residual moisture in the oil phase. The remaining aqueous and solid mixture was vacuum filtered to separate the solid products from the aqueous products and the solid residue was dried in a drying oven at 40ºC till no change in mass was observed.

Organic yields of the crude-like oil and solid phase were determined using a Weatherford Instruments Source Rock Analyser (SRA) through thermal desoption to 300ºC and subsequent pyrolysis to 650ºC following the method described by Obeid et al. (2020). Aqueous yields were determined by subtraction. Gas chromatograph-mass spectroscopy (GC-MS) on the liquid phase products were determined using a PerkinElmer SQ8. Details of the GC-MS conditions and separating capillary have been stated in previous work (Obeid et al., 2020). Chemical compounds in the liquid phase characterizable through GC-MS were interpreted by comparison to the spectral database of NIST14 spectral library using PerkinElmer TurboMass 6.1 software.

Metallic analysis on biomass feedstock was conducted by CSIRO, Waite Campus, Urrbrae, South Australia using an inductively couples plasma – optical emission spectrometry (ICP-OES). The ICP-OES was used to identify and quantify the metallic composition of the biomass using emission plasma. The quantified elements are listed in the Supplementary Information sheet. Biomass was finely ground to a particle size < 2 mm and acid digested with nitric acid.

A range of metallic elements in the inorganic content of the feedstock was determined by plasma emission in the ICP-OES and each sample was analysed in triplicates.

3. Results

3.1.Calibration and geometric constant determination

Fluid properties of the silicon oil and CMC solution were used to estimate the geometric constants of the anchor impeller on the rheo-reactor using both the Couette analogy and the Metzner-Otto principle as stated in Table 1.

Table 1: Geometric constants for anchor impeller for a rheo-reactor

Parameters	Couette	Metzner-Otto
R_i (mm)	39	-
r (mm)	43	46*
K_p	-	491
K_{pn}	-	49
$\boldsymbol{k_\tau}$ (Pa/Nm)	1516	1462
$\boldsymbol{k_\gamma}$ (rad^{-1})	31	30**

*Radius obtained from the equivalent diameter **k_γ=, k_s

The accuracy of the viscosity measurement using the Couette and Metzner-Otto principles was determined using Newtonian fluids and a Non-Newtonian fluid. High viscous silicon oil with a standard viscosity of 11.7 Pa.s at 23ºC was used to validate the accuracy of the viscosity measurement. The fluid viscosity using the Couette analogy was determined to deviate by 0.3% from the standard viscosity of the fluid while that of the Metzner-Otto deviated by 1.7% of the standard viscosity. Additionally, the viscosity of low viscous silicon oil, which is another Newtonian fluid was determined with both methods. As shown in Figure 2, the viscosity of

low viscous silicon oil averagely deviates about 3.1% from the standard fluids using the Couette's analogy while the deviation from the standard viscosity measurement is about 3.5% using the Metzner-Otto principle. This is in agreement with literature where the acceptable viscosity reading should have errors <10% (Wrolstad et al., 2005). The deviations of the determined viscosities increased when comparing the estimated viscosity of high viscous silicon oil and low viscous silicon irrespective of the type of method used.

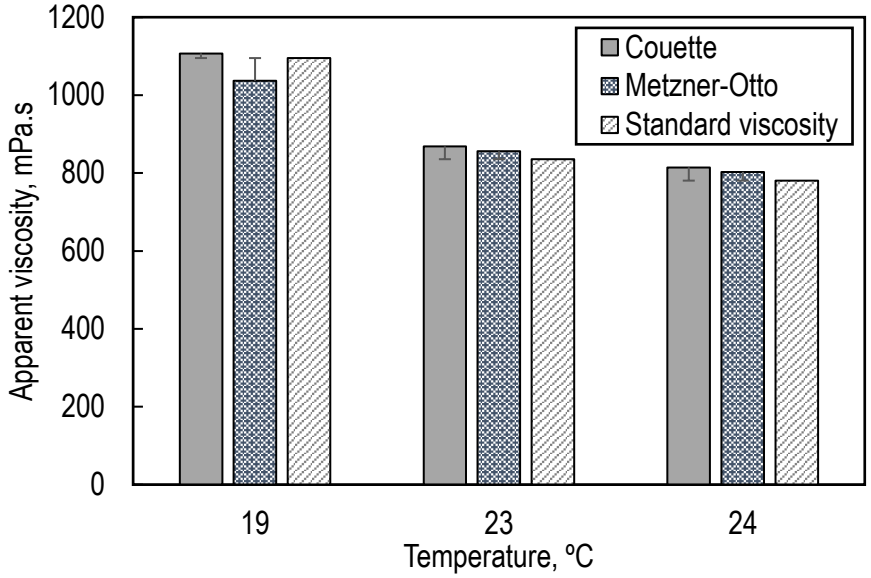

Figure 6. Comparison of the viscosity of low viscous silicon oil using Couette and Metzner-Otto principles.

One-way ANOVA was conducted to statistically analyse the difference between the viscosity data sets obtained from the Couette and Metzner-Otto methods. A Tukey HSD post-hoc test was used to predict whether the relationship between both methods was statistically significant. As stated in Table 2s from the Supplementary Information sheet, the one-way ANOVA test showed a significant difference between the viscosity values obtained from both viscosity methods. The null hypothesis was rejected as the P-value is < 0.05 and $F > 4.1$ ($F(3) = 35.1$, $p = 0.00006$). Table 3s in the Supplementary Information Sheet shows the results of the Tukey HSD test. From the conducted post hoc test, it can be inferred that there is a significant

difference between the independent variable (temperature) and each dependent variable (viscosity data obtained from different methods). However, there is no significant difference between the viscosity values obtained from each method and the standard viscosity value. Thus, implies that both the Couette and Metzner-Otto method can be used to accurately predict the fluid viscosity. The absolute difference in the mean of viscosity data obtained from the Metzner Otto method and the mean of the standard viscosity was five times lower than the absolute difference between the mean of viscosity data obtained from the Couette method and the mean of the standard viscosity. Hence, the Metzner-Otto method is statistically more accurate than the Couette method.

The apparent viscosity of a Non-Newtonian fluid at a constant temperature is dependent on the shear rate unlike the viscosity of Newtonian fluids which is independent of shear rates at any given temperature. Hence the apparent viscosity of 2w/w% CMC solution was determined within a shear rate range from 0 to 350 s^{-1}. The increase in shear stress with an increase in shear rate shown in Figure 3 depicts that CMC solution is a Non-Newtonian fluid with pseudoplastic behaviour. Apparent viscosities determined with both methods as shown in Figure 3 are similar.

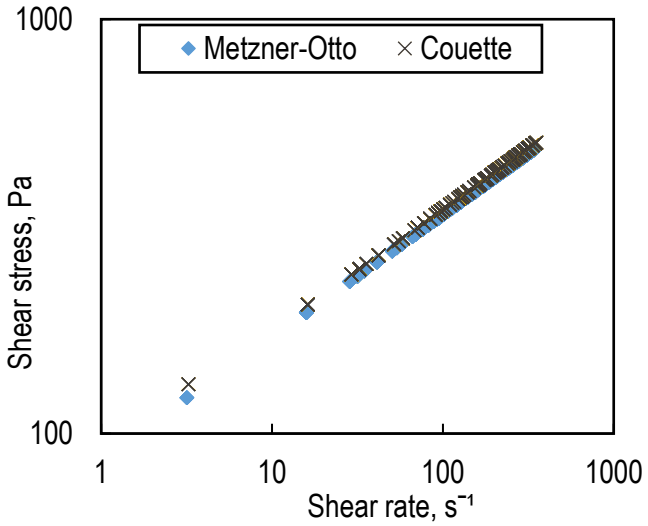

Figure 7. Flow curve 2% CMC solution using a standard rheometer, Couette and Metzner-Otto methods

A Tukey HSD test conducted on the apparent viscosity data for the two apparent viscosity methods using CMC solution showed that both Couette analogy and Metzner-Otto principle were not statistically different as the absolute difference of the mean was less than the critical range (0.08 << 194.8). Hence, both methods agree with each other and valid for apparent viscosity determination of Non-Newtonian fluids.

3.2.Factors affecting the changes in apparent viscosity of reacting sludge during HTL

During heating under subcritical conditions of water, many factors can influence the changes in the apparent viscosity of the HTL products. The apparent viscosity of reacting sludge can vary due to impose external conditions (shearing force, an increment in reaction temperature and pressure), formation of new products, phase transitions and the composition of the feedstock.

3.2.1. Apparent viscosity variation due to imposed external conditions

Apparent viscosity can be modelled as a function of temperature, pressure and solid concentration at different shear rate. Temperature has significant effects on the apparent viscosity of real biomass which includes sludge. Pressure on the other hand has negligible effects on the apparent viscosity of reacting slurries under subcritical conditions (Chen et al., 2020). However, pressures above critical conditions of water have a significant but minimal influence on the apparent viscosity of the slurry. At near critical conditions of water, the properties of water which includes polarity, dielectric constant, ionic products, solvation ability, density and fluid viscosity (Gu et al., 2020; Masoumi et al., 2020; Suryawanshi et al., 2020; Tian et al., 2020) change per degree rise in temperature and an increase in pressure. Consequently, water-based feedstock will experience significant variation in its properties at near critical and critical conditions of water. As anticipated, an increase in feedstock

concentration will increase the apparent viscosity of the slurry as increasing concentration increases internal resistance in the slurry.

HTL under subcritical water conditions occurs between 280ºC and 370ºC (Tzanetis et al., 2017). In order to attain the operating conditions of 350ºC and 200 bars, the reactor vessel was pre-pressurised with an initial amount of nitrogen. Figure 4 shows the apparent viscosity profile of sewage sludge slurries with an increase in temperature and pressure at three different shear rates. As shown in Figure 4, the changes in apparent viscosity of the reacting slurry at 124 s^{-1}, 248 s^{-1} and 372 s^{-1} was minimal during the heating up of sludge from room temperature to 120ºC. Application of heat in the form of increase in temperature breaks down the sludge structure (Li et al., 2014). The breakdown of macromolecules in the sludge during the heating process from room temperature to 120ºC has minimal effects on changes in apparent viscosity of the reacting slurry at all three shear rates. On average, the apparent viscosity at 124 s^{-1}, 248 s^{-1} and 372 s^{-1} decreases significantly between 120ºC to 220ºC and then slightly increases when the temperature of the reacting slurry increases to 280°C for all shear rates used in this study. The apparent viscosity-temperature curve for sludge at 124 s^{-1}, 248 s^{-1} and 372 s^{-1} then decreases gradually to about 320°C, peaks sharply at 335°C and finally increases as the reaction temperature increases from 335°C to 350°C.

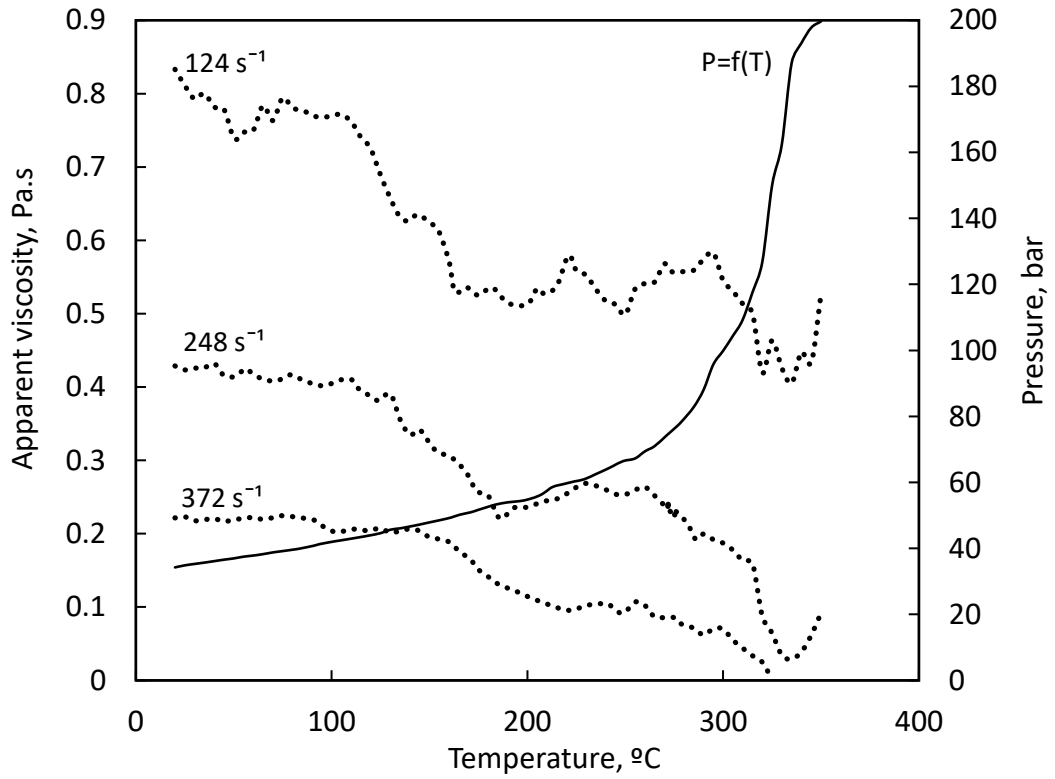

Figure 8. Apparent viscosity profile of municipal sewage sludge during heating up period and HTL process at 124 s^{-1}, 248 s^{-1} and 372 s^{-1} and a pressure-temperature curve, P = f (T).

The temperature-pressure curve as shown in Figure 4 increases linearly to 70 bar at 265°C and then exponentially as it approaches subcritical pressures of 200 bar. Operating under high pressures below critical point keeps the fluid in the liquid phase. Pressure at near critical point has minimal to no effect on the yield of biocrude (Guo et al., 2015; Qian et al., 2017). The plots of apparent viscosity at constant shear rates versus temperature as shown in Figure 4 are almost parallel to each other despite the sudden exponential increase in pressure at 265°C. This is an indication that the effect of pressure on sludge viscosity – temperature relationship may not be significant.

For all shear rates used, a gradual decrease in apparent viscosity models of HTL reacting sludge as shown in Figure 4 was observed. Apparent viscosity decreases with an increase in shear rate

at specified reaction temperatures and pressures. This clearly indicates that the sludge is non-Newtonian and shear thinning as expected.

3.2.2. Apparent viscosity variation due to new product formation

During HTL, the organics in the wet feedstock are converted by a series of chemical reactions to yield HTL products. HTL under subcritical conditions of water produces a four-fractioned product which results from the changes in molecularity, chemical and physical compositions of the intermediates during product formation. The mass yields of each product phase in the phase separation diagram shown in Figure 1s in the Supplementary Information Sheet shows the gradual decrease in solid and crude-like oil product from 200°C to 300°C. The presence of solids and crude-like oil which is a more viscous fluid compared to water increases the overall slurry viscosity. According to Saba et al. (2018), the viscosity of crude-like oil extracted using acetone and cyclohexane were determined to be quasi-Newtonian with high viscosity values. These viscosity values can increase up to 10000 times higher than conventional crude (Kumar et al., 2019). The overall decrease in sludge apparent viscosity during HTL as shown in Figure 4 is due to the gradual depletion and conversion of the organics in the solids in the feed which results in the formation of new compounds that may be present (gas and crude-like oil) or soluble in the aqueous phase.

Compounds with high molecular weights have high apparent viscosities. Consequently, fluids that contain high molecular weight compounds have relatively higher apparent viscosities than fluids with lower molecular weight compounds. According to the GCMS analysis data presented in the Supplementary information sheet, compounds detected in crude-like oil (Figure 3s, Table 3s), particularly tetracyclic triterpanes in the light oil fraction, have higher molecular weights than compounds present in the aqueous products (Figure 3s, Table 4s). Therefore, the formation of crude-like oils increases the overall viscosity values of the reacting

slurry due to the presence of high molecular weight compounds in the product (Saba et al., 2018).

3.2.3. Apparent viscosity variation with feedstock solid concentration

As expected, an increase in solid concentration increases the apparent viscosity of sludge at a constant shear rate of 372 s^{-1} mainly due to the increase of solids in the slurry. The presence of solids in a slurry increases the resistant forces in the slurry. As shown in Figure 5, viscosity of 20wt% and 25wt% sludge slurries decreases with an increase in temperature and pressure.

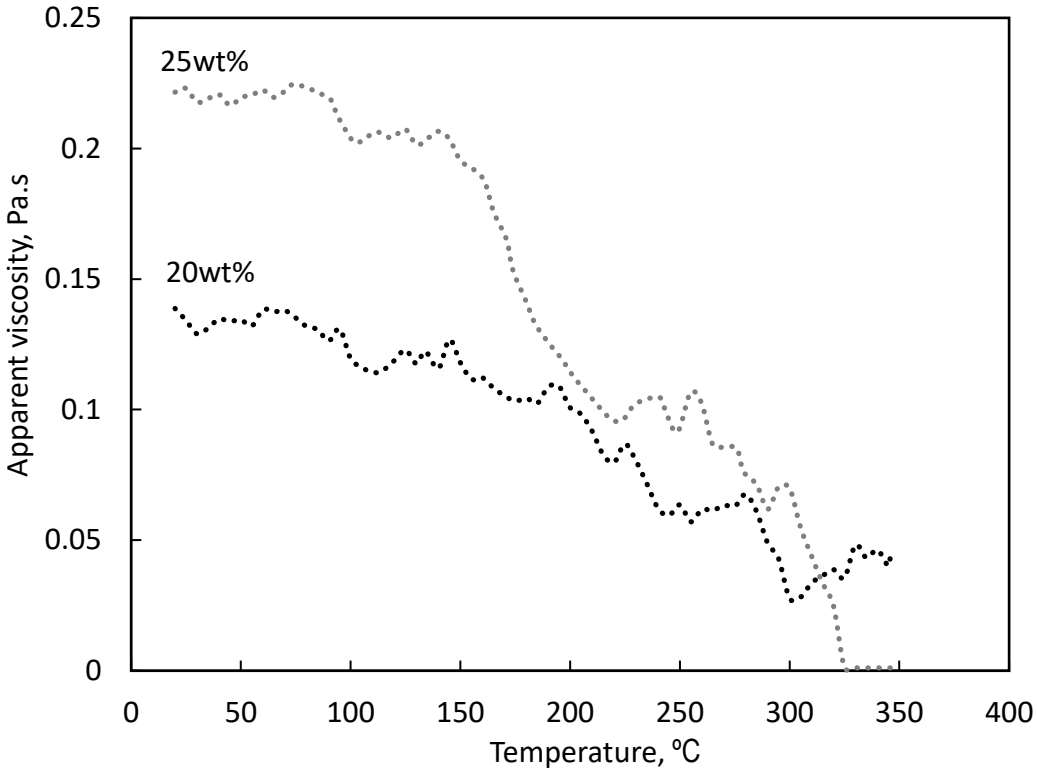

Figure 9. Apparent viscosity profile of sludge at different solid concentrations at a shear rate of 372 s^{-1}

During continuous HTL reaction process in tubular reactors, the flow and heat transfer properties can be predicted by knowing the changes in viscosity of the reacting slurry. However, the flow and heat transfer properties cannot be estimated without knowledge of the density of the reacting slurry which is yet to be determined. The feed stream at room conditions

for highly viscous feedstock such as 25wt% sludge in this study, can be pre-heated to reduce the viscosity of the feedstock to ease transportation. Knowledge of slurry viscosity and density can be used to determine dimensionless numbers such as Reynolds, Prandtl and Nusselt numbers. These dimensionless numbers are useful in specifying flow velocity of HTL slurries in pipes, estimating the heat requirements for HTL of real biomass and heat exchanger design, particularly with scale-up design and optimisation. High viscosity leads to low Reynold number and low heat transfer coefficients. It is desirable to process a low viscous fluid as it reduces transportation issues and enhances effective heat transfer during HTL. Heat transfer for less viscous fluids like water have a high heat transfer capacity which is contrary to viscous fluids which have low heat transfer capacities.

3.2.4. Apparent viscosity variation with feedstock composition

The variability in the apparent viscosity profile of sludge slurries under subcritical conditions of water can be influenced by the organic compositions of the feedstock. Individual macromolecules of biomass which includes proteins, carbohydrates, lipids and lignin will have different viscosity profiles under subcritical water conditions. Consequently, biomass slurries with variable organic components exhibit unique viscosity profiles under elevated temperatures and pressures (Edifor et al., 2020). Currently, there is no information on the effects of the inorganics in the biomass on the changes in viscosity of the reacting slurry. Metallic compounds in the inorganic fractions of the biomass can potentially affect the chemical speciation of the compounds produced and hence influence the variations in the viscosity of the reacting slurry.

Sludge is a lignin-high ash biomass containing sulphur, phosphorus, iron and calcium ions which can potentially catalyse or inhibit HTL reactions (Obeid, 2020) **.** To determine the effects of the inorganic fraction on the apparent viscosity profile of sewage sludge, the apparent

viscosity profile of sludge was compared to that of mixtures of model compounds with the same composition (Table 1s) as that in sludge. As shown in Figure 6, the apparent viscosity profile of sludge biomass at temperatures below 175ºC was slightly higher than the viscosity of mixtures of model compounds. However, above 175ºC, the apparent viscosity of sludge biomass decreased while the apparent viscosity of mixtures of model compounds increased with temperature. The difference between the apparent viscosities of sludge biomass and mixtures of model compounds was about 0.1 Pa.s at 372 s^{-1}. According to the mass yield data shown in Figure 4s of the Supplementary Information, sludge biomass produces solids and crude-like oil with mass yield of 25% higher than the mass yield of solids and crude-like oil produced from mixtures of model compound. The high solid yield results from the interactions of high amounts of carbohydrates, the presence of lignin and high ash content in the biomass feedstock (Smith et al., 2016) while the crude-like oil yields results from the high lipids in the feedstock. Insoluble inorganic metals in the ash remains in the solid products after HTL. Comparing the mass yield of produced solids and crude-like oil, we expect the viscosity of sludge biomass to be higher than the viscosity of mixtures of model at 350ºC due to the high solid and crude-like oil yields. Contrarily, the apparent viscosity of sludge biomass was less than the apparent viscosity of mixtures of model compounds. This deviation is likely due to the effects of metallic compounds in the feed and the presence of lignin in the sludge biomass which can potentially alter the HTL pathway and mechanism to yield products that are less viscous. According to Durak and Genel (2020), catalysts such as iron, zinc and a combination of iron and zinc speeds up reaction and increase the crude-like oil yields in the order Zn < Zn + Fe < Fe. The addition of iron to biomass can increase the production of heavy oils and solids in the product phase. Even though the iron concentration in the sludge is three times less than that used by Durak and Genel (2020), the presence of iron and other metallic elements can have

a minimal catalytic effect which can affect yield of crude-like oil and solid and consequently affect the apparent viscosity of the reacting slurry.

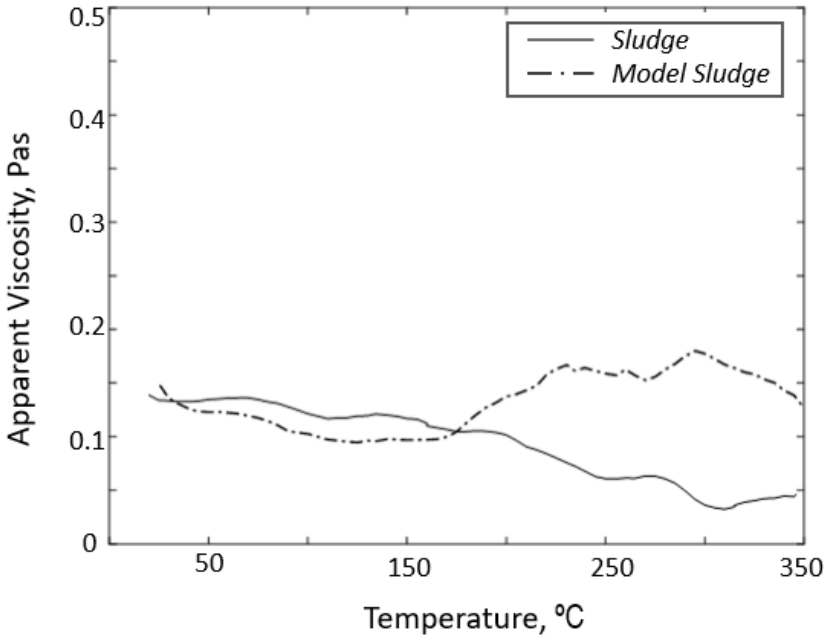

Figure 10. Apparent viscosity profile of sludge biomass and mixtures of model compounds at 372 s^{-1}

To further analyse the effects of inorganics in biomass, the viscosity profile of a high ash-no lignin algae (*Tetraselmis sp*) was compared to the viscosity profile of mixtures of model compounds shown in Figure 7. *Tetraselmis sp* is rich in sodium, aluminium, magnesium and calcium salts as it was cultured in salt water. *Tetraselmis sp* contains high carbohydrate and protein compounds hence produces more solid products with dense crude-like oils. Mass yields of solids and crude-like oil of *Tetraselmis sp* shown in Figure 4s in the Supplementary information is about 40% higher than that produced by model compounds. Despite the mass yields of algae, the overall apparent viscosity profile of *Tetraselmis sp* decreases from the apparent viscosity profile model compounds when T>50°C with an average variation of 0.05 Pa.s. The lower viscosity of the real biomass compared to the viscosity of the mixtures of model

compounds at T>175°C is due to the effects of high ash content similar to that observed in the viscosity profile of sludge slurries. Comparing the average differences in apparent viscosity variations as shown in Figure 6 and Figure 7, the difference in apparent viscosity variations between the biomass and mixtures of model compounds is greater in sludge than in *Tetraselmis sp*. This difference may be a result of the effect of lignin on the reaction pathway of sludge feedstock and the effect of salts in *Tetraselmis sp*. According to the data shown in Table 6s in the Supplementary Information, the high amounts of salts which is evident by the presence of sodium can yield a catalytic effect during HTL of algae. High ash content in biomass can significantly affect the physicochemical properties of crude-like oil produced via HTL through the catalytic effect of these metal ions on polymerization reactions (Díaz-Vázquez et al., 2015). Additionally, alkali metals and alkaline earth metals promote reactions and inhibit reactions respectively as their catalytic effects during thermal decomposition (Jiang et al 2013). Catalytic and inhibitory effects increase conversion rates and may have potentially increase the mass yields of the HTL products which can affect the apparent viscosity of the product. The effects of metallic ions on yield of crude-like oil can be minimal due to the small concentrations of these elements which could produce significant catalytic effects. Hence the presence of metal ions in real biomass affects the viscosity profile of the reacting slurry under HTL conditions.

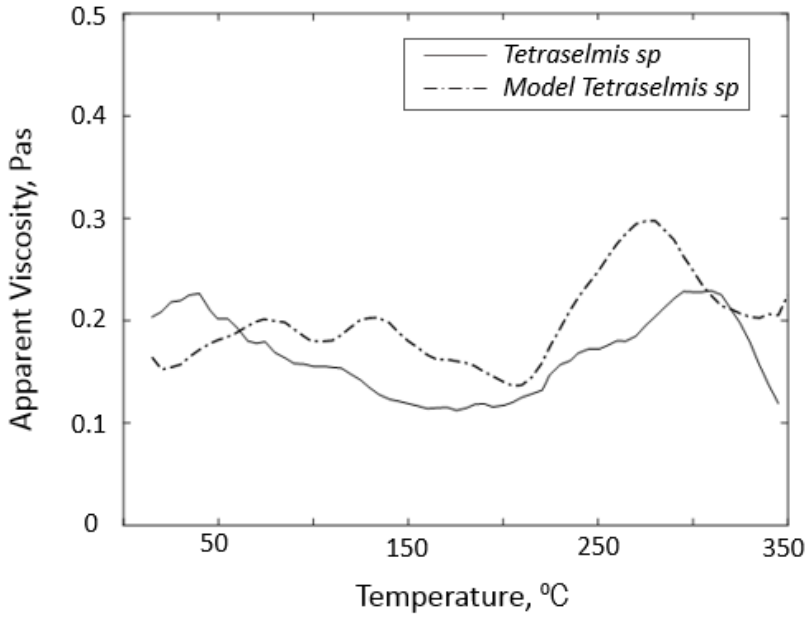

Figure 11. Apparent viscosity profile of *Tetraselmis sp* and mixtures of model compounds at 372 s^{-1}

To determine the effects of low ash on the apparent viscosity profile of biomass slurries, *Spirulina sp* was used as a low-ash/no-lignin biomass. *Spirulina sp* contains low carbohydrates, no ash and no lignin, hence no solids were formed at the end of the reaction process. Consequently, the mass yields shown in Figure 4s for *Spirulina sp* were identical to the mass yields of each product in mixtures of model compound. *Spirulina sp* contains high amounts of proteins of which produced a thick and sticky viscous crude-like oil. A significant change in the apparent viscosity profile of *Spirulina sp* and mixtures of model compounds was shown in Figure 8. The viscosity of *Spirulina sp* within a temperature range of 100°C< T<340° was lower than the apparent viscosity of the model *Spirulina sp*. The changes in apparent viscosity values of the biomass from the apparent viscosity of the mixtures of model compounds in *Spirulina sp* was similar to that in *Tetraselmis sp*. This variation within the stated temperature range is again due to the catalytic and inhibitory effects of the inorganics in the biomass even

though *Spirulina sp* contained less ash but high amounts of potassium (alkali earth metals) which would catalyse the reaction and affect the yield of products.

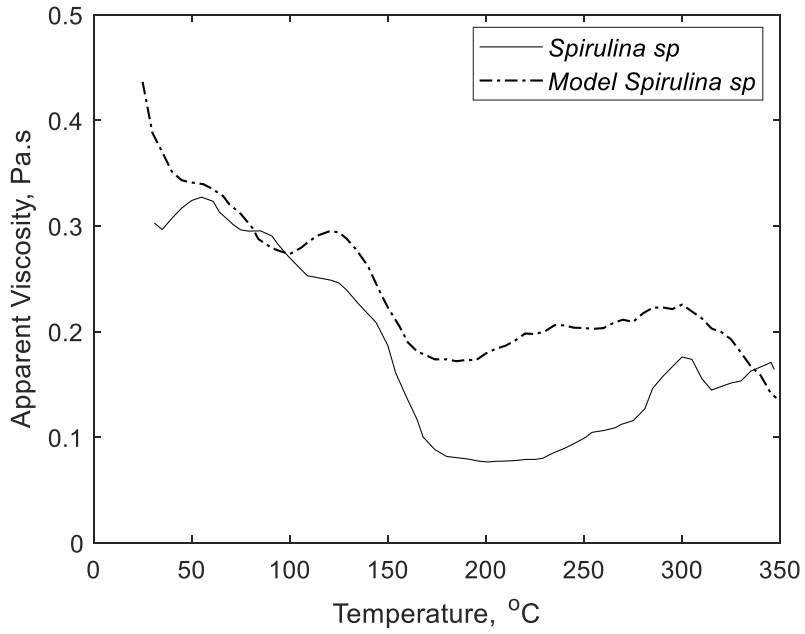

Figure 12. Apparent viscosity profile of *Spirulina sp* and mixtures of model compounds at 372 s^{-1}

In addition to the effects of the various macromolecules on the apparent viscosity changed of biomass, the presence of certain metallic compounds in the inorganic fraction of biomass greatly influences the viscosity profile of biomass under HTL conditions.

4. Conclusion

Rheo-reactors can be used for real-time viscosity measurement of slurries under subcritical conditions of water using the torque-impeller speed raw data. The Metzner-Otto method and Couette principle were valid for determining the viscosity for both Newtonian (errors <5%) and non-Newtonian fluids. Statistically, the viscosity data obtained from both methods agreed with the viscosity values from the viscosity standard.

As expected, temperature and pressure are major factors that influence changes in the apparent viscosity of reacting slurries. Biochemical composition as well as the presence of mineral elements in the ash component of biomass can adversely affect the reaction mechanism of the feedstock biomass under HTL conditions. The dominance and mixtures of certain macromolecules (lipids, proteins, lipids and lignin) in biomass can predict the apparent viscosity profile of the reacting slurry. However, the presence of certain metallic ions can catalyse the reaction by promoting or inhibiting the reaction mechanism that causes variations in the physicochemical properties of the feedstock, particularly slurry viscosity. Elucidating the apparent viscosity variations in biomass is necessary for estimating flow properties and the heat requirements of real biomass during plant design and scale-up procedures.

Acknowledgement

The authors wish to acknowledge Melbourne Water for providing the feedstock.

Funding: This work was supported by Southern Oil Refining and the Australian Research Council's Linkage Projects funding scheme [Project LP150101241].

References

Aït-Kadi, A., Marchal, P., Choplin, L., Chrissemant, A.-S., & Bousmina, M. (2002). Quantitative Analysis of Mixer-Type Rheometers using the Couette Analogy. *The Canadian Journal of Chemical Engineering, 80*, 1166-1174.

Bbosa, B., DelleCase, E., Volk, M., & Ozbayoglu, E. (2017). Development of a mixer-viscometer for studying rheological behavior of settling and non-settling slurries. *J Petrol Explor Prod Technol, 7*, 511-520.

Castell-Perez, M. E., Steffe, J. F., & Moreira, R. G. (1991). Simple determination of power law flow curves using a paddle type mixer viscometer. *Journal of Texture Studies, 22*, 303-316.

Chen, W., Haque, M. A., Lu, T., Aierzhati, A., & Reimonn, G. (2020). A perspective on hydrothermal processing of sewage sludge. *Current Opinion in Environmental Science & Health, 14*, 63-73.

Choplin, L., & Marchal, P. (2010). Mixer-type rheometer. In C. Gallegos (Ed.), *Rheology* (Vol. II, pp. 32-51). United Kingdom: Encyclopedia of Life Support Systems.

Díaz-Vázquez, L. M., Rojas-Pérez, A., Fuentes-Caraballo, M., Robles, I. V., Jena, U., & Das, K. C. (2015). Demineralization of Sargassum spp. macroalgae biomass: selective hydrothermal liquefaction process for bio-oil production. *Frontiers in Energy Research, 3*.

Durak, H., & Genel, S. (2020). Catalytic hydrothermal liquefaction of lactuca scariola with a heterogeneous catalyst: The investigation of temperature, reaction time and synergistic effect of catalysts. *Bioresour Technol, 309*.

Edifor, S. Y., Nguyen, Q. D., van Eyk, P., Biller, P., & Lewis, D. M. (2020). *Viscosity variation of model compounds during hydrothermal liquefaction under subcritical conditions of water*.

Gu, X., Martinez-Fernandez, J. S., Pang, N., Fu, X., & Chen, S. (2020). Recent development of hydrothermal liquefaction for algal biorefinery. *Renewable and Sustainable Energy Reviews, 121*.

Guo, Y., Yeh, T., Song, W., Xu, D., & Wang, S. (2015). A review of bio-oil production from hydrothermal liquefaction of algae. *Renewable and Sustainable Energy Reviews, 48*, 776-790.

Jo, H. J., Jang, H. K., Kim, Y. J., & Hwang, W. R. (2017). Process viscometry in flows of non-Newtonian fluids using an anchor agitator. *Korea-Australia Rheology Journal, 29*(4), 317-323.

Kumar, V., Kumar, S., Chauhan, P. K., Verma, M., Bahuguna, V., Joshi, H. C., Ahmad, W., Negi, P., Sharma, N., Ramola, B., Rautela, I., Nanda, M., & Vlaskin, M. S. (2019). Low-temperature catalyst based Hydrothermal liquefaction of harmful Macroalgal blooms, and aqueous phase nutrient recycling by microalgae.

Li, B., Wang, F., Chi, Y., & Yan, J. H. (2014). Adhesion and Cohesion Characteristics of Sewage Sludge During Drying. *Drying Technology, 32*(13), 1598-1607. doi: 10.1080/07373937.2014.910522

Luan, D., Chen, Q., & Zhou, S. (2014). Numerical Simulation and Analysis of Power Consumption and Metzner-Otto Constant for Impeller of 6PBT. *Chinese Journal of Mechanical Engineering, 27*(3), 635-640. doi: 10.3901/CJME.2014.03.635

Masoumi, S., Borugadda, V. B., & Dalai, A. K. (2020). Biocrude Oil Production via Hydrothermal Liquefaction of Algae and Upgradation Techniques to Liquid Transportation Fuels *Biorefinery of Alternative Resources: Targeting Green Fuels and Platform Chemicals* (pp. 249-270). Singapore: Springer.

Metzner, A. B., & Otto, R. E. (1957). Agitation of Non-Newtonian Fluids. *A.I.Ch.E., 3*(1).

Obeid, R. (2020). *Reaction Kinetics for Hydrothermal Liquefaction of Biomass.* (Doctor of Philisiphy Thesis by Publication), The University of Adelaide, Australia.

Obeid, R., Lewis, D. M., Smith, N., Hall, T., & van Eyk, P. (2020). Reaction Kinetics and Characterization of Species in Renewable Crude from Hydrothermal Liquefaction of Mixtures of Polymer Compounds To Represent Organic Fractions of Biomass Feedstocks. *Energy & Fuels, 34*(1), 419-429.

Pollak, S., Hüttemann, S., Qui~nones-Cisneros, S. E., & Weidner, E. (2017). Development and calibration of a high pressure high shear rate capillary rheometer. *Journal of Petroleum Science and Engineering, 157*, 581-587.

Qian, L., Wang, S., & Savage, P. E. (2017). Hydrothermal liquefaction of sewage sludge under isothermal and fast conditions. *Bioresour Technol, 232*, 27-34. doi: 10.1016/j.biortech.2017.02.017

Saba, A., Lopez, B., Lynam, J. G., & Reza, T. M. (2018). Hydrothermal Liquefaction of Loblolly Pine: Effects of Various Wastes on Produced Biocrude. *ASC Omega, 3*, 3051-3059.

Smith, A. M., Singh, S., & Ross, A. B. (2016). Fate of inorganic material during hydrothermal carbonisation of biomass: influence of feedstock on combustion behaviour of hydrochar. *Fuel, 169*, 135-145.

Suryawanshi, P. G., Das, S., Borugadda, V. B., Goud, V. V., & Dalai, A. K. (2020). Process Improvements and TechnoEconomic Feasibility of Hydrothermal Liquefaction and Pyrolysis of Biomass for Biocrude Oil Production *Biorefinery of Alternative Resources: Targeting Green Fuels and Platform Chemicals* (pp. 221-248).

Tian, Y., Wang, F., Djandja, J. O., Zhang, S., Xu, Y., & Duan, P. (2020). Hydrothermal liquefaction of crop straws: Effect of feedstock composition. *Fuel, 265*.

Tzanetis, K. F., Posada, J. A., & Ramirez, A. (2017). Analysis of biomass hydrothermal liquefaction and biocrude-oil upgrading for renewable jet fuel production: The impact of reaction conditions on production costs and GHG emissions performance. *Renewable Energy, 113*, 1388-1398. doi: 10.1016/j.renene.2017.06.104

Wang, W., Yu, Q., Meng, H., Han, W., Li, J., & Zhang, J. (2018). Catalytic liquefaction of municipal sewage sludge over transition metal catalysts in ethanol-water co-solvent. *Bioresour Technol, 249*, 361-367.

Wrolstad, R. E., Acree, T. A., Decker, E. A., Penner, M. H., Reid, D., Schwartz, S. J., Shoemaker, C. F., Smith, D., & Sporns, P. (2005). *Viscosity of Liquids, Solutions and Fine Suspensions* (Vol. 2): Newark: Wiley.

Xue, Y., Chen, H., Zhao, W., Yang, C., Ma, P., & Han, S. (2016). A review on the operating conditions of producing biooil from hydrothermal liquefaction of biomass. *40*, 865-877.

Yang, J., He, Q., & Yang, L. (2019). A review on hydrothermal co-liquefaction of biomass. *Applied Energy*, *250*, 926-945.

Yen, P. S., Chen, L. C., Chien, C. Y., R.M., W., & Lee, D. J. (2002). Network strength and dewaterability of flocculated sludge *Water Research*, 539-550.

Supplementary Information

Real-time viscosity variations of sewage sludge during hydrothermal liquefaction under subcritical water conditions

Sylvia Y. Edifor[a]* Quoc D. Nguyen[a] Philip van Eyk[a] Patrick Biller[b] Tony Hall[c] David M. Lewis[a]

[a]School of Chemical Engineering and Advanced Materials, The University of Adelaide, South Australia 5005, Australia

[b]Department of Engineering-Biological and Chemical Engineering, Aarhus University, 8200 Aarhus, Denmark

[c]Faculty of Science, The University of Adelaide, South Australia 5005, Australia

Table 1s. Composition of sewage sludge, Tetraselmis sp and Spirulina sp

Composition	Sludge	*Tetraselmis sp*	*Spirulina sp*
Organic, %			
Lipid	19.9	4.7	6.6
Carbohydrate	21.5	22.3	16
Protein	9.6	11.7	62
Lignin	1.4	0	0
Inorganic, %			
Ash	47.6	61.3	15.4

*Composition of *Spirulina sp* is given by Bulk Nutrients

Table 2s. ANOVA data for viscosity data comparing two different methods for viscosity measurement

Source of Variation	SS	df	MS	F	P-value	F crit
Between Groups	1778806	3	592935.2	35.1	5.92E-05	4.1
Within Groups	135016.2	8	16877.0			
Total	1913822	11				

Table 3s. Tukey HSD Test for viscosity data for silicon oil

Comparison	Absolute difference	Critical range	Results
Temperature-Couette	907.9	272.7	Means significantly different
Temperature-Metzner-Otto	876.6	272.7	Means significantly different
Temperature-Standard viscosity	881.7	272.7	Means significantly different
Couette-Metzner-Otto	31.3	272.7	Not Significantly different
Couette-Standard viscosity	26.2	272.7	Not Significantly different
Metzner Otto-Standard viscosity	5.1	272.7	Not Significantly different

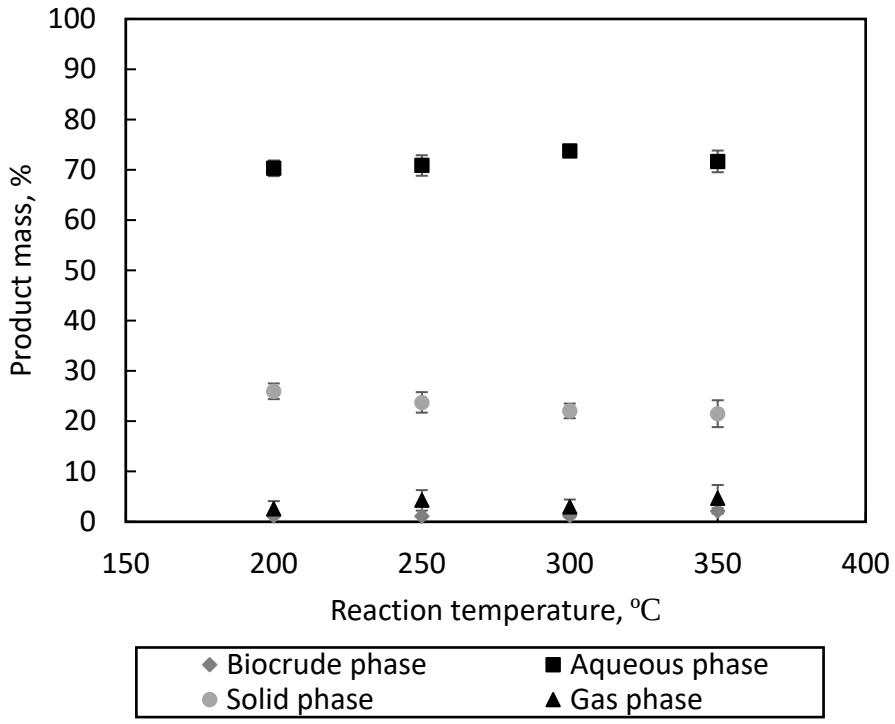

Figure 1s. Phase separation of HTL products

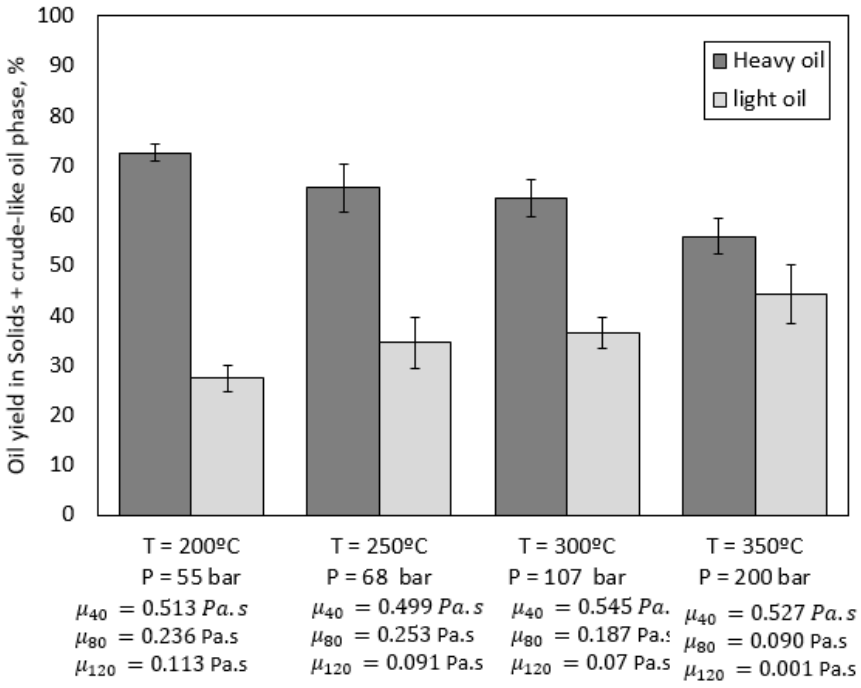

Figure 2s. Oil yields of solid and crude-like oil phase

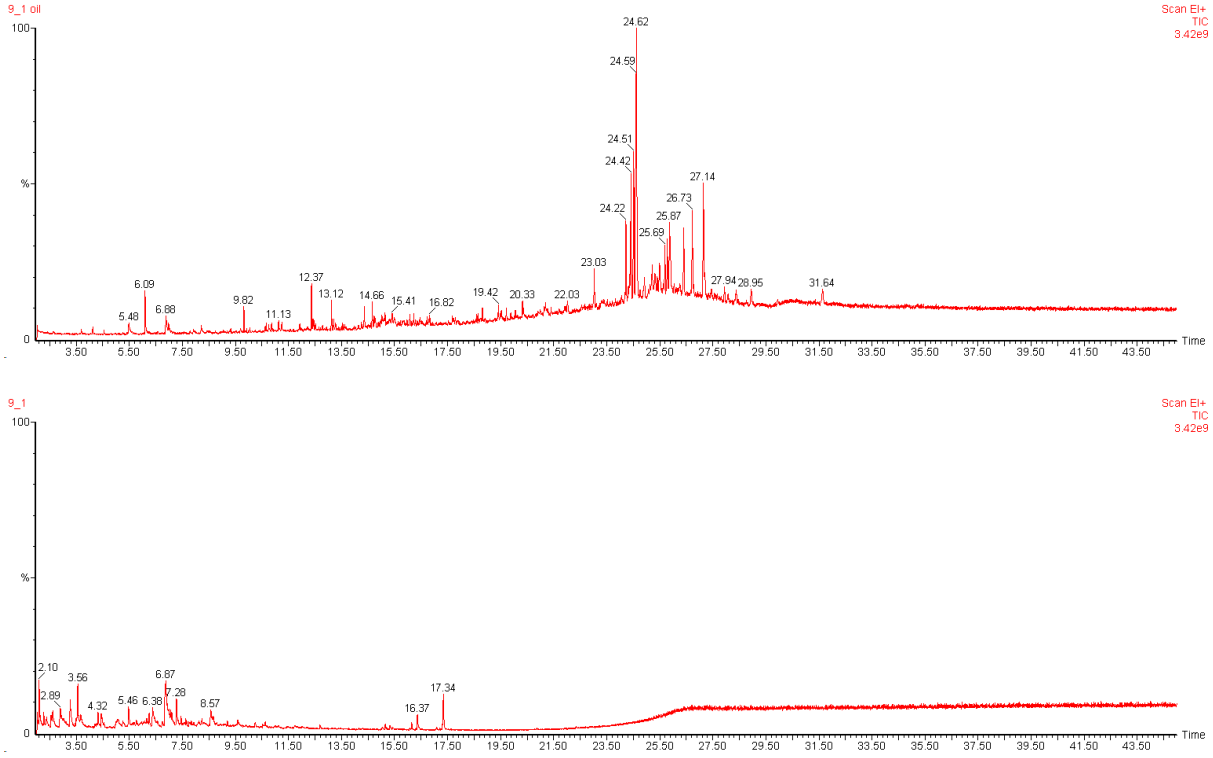

Figure 3s. Total ion chromatograms for crude-like oil phase (upper) and aqueous phase (lower)

Table 4s. GCMS data of crude-like oil product after HTL of sludge at 350ºC

Retention time, min	% by Response	Name	Molecular weight
24.622	8.33	Cholestane	372
24.592	6.25	Cholest-2-ene	370
27.143	4.34	Stigmastan-3-one	424
24.512	3.88	Cholestene isomer	370
24.417	3.70	Cholestene isomer	370
26.728	2.95	Cholestan-3-one	386
24.222	2.60	Cholestene isomer	370
26.403	2.52	Cholestan-2-one	386
25.873	2.09	Stigmast-2-ene	398
3.694	1.58	Ethylbenzene	106
23.027	1.57	Cholestene isomer	370
25.493	1.54	Stigmasterol	412
25.213	1.46	Ergost-2-ene	384
25.693	1.45	Stigmastene isomer	398
6.09	1.44	1-hexanol, 2-ethyl-	130
25.788	1.42	Stigmastene isomer	398
25.313	1.41	Ergostane	386
24.922	1.23	Cholestdiene isomer	368
25.903	1.12	Stigmastane	400
28.949	1.04	Butylcholestanone isomer	432
28.384	1.01	Propylcholestane isomer	414

12.372	1.01	Undecene	154
6.88	1.00	Phenol, 3-methyl-	108
27.193	1.00	Propylcholestane isomer	414
5.48	0.99	Phenol	94
2.659	0.97	Toluene	92
24.362	0.83	Coprostane	372
4.124	0.82	Styrene	104
13.123	0.70	Dodecene	168

Table 5s. GCMS data of aqueous product after HTL of sludge at 350ºC

Retention time, min	% by Response	Name	Molecular weight
6.87	6.3	2(3h)-furanone, 5-ethyldihydro-	114
3.559	2.4	Butanoic acid, 3-methyl-	102
6.375	2.2	2-pyrrolidinone, 1-methyl-	99
17.345	1.9	5,10-diethoxy-2,3,7,8-tetrahydro-1h,6h-dipyrrolo91,2',2'-d0pyrazine	250
2.889	1.7	Propanediamide	102
3.279	1.7	Pyrazine, methyl-	94
2.103	1.6	Propanoic acid	74
5.06	1.5	Pentanoic acid, 4-methyl-	116
7.281	1.4	1-ethyl-2-pyrrolidinone	113
8.571	1.4	1,2 dimethylpiperidine	113
3.674	1.3	Butanoic acid, 2-methyl-	102

2.619	1.3	Propanoic acid, 2-methyl-	88
5.465	1.2	Phenol	94
16.374	1.0	Pyrrolo[1,2-a]pyrazine-1,4-dione, hexahydro-3-(2-methylpropyl)	210
4.439	0.9	Pyrazine, 2,5-dimethyl-	108
7.1	0.8	1,5-dimethyl-2-pyrrolidinone	113
7.055	0.8	2,5-pyrrolidinedione, 1-methyl-	113
4.324	0.8	2-cyclopenten-1-one, 2-methyl-	96
8.666	0.7	2,5-pyrrolidinedione, 3-ethyl-1,3-dimeth	155
2.554	0.6	Pyridine	79
9.592	0.6	N-[2-hydroxyethyl]succinimide	143
2.374	0.6	Pyrazine	80
8.136	0.5	3,3 dimethylpiperidine	113
8.236	0.5	Octanoic acid	144
3.504	0.4	Acetamide, n-methyl-	73
16.149	0.4	3,6-diisopropylpiperazin-2,5-dione	198
5.26	0.4	2-cyclopenten-1-one, 2-methyl-	96
7.741	0.4	N-(3-methylbutyl)acetamide	129
2.279	0.4	Dimethyl ethanethioamide	103
7.451	0.4	1,4-dioxaspiro[2.4]heptan-5-one, 7,7-dim	142
6.25	0.4	2-cyclopenten-1-one, 2,3-dimethyl-	110

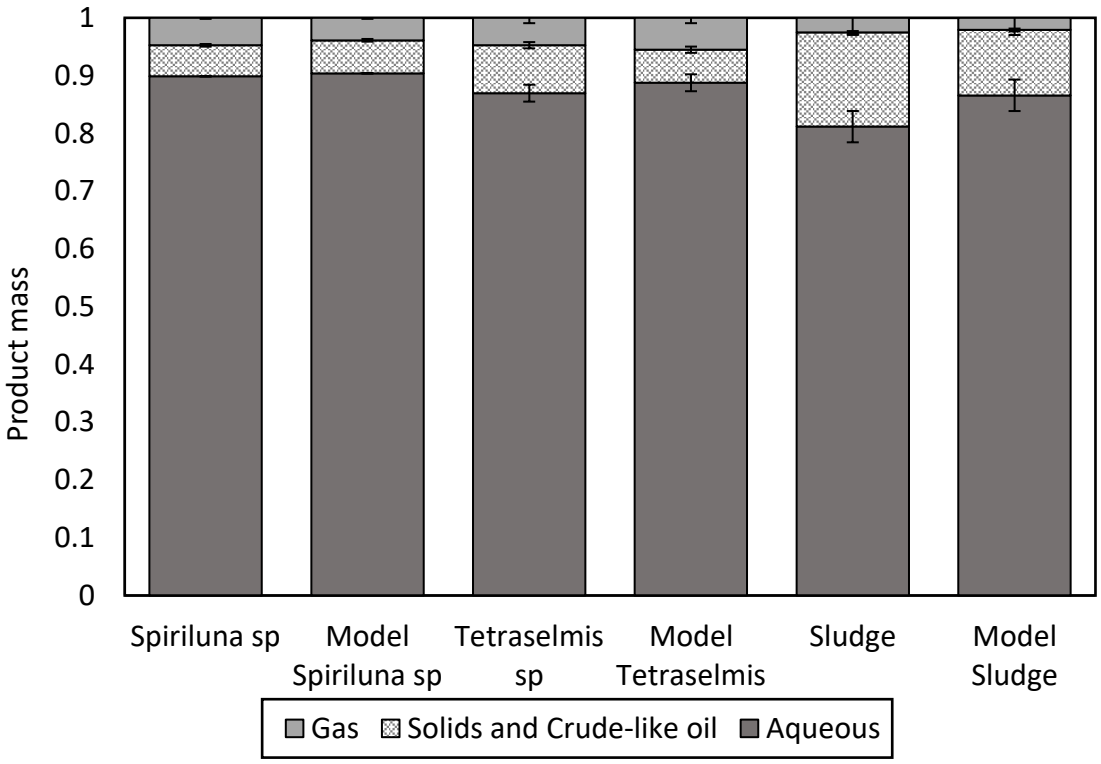

Figure 4s. Product mass of real biomass and mixtures of model compounds from phase separation after HTL at 350ºC *no solids formed in Spiriluna sp

Table 6s. Elemental analysis of real biomass

Inorganic composition, %			
Metals	Sludge	Tetraselmis sp	Spiriluna sp
Calcium	16.7	6.7	3.4
Iron	22.2	<1	1.3
Magnesium	5.4	7.9	6.9
Phosphorus	22.9	1.3	35.4
Potassium	1.9	1.6	45.5
Chromium	0.05	0	6.7
Sodium	2.2	60.8	<1
Sulphur	15.5	3.7	<1
Aluminium	9.7	17.6	<1
Others	<1	<1	<1

Chapter 7:

Conclusions

7. Conclusion

This PhD investigation has provided additional knowledge to the fundamental fluid properties of sewage sludge during the transformation of HTL reacting slurries. It has expanded existing research on the hydrothermal liquefaction of sewage sludge and biosolids, specifically, the quantification of flow properties for design purposes. This body of work has highlighted an important design parameter, viscosity, which has been ignored in current scientific research. One major contribution of this study was to characterise biosolid slurries by assessing its processability in terms of stability and pumpability. Secondly, this body of work determined the rheological characteristic of different types of sludge obtained from different parts of a waste treatment plant. Another major contribution of this study was the elucidation of apparent viscosity profile of model compound feedstock which is useful for predicting the apparent viscosity profile of actual biomass slurries. The fourth major contribution quantified the apparent viscosity of sludge slurries, which helps in design purposes and is useful for process control and monitoring. This is the first study on the changes in apparent viscosity of reacting HTL feedstock ever conducted under subcritical water conditions. Conclusions on the individual studies are stated below:

7.1. Conclusions from individual studies

7.1.1. The influence of feedstock characteristics on the processability of biosolid slurries for conversion to renewable crude oil via hydrothermal liquefaction

This study assessed the influence of biosolid feedstock characteristics for renewable crude-like oil production. The stability and pumpability of biosolid slurries at different solid concentrations and particle sizes were analysed. From this study, the following conclusions were made:

a. The effects of particle size in the hundreds of micron ranges used in the study had negligible effects on the slurry stability. Hence biosolid particle size can be limited to >750 µm for transportation purposes without a further breakdown in particle size.
b. An increase in solid concentration of biosolid slurries improves the stability of the slurry. Though higher solid loading is highly desired for higher throughputs and crude-like oil yields, high solids in HTL feedstock increase transportation cost of slurries.
c. Solid concentrations <60%w/w dry biosolids settle quickly within a period of 30 minutes. The settling characteristics of biosolid slurries can lead to the transportation issues, including blockages of pipe and clogging of pumps.
d. Transporting concentrated biosolid slurries requires high pumping energy. Additionally, processing high solid concentrated biosolids require high capital and operational costs.

7.1.2. Rheological studies of municipal sewage sludge slurries for hydrothermal liquefaction biorefinery applications

The rheological behaviour of different types of sludge was elucidated for HTL applications. The rheological parameters were determined using rheological models to fully characterise the feedstock. The conclusions drawn from this study are as follows:

a. Sewage sludge slurries prepared from feedstock obtained from different WWTPs vary per the source of the feedstock.
b. Sewage sludge and biosolid slurries were determined to be non-Newtonian fluids exhibiting shear thickening behaviour.
c. Rheological data for sludge slurries best fit into the Herschel-Bulkley viscosity model. The rheological parameters obtained from this model was used to estimate the design parameters for pipeline design purposes.

d. Pumping power required for pumping sewage sludge slurries at a specific solid concentration was higher than slurries prepared from stockpiled biosolids.

7.1.3. Viscosity variation of model compounds during hydrothermal liquefaction under subcritical conditions of water

This study focused on reacting slurries of model compounds, specifically viscosity, under subcritical water conditions. The real-time viscosity variations of sunflower oil, soy protein, granulated sucrose and mixtures of model compounds feedstock were quantified using the Metzner-Otto correlation for viscosity measurement in a stirred tank reactor. The following conclusions were made at the end of this study:

a. HTL feedstock slurries prepared from models of lipids, proteins and carbohydrates exhibits unique viscosity profiles under HTL conditions. The apparent viscosity changes in lipids are insignificant compared to the apparent viscosity changes in other model compounds under subcritical water conditions. Apparent viscosity of protein feedstock decreases significantly from room temperature to 100ºC and changes insignificantly until 350ºC. The apparent viscosity of reacting slurries of carbohydrate feedstock changes insignificantly from room temperature to 250ºC and increases as solids precipitate out of solution.
b. Factors that affected the changes in the apparent viscosity of reacting slurries of model compounds included temperature, pressure, chemical composition, phase change and the shearing forces.
c. Apparent viscosity profile of binary and ternary mixtures of model compounds gives a prediction of the apparent viscosity of actual biomass with similar compositions.

7.1.4. *Real-time viscosity variations of sewage sludge during hydrothermal liquefaction under subcritical water conditions*

In this study, the real-time viscosity changes of sewage sludge slurries were quantified under subcritical water conditions. Apparent viscosity measurement was estimated using the Couette and Metzner-Otto methods in a batch reactor. A comparison was made between the apparent viscosities of the reacting sludge slurries to reacting microalgae and mixtures of model compounds. The following conclusions were made from this study:

a. Generally, the apparent viscosity of sewage sludge slurries decreases with an increase in temperature from room temperature to about 320ºC.
b. Changes in apparent viscosity of sewage sludge are due to dominant macromolecules in sludge that react under elevated conditions.
c. The inorganic composition of sewage sludge catalyses HTL reaction mechanism which causes changes in the physical and chemical composition and eventually affects the slurry viscosity.

7.2. Recommendations for future work

The results reported in this thesis have broadened our understanding of the rheological characteristics of biosolids and sewage sludge slurries before HTL during upstream processes (pipe flow and pumping) and the changes in the viscosity of reacting slurries during HTL under subcritical conditions. However, a few gaps were identified, and further studies may be required to fully elucidate the rheological characteristics of the sludge feedstock during HTL:

a. Biomass comprises of proteins, carbohydrates, lipids and lignin. Most lignocellulosic biomass feedstock contains significant amounts of lignin which potentially affects the changes in the apparent viscosity of biomass under subcritical water conditions. Lignin is largely made up of insoluble solids whose presence will increase the solid product and

change the apparent viscosity of the reacting slurry. The nature of lignin model compounds, such as alkaline lignin, sticks to its containing vessel walls. Considering the sticky nature of lignin feedstock, the impeller configuration used was a limitation due to the small clearance between the impeller blades and the reactor vessel walls. An obstruction to the free rotation of the impeller was observed during apparent viscosity measurement. To fully mimic the viscosity changes in biomass, especially the lignin-containing biomass, viscosity changes of lignin can be determined with a different impeller configuration that will keep the slurry homogenous during measurement.

b. Further experiments can be conducted to fully quantify the viscosity changes of the inorganic fraction of biomass using models under subcritical water conditions.
c. Future investigations can be conducted on the effects of the catalysis of clays in sewage sludge on the conversion of organics and the changes in the apparent viscosity of reacting slurries. This should include detailed characterisation of clays in different sludge feedstock and assessing the effect of different types and concentration of clays to HTL product formation.
d. This study quantified the apparent viscosity of model compounds at a fixed rotational speed (shear rate). Further experiments can be conducted at different rotational speeds to fully characterise the rheological behaviour of each model compound, mixtures of model compounds, sewage sludge slurries, and other biomass samples at specific reaction conditions.
e. The data obtained after fully quantifying each feedstock's rheological properties used in this study can be used to model the apparent viscosity as a function of temperature, pressure, and composition. This will clearly explain how these factors and reaction conditions affect viscosity.

f. The data obtained from the viscosity changes of mixtures of model compounds of each macromolecule can be used to derive a relation as a function of the individual model compounds. Developing such a relation will help predict the viscosity changes of other biomass feedstock once the organic and inorganic components are known.

g. Viscosity data at different reaction conditions can be used to determine dimensionless parameters such as Reynolds number, Nusselts number and even heat transfer parameters including the heat transfer coefficient. Other parameters, such as density, can also be determined to fully characterise the fluid's flow and heat transfer properties.